Non-Linear Extreme Tension Statistics of Towing Hawsers

by

Fernando de Carvalho Frimm

B.S., Naval Architecture
University of São Paulo, Brazil
(1976)
M.S., Ocean Engineering
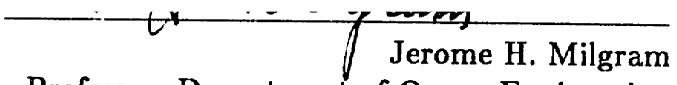University of São Paulo, Brazil
(1983)

SUBMITTED TO THE DEPARTMENT OF
DEPARTMENT OF OCEAN ENGINEERING
IN PARTIAL FULFILLMENT OF THE
REQUIREMENTS FOR THE
DEGREE OF
DOCTOR OF PHILOSIPHY IN OCEAN ENGINEERING
at the
MASSACHUSETTS INSTITUTE OF TECHNOLOGY
October 1987
© 1987 Massachusetts Institute of Technology

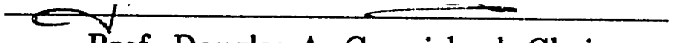Signature of Author: _____
Department of Ocean Engineering

Certified by: _____
Jerome H. Milgram
Professor, Department of Ocean Engineering
Thesis Supervisor

Accepted by: _____
Prof. Douglas A. Carmichael, Chairman
Departmental Graduate Committee

Non-Linear Extreme Tension Statistics
of Towing Hawsers

by

Fernando de Carvalho Frimm

Submitted to the Department of Department of Ocean Engineering
on October 30, 1987 in partial fulfillment of the
requirements for the Degree of
Doctor of Philosophy in Ocean Engineering

ABSTRACT

The study of towing operations in a random seaway is undertaken with the purpose of predicting extreme values for the towline tension. In a statistical sense, such extremes are tension values that have a given probability of occurrence during a certain period of time.

This statistical study takes into account the non-linear dependence of towline tension and ship motions. On a quasi-static basis, the tension-extension relationship presents two distinct regimes: one in which large extensions are accommodated by the cable catenary producing small tension variations; and a second one where small extensions, being accommodated by the cable stretch, cause very large tensions. Dynamically, as the cable oscillates in the water, the transverse hydrodynamic drag on the cable causes even more non-linearity. Making extensive use of time domain simulations, a polynomial expression for the towline tension in terms of the end motions is determined. This relationship is then used in the non-linear statistical calculations.

The tug and tow ships connected by the hawser constitute a twelve degree of freedom dynamic system, which is solved for the ships motions under the scope of linear seakeeping theory. For that purpose, the hawser forces are linearized using the method of equivalent linearization. The resulting motions combine to make up the cable extension which is the input to the non-linear statistical analysis of extremes.

Two methods are developed for evaluating the tension extremes. The first one consists of systematic development for an approximate probability density function (pdf) for the extremes. It is based on the bivariate Gram-Charlier Series obtained with the joint cumulants of the tension and its time derivative. The second one is fully non-linear. Starting with the known triple joint pdf of the cable extension and its first two time derivatives, a non-linear mapping is developed using a mathematical model relating tension to motion, and the probability for extremes determined numerically.

Thesis Advisor: Jerome H. Milgram
Professor, Department of Ocean Engineering

ACKNOWLEDGMENTS

I would like to express my appreciation to Prof. Jerome Milgram, my thesis supervisor, for his guidance during the course of this work. His enthusiasm and dedication constituted a very important factor for the conclusion and achievements of this work.

I would like also to thank the thesis committee members, Prof. Dick Yue and Prof. Mike Triantafyllou, for their comments and suggestions, specially Prof. Triantafyllou, for his efforts in providing the necessary cable dynamics "tools" for this thesis.

To my friends in the Sailing Lab., Jim, Penn, Buddy and Bob, thanks for your support and encouragement, and most of all for providing such nice environment to be working in. To George Anagnostou my sincere thanks for the long hours discussing towlines, hawsers, spring constants, damping coefficients ... It was a great help!

To Jim Burgess and Elleanor Swett my sincere thanks for their support, friendship and encouragement to myself and my family.

Finally, I express the most gratefulness and thanks to my wife Rosa for the her patience, companionship, understanding and caring. Also to my little ones, Renato and Daniel, for giving me such joy. They made this effort worthwhile !

Contents

4

List of Figures

List of Tables

Chapter 1

Introduction

This thesis intends to provide the necessary tools for the prediction of extreme tensions in a towline during actual tow operations in the seaway.

The current practice of towing operations [1] consists of a simple static analysis. The hawser geometry is defined by the cable catenary configuration with only one load considered: the maximum static pull in the towline, which is accounted for through estimates of the tow's resistance and then a safety factor is applied to it. The resulting number is compared to the towline's breaking strength. It is the safety factor, in fact, that takes into account the dynamic loading.

This approach is too simplistic, and clearly is not sufficient to assure the safety and efficiency of offshore towing operations. Since the tow can be subject to a variety of combinations of speed and angles to the waves, each of them resulting in different dynamic loads; it is clear that a single factor of safety is inadequate.

To be able to include in the analysis the dynamic component of the towline tension, other variables pertinent to the problem like the seakeeping qualities of the tug and tow vessels, the length of the towline, its weight and elastic behavior, need to be considered. For that purpose the towing problem has to be studied as a dynamic system where the individual dynamic characteristics of each element: the tug, the hawser, the towed vessel and their interactions are accounted for.

Previous works on the dynamics of towing systems by Abkowitz [2], Bernitsas [3], Miller [5] dealt more with the maneuvering motions of the ships and the quasi-static low frequency stretch of the towline. The seakeeping, i.e. the fast motions of the vessels and their influence on the dynamic tension were not considered.

More recently, studies in the area of cable dynamics had been developed by Triantalyllou [6], Shin [7], Burgess [8] and Bliek [9]. They provided a big step to the understanding of the dynamic behavior of cables and systems with cables. These studies indicate that the dynamic tension in a towline is a factor too important to be left out in the analysis, and also that it is heavily influenced by the seakeeping motions of the tug and the tow. Therefore, the dynamic effects of these motions on the hawser and their interactions with the line itself are to be considered for a more accurate prediction of the maximum loads a towing hawser can undergo in the seaway.

The main purpose of this thesis is the stochastic analysis of such dynamic system to determine extreme tensions on the hawser. In a statistical sense the extreme load

11

is some tension level with a probability value associated to it. Actually, it is defined as extreme tension, the magnitude of the tension that has a pre-defined probability of occurrence during a given period of time.

The basis for the analysis of the probability of extremes in linear dynamic systems was introduced by Rice [28], and applied in ocean engineering and naval architecture by Longett-Higgings [10], and Ochi [11]. In Ochi's work, the analysis of extremes for the linear seakeeping motions of a single body is complete. However, his results cannot be directly applied to the towing problem because of the need to consider both the tug and the tow acting together on the towline, which consists of a twelve degree of freedom problem, and also because of the fact that the towline can present a highly non-linear behavior.

There are basically two strong non-linearities in this problem. One is the hydrodynamic drag acting transverse to the cable due to its oscillations in response to the exciting motions at the ends. The second one is the towing hawser tension-extension relationship; in the range of amplitudes of the tug and tow motions, the cable can undergo a substantial change in span going from a completely slack condition to a completely taut one.

Chapter 2 in this work deals with the towing dynamics problem, which is solved under the scope of linear seakeeping theory. The main hypothesis there is that although the towline tension depends non-linearly on the vessels' motions its influence on the motions themselves is small. Therefore, the towline force can be linearized,

using the equivalent linearization method, and the motions determined through the solution of the linearized twelve degree of freedom problem. The towline elongation Response Amplitude Operator (RAO) is obtained and the prediction of the 'linear' extreme tensions according to Rice's theory [28] is introduced in Chapter 3. The effects of the non-linearities and the errors in the extreme values obtained within the linear theory are discussed.

In Chapter 4 one non-linear statistical analysis for the hawser is undertaken. It is developed from the Gram-Charlier method for the statistical analysis of the tension. It consists of a series representation of the joint probability function (pdf) of the tension and its time derivative, in terms of Hermite Polynomials. This pdf is then applied to determine the statistical distribution of the extremes. The method proved successful for slightly non-linear cables but as the non-linear behavior is accentuated it fails to predict the extreme tensions satisfactorily.

In chapter 5 the non-linear statistical problem is dealt with by means of an alternative approach. Using time domain simulations of the hawser dynamic equations, a polynomial representation for the tension is obtained in terms of the hawser extension and the extension rate of change (Appendix A). This polynomial representation is treated as a mapping function for the tension in the plane defined by the extension and the extension derivative. Because the vessels' motions combine linearly to make up the hawser extension, the extension and its time derivatives are jointly Gaussian distributed. Thus, the probability distribution of the non-linear

tension extremes is determined through the direct integration of this polynomial mapping function together with the joint pdf of the extension and its first and second time derivatives. This approach resulted in more accurate predictions of extreme tensions, even for the case when the towline presents very strong non-linear characteristics.

Chapter 2

Towing Dynamics

2.1   Introduction

In this chapter the dynamical aspects of the towing problem are introduced. The objective is to determine the motions at both ends of the hawser that combine to make up the cable extension. The block diagram in Figure 2.1 illustrates the procedures adopted to solve this problem.

As Figure 2.1 suggests, both vessels are excited by the sea waves, which are the main force input to the problem. The wave forces excite the ships which respond to these forces and those of the hawser. Therefore, the hawser acts as a restoring force on the ships, thus affecting the motions themselves.

15
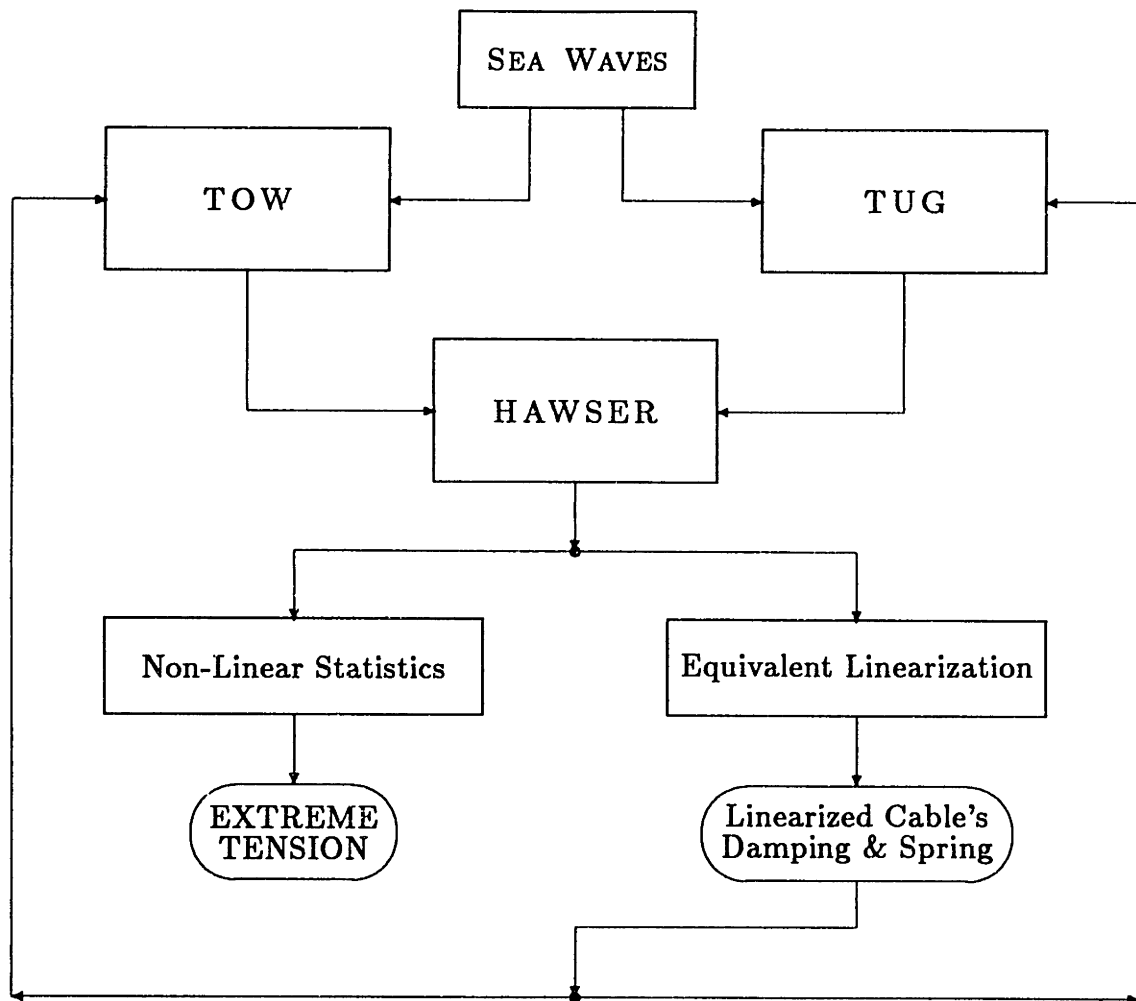
Figure 2.1: Block Diagram for the Dynamic Problem

The solution to the problem is complicated by the non-linear dependence between hawser force and motions. To be able to determine the ship motions the cable tension is "linearized" using the equivalent linearization approach such that linear seakeeping theory can be applied.

16

The methodology is justified on the basis that the motions amplitudes obtained this way are conservative. Due to the nature of the equivalent linearization method, the extreme "linearized force" is smaller that the true non-linear one, therefore the extreme motion amplitudes are larger than they would be otherwise. This happens because the cable extension is mostly determined by the surge motion, which is largely dependent on the inertial forces and the the hawser action is the only restoring force present. For all the other motions the hawser restoring force is small when compared to the hydrostatic ones.

Once the forces are identified, the tug and tow motions are determined under the scope of linear seakeeping theory. The final step is the evaluation of the cable extension to be used in the non-linear statistical calculations of the extreme tension.

2.2   Tension Linearization

As discussed in Appendix A, to determine the tension end-motion realtionship, a least minimum squares fit is performed on tension time histories obtained with simulations of the cable non-linear dynamic equations. The input to these simulations are sinusoidal end motions with known amplitude and frequency. It is necessary to consider enough data to cover the whole range of frequencies and elongation amplitudes present in realistic towing operations.

17

It is concluded that a third order polynomial on the cable's end point elongation $x(t)$ and elongation time derivative $\dot{x}(t) = \frac{dx}{dt}$ represent the cable tension adequately:

$$T(x, \dot{x}) = \sum_{m=0}^{3} \sum_{n=0}^{3} a_{mn} \, x^m(t) \, \dot{x}^n(t) \; , \qquad \text{with:} \; \begin{cases} m + n \; \leq 3 \\[2mm] (m, n) \; \neq (0, 0) \end{cases} \qquad (2.1)$$

For the linear case, the tension is assumed to be related to the end-point extension and extension derivative in the following way:

$$T(x, \dot{x}) = k_{eq} \, x(t) \; + \; b_{eq} \, \dot{x}(t) \qquad (2.2)$$

such that the coefficients k_{eq} and b_{eq} represent the linearized effects of the cable's restoring and damping forces, respectively.

Given the non-linear system, equation (2.1), and the linear approximation, (2.2), the method of equivalent linearization consists of equating the crosscorrelation functions, between input and output, for both realizations in order to determine the "best" linear representation [15].

The resulting linear system is "optimum" in a mean square sense. I.e., when responding to a stochastic input, the equivalent linearized version is the one that presents the minimum root mean square deviation with respect to the response of

18

the actual non-linear system it is approximating. (Figure 2.2)

Defining $R_{xx}(\tau)$ as the autocorrelation function for the extension $x(t)$ at the ends of the cable; then, since $x(t)$ is a Gaussian distributed random variable, the following holds:

$$
\begin{aligned}
E\left[x^2(t)\right] &= R_{xx}(0) = m_{0_x} \\
E\left[x(t)\,\dot{x}(t)\right] &= \left.\frac{dR_{xx}(\tau)}{d\tau}\right|_{\tau=0} = 0 \\
E\left[\dot{x}(t)\,\dot{x}(t)\right] &= -\left.\frac{d^2 R_{xx}(\tau)}{d\tau^2}\right|_{\tau=0} = m_{2_x} \\
E\left[x(t)\,\ddot{x}(t)\right] &= \left.\frac{d^2 R_{xx}(\tau)}{d\tau^2}\right|_{\tau=0} = -m_{2_x}
\end{aligned}
\tag{2.3}
$$

where m_{0_x} and m_{2_x} are the spectral moments of zero and second order, respectively; and also [16]:

$$
E\left[x^p\,\dot{x}^q\right] = \begin{cases} \dfrac{1}{2^{n+m}}\ \dfrac{(2n)!\,(2m)!}{n!\,m!}\ m_{0_x}^{2n}\,m_{2_x}^{2m} & p = 2n,\ q = 2m \\[2ex] 0 & p,\ q\ otherwise. \end{cases}
\tag{2.4}
$$

$R_{NL}(\tau)$ is the crosscorrelation function between non-linear tension and extension; and $R_L(\tau)$ is the crosscorrelation function between the linearized tension and the extension:

$$
R_{NL}(\tau) = E\left[T_{NL}(t)\,x(t+\tau)\right] \qquad R_L(\tau) = E\left[T_L(t)\,x(t+\tau)\right]
\tag{2.5}
$$

19
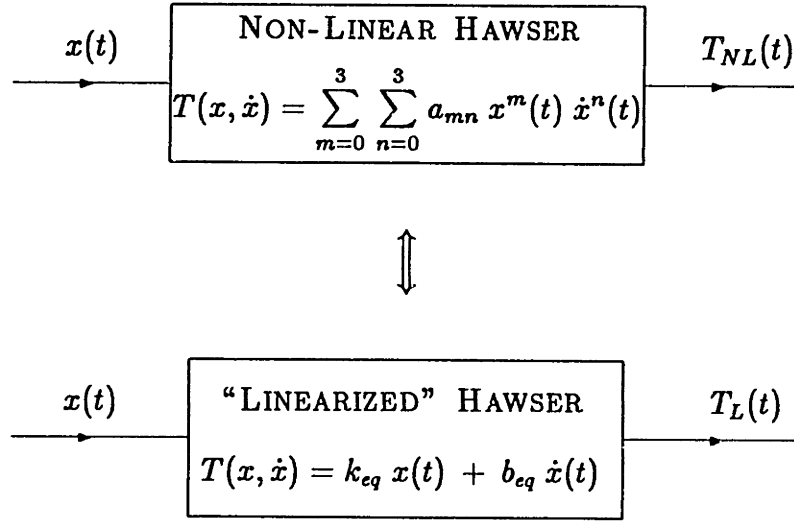
Figure 2.2: Equivalent Linearization

Given the coefficients a_{mn}, we wish to determine k_{eq} and b_{eq} such that the two crosscorrelations $R_{NL}(0)$ and $R_L(0)$ are equal. The result is:

$$k_{eq} = a_{10} + 3\,a_{30}\,m_{0x} + a_{12}\,m_{2x} \tag{2.6}$$

$$b_{eq} = a_{01} + 3\,a_{03}\,m_{2x} + a_{21}\,m_{0x} \tag{2.7}$$

2.3 Dynamic Equations

In the frequency domain the equations of motion for each of the vessels can be written:

– for the tug:

$$\left[-w_e^2 \left(M_1 + A_1(w_e) \right) + iw_e\, B_1(w_e) + C_1 \right] X_1\, e^{iw_e t} = F_1(w_e)\, e^{iw_e t} + F_{H_1} \quad (2.8)$$

– for the tow:

$$\left[-w_e^2 \left(M_2 + A_2(w_e) \right) + iw_e\, B_2(w_e) + C_2 \right] X_2\, e^{iw_e t} = F_2(w_e)\, e^{i(w_e t + \theta)} + F_{H_2} \quad (2.9)$$

where:

$M_{1,2}$ – generalized mass matrix for tug and tow

$A_{1,2}$ – added mass matrix for tug and tow

$B_{1,2}$ – damping coefficient matrix for tug and tow

$C_{1,2}$ – hydrostatic restoring force matrix for tug and tow

$F_{1,2}$ – unit amplitude waves exciting force vector for tug and tow

$X_{1,2}$ – motions response vector for tug and tow

$F_{H_{1,2}}$ – cable force vector acting on the tug and tow

w_e - waves encounter frequency

θ - phase difference between tug and tow

Regular strip theory [17] computations are applied to both vessels to determine the frequency dependent hydrodynamic coefficients and the wave exciting forces. For that purpose, the MIT five degrees of freedom seakeeping program [18] is used for the motions: sway, heave, pitch, roll and yaw.

The surge problem is solved separately, and included afterwards to complete the six degrees of freedom equations for each ship. The basic simplifications and hypothesis considered are as follows:

Surge added mass – The added masses for both vessels are taken as constants: 5% of the mass.

Surge damping coefficients – The surge damping coefficients are considered frequency independent constants. For the towed vessel it is taken as the slope of the calm water resistance curve with a locked propeller as appendage. For the tug, it is assumed a constant torque propulsion plant, and the damping calculated as the change in trust per unit change in velocity at the propeller point of operation.

Surge exciting force – The exciting force is obtained through the Froude-Krylov approximation, i.e., integrating of the wave pressure field on the ships' surface, assuming no disturbance due to the ships' presence.

Further details on the surge motion analysis can be found in references [19,32] and in the appendix B.

2.4   The Coupled Equation of Motion

The individual equations of motion (2.8) and (2.9), for the tug and the tow, can be coupled together when the hawser effects are accounted for.

Because of the forces transmitted by the hawser, motions of one vessel influence the hawser forces not only on itself, but also on the ship at the other end of the towline. Therefore, the coupling effects can be represented by influence matrices that translate the hawser force acting on the ships due to unit change of motions and velocities at both extremities of the line.

Considering:

K_{11} – Hawser force on the tug due to unit motions at the tug,

K_{12} – Hawser force on the tug due to unit motions at the tow,

K_{22} – Hawser force on the tow due to unit motions at the tow,

K_{21} – Hawser force on the tow due to unit motions at the tug;

D_{ij} – Similarly, hawser forces on the tug and tow due to unit velocities at the tug or tow.

Then, for the hawser forces on the tug and the tow:

$$F_{H_1} = K_{11} X_1 + K_{12} X_2 + D_{11} \dot{X}_1 + D_{12} \dot{X}_2 \qquad (2.10)$$

and

$$F_{H_2} = K_{12} X_1 + K_{22} X_2 + D_{21} \dot{X}_1 + D_{22} \dot{X}_2 \qquad (2.11)$$

or in matrix form:

$$F_H \;=\; \begin{bmatrix} K_{11} + iw_e D_{11} & K_{12} + iw_e D_{12} \\ K_{21} + iw_e D_{21} & K_{22} + iw_e D_{22} \end{bmatrix} \begin{bmatrix} X_1 \\ X_2 \end{bmatrix} \qquad (2.12)$$

Thus, the (12×12) coupled equations of motion be written[1]:

$$\left[-w_e^2 M(w_e) + iw_e B(w_e) + C \right] X \, e^{iw_e t} \;=\; F(w_e) \, e^{iw_e t} \qquad (2.13)$$

where:

$$M(w_e) \;=\; \begin{bmatrix} M_1 + A_1(w_e) & 0 \\ 0 & M_2 + A_2(w_e) \end{bmatrix}_{12 \times 12}$$

$$C \;=\; \begin{bmatrix} C_1 - K_{11} & -K_{12} \\ -K_{21} & C_2 - K_{22} \end{bmatrix}_{12 \times 12}$$

---

[1]The coupling or influence matrices K_{ij} and D_{ij}, are described in the Appendix B.

$$
B(w_e) = \begin{bmatrix} B_1(we) - D_{11} & -D_{12} \\ -D_{21} & B_2(we) - D_{22} \end{bmatrix}_{12\times12}
$$

$$
X = \begin{bmatrix} X_1 \\ X_2 \end{bmatrix}_{12\times1} \qquad \text{and} \qquad F(w_e) = \begin{bmatrix} F_1(w_e) \\ F_2(w_e)\,e^{i\theta} \end{bmatrix}_{12\times1}
$$

2.5 The Cable Elongation

For the tension calculations, according to the equations (2.2) and (2.1) it is necessary to compute the total cable elongation (or extension) x caused by the ship motions.

The motion vector X is determined through the solution of the coupled equation of motion (2.13). Knowing also the attitude of the tow relative to the tug, and the static configuration the hawser presents; the cable extension at each end is computed as the projection of the motion vectors X_1 or X_2 in the direction tangent to the cable at that extremity. It is along this direction that the dynamic tension is mostly influenced by the ship motions. The total elongation x in then assumed to be the sum of both extensions thus determined.

The total elongation the hawser undergoes due to the motions of tug and tow, is then:

$$x = S_1' \cdot X_1 + S_2' \cdot X_2 \tag{2.14}$$

or in matrix form:

$$x = \left[\; S_1' \; \vdots \; S_2' \; \right] \begin{bmatrix} X_1 \\ X_2 \end{bmatrix} \tag{2.15}$$

where $S_{1,2}'$ are influence row vectors for hawser extension due to unit motions at the tug and tow ends respectively.[2]

The wave exciting force vector (for unit wave amplitude) is:

$$F(w_e) = \mid F(w_e) \mid e^{i\,w_e\,t} \tag{2.16}$$

and the motion vector is:

$$X(w_e) = \left| X \right| e^{i\,w_e\,t} \tag{2.17}$$

The frequency domain solution of the equation of motions, equation (2.13), gives the ship motions amplitude vector for every frequency w_e :

$$X(w_e) = \left[-w_e^2\, M(w_e) + i w_e\, B(w_e) + C \right]^{-1} \left| F(w_e) \right| \tag{2.18}$$

---

[2] The row vector $S' = [\; S_1' \; \vdots \; S_2' \;]$ is described in the Appendix B.

The 12 degree of freedom motions transfer function can be identified as the (12×12) matrix:

$$H(w_e) = \left[-w_e^2 M(w_e) + i w_e B(w_e) + C \right]^{-1} \qquad (2.19)$$

The scalar elongation can be written as:

$$x(t) = S' \; H(w_e) \; X \; e^{i w_e t} \qquad (2.20)$$

where the cable elongation response amplitude operator, i.e. the elongation per unit wave amplitude, is identified as:

$$G_x(w_e) = S' \; H(w_e) \; X \qquad (2.21)$$

Figure 2.3 presents the elongation RAO for a 1200ft long, 2 in diameter steel hawser when an ARS-50 class tug is towing a Frigate in 30 knots wind and speed of advance of 3 knots. The oscillations in the curve are due to the phase differences between the wave exciting forces at the tug and tow.

Given the sea wave power density spectrum, $S_W(w_e)$, according to linear systems theory [20], the elongation power spectrum density, or simply the "elongation spectrum" is given by:

$$S_x(w_e) = \left| G_x(w_e) \right|^2 S_W(w_e) \qquad (2.22)$$
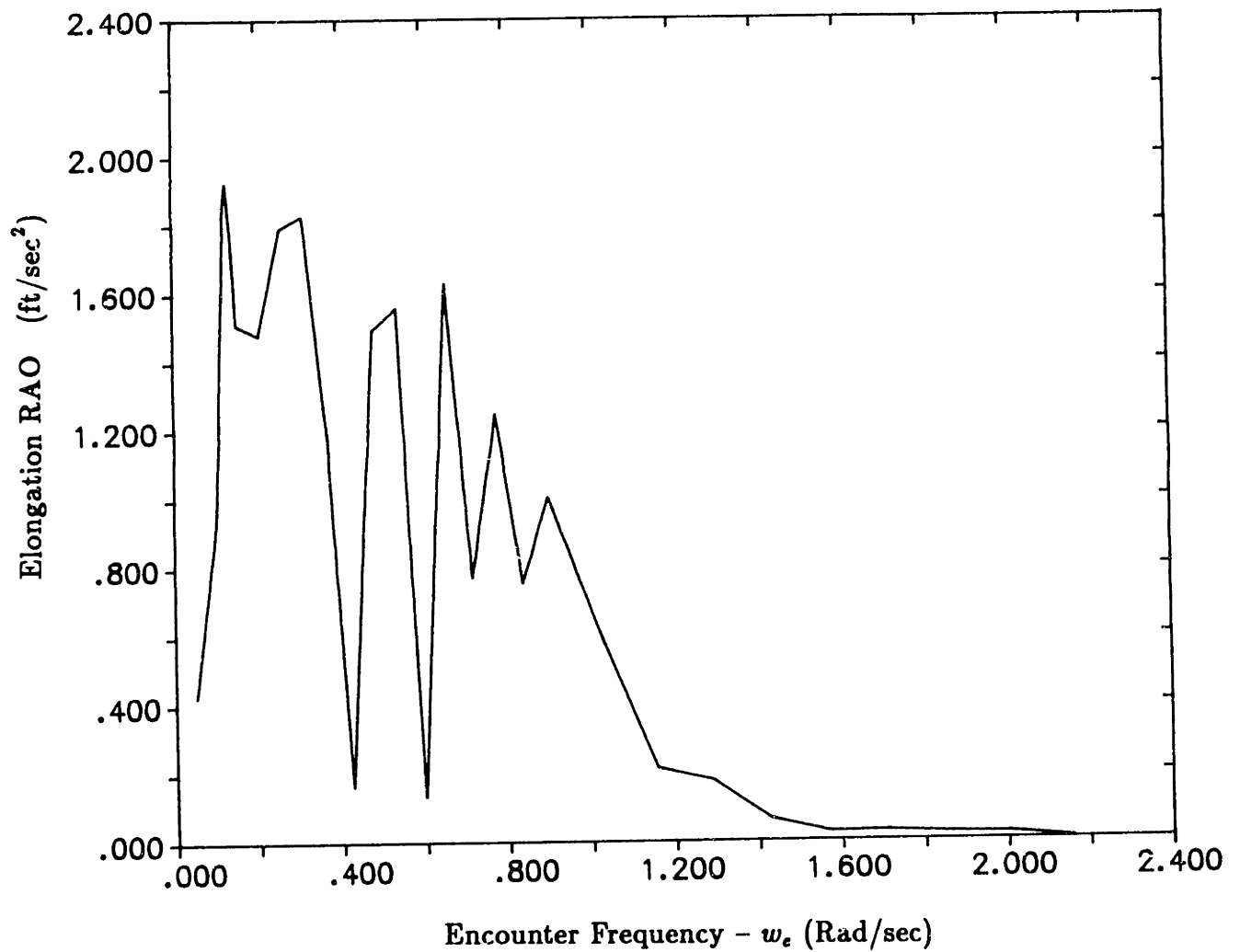
Figure 2.3: Towline Elongation RAO
Hawser Length: 1200 ft – Diameter: 2 in
Static Tension: 20.0 kips
Tug ARS-50 towing a Frigate at 3 knots
Wind Velocity: 30 knots.

and the elongation spectral moments can be evaluated:

$$m_{n_x} = \int_0^\infty w_e{}^n S_x(w_e)\, dw_e \qquad (2.23)$$

Chapter 3

The Linear Statistics

of Extremes

The goal in this chapter is the introduction of the theory for the analysis of extreme tension within the scope of linear systems theory.

Considering the cable elongation $x(t)$ as a stationary and Gaussian distributed random process, the theory of linear time-invariant systems assures that the resulting equivalent linearized tension $T_L(t)$, given by equation (2.2), will also be stationary and Gaussian distributed.

For the elongation, the joint Gaussian pdf - probability density function of the elongation and its first and second time-derivatives is given by:

$$p_x(x, \dot{x}, \ddot{x}) = \frac{1}{(2\pi)^{\frac{3}{2}}\sqrt{m_{2_x}\Delta}} \exp\left[-\frac{1}{2\Delta}\left(m_{4_x}x^2 + \frac{\Delta}{m_{2_x}}\dot{x}^2 + m_{0_x}\ddot{x}^2 + 2m_{2_x}x\ddot{x}\right)\right] \quad (3.1)$$

with $\Delta = m_{0_x} m_{4_x} - m_{2_x}^2$ and the spectral moments $m_{0_x}, m_{2_x}, m_{4_x}$ given by equation (2.23).

Similarly, the joint Gaussian pdf for the linearized tension and its time derivatives, $p_T(T, \dot{T}, \ddot{T})$, could be determined using equation (2.2) with (2.23).

3.1 The Number of Local Maxima

In the analysis of extreme values we shall look for conditions for local positive maxima to occur. At these local peaks, the tension $T_L(t)$ is positive, its first derivative is zero and the second derivative is negative. As first considered by Rice [28], given the joint pdf $p_T(T, \dot{T}, \ddot{T})$, for the tension and its first and second derivatives; the expected number of peaks per unit time, above the specified level T_0, is given by:

$$M(T_0) = \int_{T_0}^{\infty} dT \int_{-\infty}^{0} \left| \ddot{T} \right| p_T(T, 0, \ddot{T}) \, d\ddot{T} \qquad (3.2)$$

where $T = T_L(t)$, as in equation (2.2).

Considering the expected value for the total number of peaks as given by the number of all local maxima above the level $T_0 = 0$:

$$M(0) = \int_{0}^{\infty} dT \int_{-\infty}^{0} \left| \ddot{T} \right| p_T(T, 0, \ddot{T}) \, d\ddot{T} \qquad (3.3)$$

Then, the ratio $M(T_0) / M(0)$ can be interpreted as the probability for one local maxima to be larger or above the reference level T_0; thus determining the PDF - probability distribution function, for T_0 to be exceeded once:

$$F_M(T \geq T_0) = \frac{M(T_0)}{M(0)} \tag{3.4}$$

In equation (3.4) above, an important implicit assumption is that every zero up-crossing generates a local maxima. This hypothesis is not as restrictive as it may seem. It translates that probability values are assigned to the peaks neglecting those rare instances, when a local maxima is followed by another one without the occurrence of a zero crossing event. Its adoption is justified on the basis that the extreme tension, we want to determine, is a fairly large tension level, for which the occurrences of these "double peaks" are unlike to happen. Furthermore, the linear tension results from a narrow-band process; the sea spectrum with the cable elongation RAO, which in a certain way guarantees the unlikelihood of these peaks to occur.

Actually, once it is assumed that every level crossing generates one local maxima, this hypothesis can be carried further on, and the probability distribution of peaks determined directly from the frequency of crossings. The classical result obtained by Rice [28] is the formula for the average number of up-crossing events of an arbitrary level in a stationary random process. In the present case, let $p_T(T, \dot{T})$ be the joint

32

probability distribution function of the linearized tension and its time derivative; then, for an arbitrary tension level T_0, the average number of up-crossings or simply the "frequency" of crossings is:

$$N(T_0) = \int_0^\infty \dot{T} \, p_T(T, \dot{T}) \, d\dot{T} \qquad (3.5)$$

The expression (3.5) above is much simpler than equation for the frequency of peaks, (3.2), due to the fact that it involves the joint pdf $p_T(T, \dot{T})$ of the tension and its first time derivative instead of the joint pdf $p_T(T, \dot{T}, \ddot{T})$, for the tension and its first and second derivatives. This simplification, although not necessary for the extreme linear tension analysis in the present section, since both $p_T(T, \dot{T})$ and $p_T(T, \dot{T}, \ddot{T})$ are known; facilitates the subsequent non-linear tension extremes problem. There, it would be much more difficult to evaluate the joint pdf of the non-linear tensions and its derivatives, $f(T, \dot{T}, \ddot{T})$, in a systematic way; although it can be done for $f(T, \dot{T})$, as introduced in Chapters 4 and 5.

3.2 The Probability for the Extremes

As mentioned in the previous section, the PDF for the peaks can be evaluated directly with the frequency of crossings. Thus, the probability that the tension T_0 be exceeded, given that the zero crossing event happened (and before it is exceeded again) is:

$$P(T \geq T_0) = \frac{N(T_0)}{N(0)} \qquad (3.6)$$

or for the tension to be below the level T_0 :

$$P(T \leq T_0) = 1 - \frac{N(T_0)}{N(0)} \qquad (3.7)$$

Differentiating equation (3.7) above, the pdf - probability density function for the tension to be below the reference value is:

$$p(T \leq T_0) = -\frac{1}{N(0)} \frac{d}{dT_0} N(T_0) \qquad (3.8)$$

Rice [28] and Longett-Higgings [10] had shown that for a narrow-banded Gaussian random process, this pdf for the maxima converge to a Rayleigh distribution, which is exact when the process is infinitely narrow, i.e.:

$$p(T \leq T_0) = \frac{T_0}{m_{0_T}} \exp[-\frac{1}{2} \frac{T_0^2}{m_{0_T}}] \qquad (3.9)$$

where m_{0_T} is the mean square value of the linearized tension, which can be related to the elongation spectral moments:

$$m_{0_T} = k_{eq}^2 \, m_{0_x} \; + \; b_{eq}^2 \, m_{2_x} \tag{3.10}$$

It is important to note that when narrow-bandness is assumed, the Rayleigh distribution for the maxima in equation (3.9) is obtained using either the number of peaks or the number of crossings, i.e. equation (3.2) or (3.5), as shown in Rice's work [28].

3.3 The Linear Extreme Tension

For practical purposes it is worth considering the extreme tension, T_{ext}, as the tension level which has a given probability, α, of not being exceeded in a given period of time, Δt.

Assuming $T(t)$ a stationary random process for the prescribed period of time, the total number of peaks (or up-crossings) is:

$$M \; = \; \Delta t \; N(0) \tag{3.11}$$

Assuming that the extreme tension is adequately large such that its occurrences are infrequent enough to be considered independent; the total probability that the

level T_0 is not exceeded during the time period Δt, is:

$$P_\Delta(T \leq T_0) = \left[1 - \frac{N(T_0)}{N(0)}\right]^M \qquad (3.12)$$

The assumption of independence among local peaks leads to somewhat larger probabilities of any arbitrary tension level be exceeded. Therefore, the analysis indicates that extremes are more probable then they would actually be, thus on the conservative side. This fact can be proven heuristically using elementary algebra of sets and conditional probability arguments [21], and was verified for narrow-band processes by Naess [22], where the peak values were subject to a Markov chain condition.

Therefore, using (3.12) with $P_\Delta(T \leq T_{ext}) = \alpha$:

$$\left[1 - \frac{N(T_{ext})}{N(0)}\right]^M = \alpha \qquad (3.13)$$

the extreme tension is determined solving numerically equation (3.13) above, for T_{ext}.

3.3.1 Linear Extreme Tension Results

This section presents the prediction of the extreme tension for a US Navy ARS-50 class tug towing the US Navy Frigate Page at a speed of advance of 3 knots. The characteristics of these vessels are given in Table 3.1.

36

The towline hawser is a 1200 ft long fiber-core wire hope with 2 in diameter.

		ARS50	PAGE
Length	(ft)	240	390
Beam	(ft)	50	43
Draft	(ft)	15.5	14.5
Displacement	(l.tons)	2881	3840

Table 3.1: Tug and Tow characteristics

According to the adopted definition for the extreme tension, in these calculations it is considered:

$$\Delta t = 24.0 \text{ hours} = 86400 \text{ sec} \qquad \text{and} \qquad \alpha = 0.001$$

I.e., T_{ext} is the tension level which has 99.9% probability of not being exceeded in 24 hours.

The equation of motion, (2.13), is solved for the 12 degrees of freedom problem and considering a Pierson-Moskowitz sea spectrum [27] for 30.0 knots wind, for the elongation moments are determined:

$$m_{0_x} = 19.203 \text{ ft}^2 \qquad m_{2_x} = 8.716 \text{ ft}^4 \qquad m_{4_x} = 4.823 \text{ ft}^8$$

Which results for the coefficients of the linearized tension model:

$$k_{eq} = 1.937 \text{ kips/ft} \qquad \text{and} \qquad b_{eq} = 4.003 \text{ kips} \cdot \text{sec/ft}$$

The pdf for the extreme tension, obtained numerically with equation (3.8) is shown

in Figure 3.1.

The resulting extreme values for the linear statistical analysis are:

Extreme Elongation: $\quad x_{ext} = \quad$ 24.82 ft

Extreme Tension: $\qquad T_{ext} = \quad$ 84.50 kips.
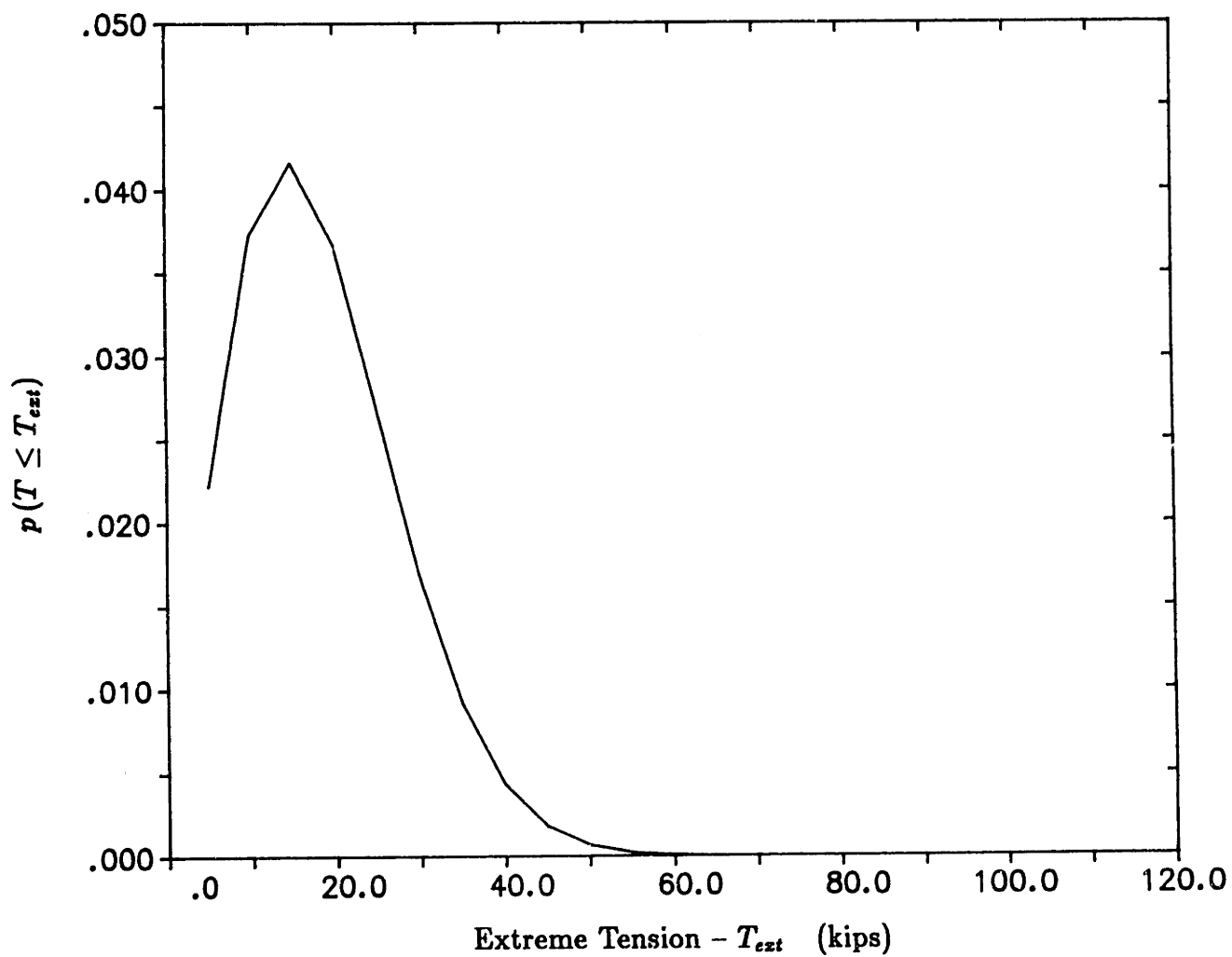
Figure 3.1: Probability Density Function - $p(T \leq T_{ext})$
Hawser Length: 1200 ft – Diameter: 2 in
Static Tension: 20.0 kips
ARS-50 Towing Frigate PAGE at 3 knots
Wind Speed: 30 knots.

3.3.2 Comments on The Linear Extremes

The extreme tension obtained with linear theory is completely unreasonable. According to Figure 3.2, the resulting extreme elongation: 24.82 ft, which results in a change in span of approximately 23.5 ft, should give at least 280.0 kips for the extreme tension, which is much greater than this linear analysis result.

The reason for such a small calculated extreme tension value resides in the fact that the cable's elastic properties are being approximated by the equivalent linearized spring constant k_{eq}. While the actual hawser, for large elongations, behaves elastically on the steep slope of the static curve, the equivalent linearized relation follows the tension-elongation according to k_{eq} which is much smaller. This happens because of the nature of the equivalent linearization process, where the linear coefficients are determined to approximate well the non-linear tension for elongations of the order $\sqrt{m_{0_x}}$.

To retrieve in the statistical analysis, the fully non-linear behavior of the hawser tension-elongation characteristic, as well as the effects of the non-linear hydrodynamic cross flow drag, the cable tension model obtained through the equivalent linearization method is not appropriate. In the following chapters, the third order polynomial tension model, introduced in Chapter 2 and Appendix B, is considered and the fully non-linear statistical analysis is undertaken.
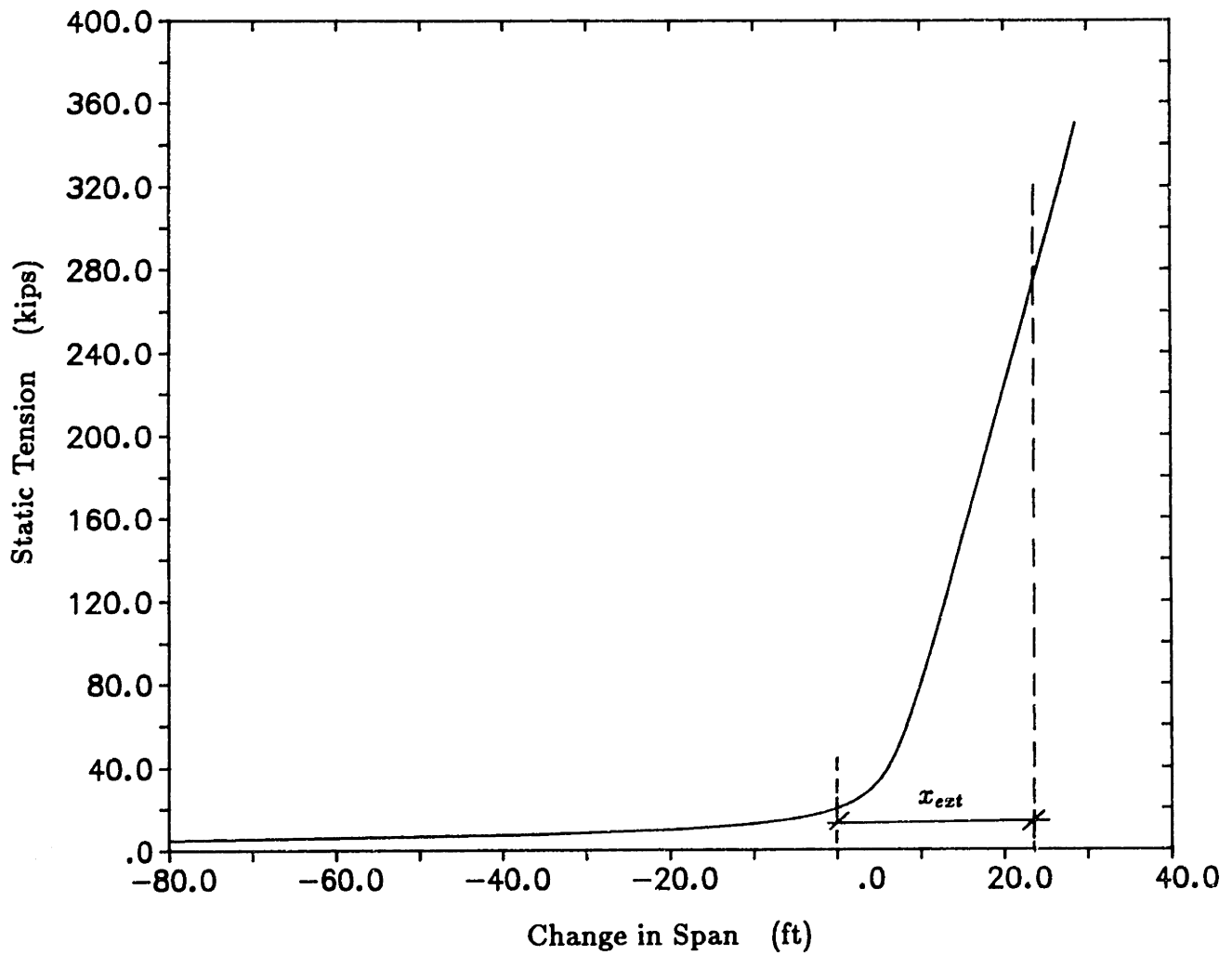
Figure 3.2: Static Curve - Tension × Change in Span
Length: 1200 ft – Diameter: 2 in
Fiber Core Wire Hawser.

Chapter 4

Gram-Charlier Series

4.1 Preliminaries

We want to write the joint probability density function - pdf, $f(T, \dot{T})$ of the tension $T(t)$ and its derivative $\dot{T}(t) = \frac{dT(t)}{dt}$ such that the number of up-crossings per unit time, or average frequency of crossings, at certain level T_0 can be determined:

$$N(T_0) = \int_0^{\infty} \dot{T} f(T_0, \dot{T}) \, d\dot{T}. \tag{4.1}$$

This joint pdf $f(T, \dot{T})$ can be written in terms of the Fourier Transform of its characteristic function $M(iv_1, iv_2)$:

$$f(T, \dot{T}) = \frac{1}{(2\pi)^2} \int_{-\infty}^{\infty} \int_{-\infty}^{\infty} M(iv_1, iv_2) e^{-iv_1 T} e^{-iv_2 \dot{T}} \, dv_1 \, dv_2. \tag{4.2}$$

Therefore, if the characteristic function is known, the number of crossings can be evaluated by performing the $\dot{T}$ integration in equation (4.1). This can be accomplished, at least theoretically, by either one of the two methods:

1. Writing $M(iv_1, iv_2)$ in terms of the *moments* of the joint distribution of $T(t)$ and $\dot{T}(t)$ and performing the integration in (4.1).

2. Writing $M(iv_1, iv_2)$ in terms of the *cumulants* of the joint distribution of $T(t)$ and $\dot{T}(t)$ and performing the integration in (4.1).

Using *method 1* we would write:

$$M(iv_1, iv_2) = \sum_{p=0}^{\infty} \sum_{q=0}^{\infty} \frac{M_{pq}}{p!\, q!} (iv_1)^p (iv_2)^q \qquad (4.3)$$

where M_{pq} is the joint moment of T and $\dot{T}$ of order pq, i.e. $M_{pq} = E[T^p \dot{T}^q]$.

Combining the above expansion of the characteristic function with (4.2), we get for the joint pdf:

$$f(T, \dot{T}) = \frac{1}{(2\pi)^2} \sum_{p=0}^{\infty} \sum_{q=0}^{\infty} \frac{M_{pq}}{p!\, q!} \int_{-\infty}^{\infty} (iv_1)^p e^{-iv_1 T} dv_1 \int_{-\infty}^{\infty} (iv_2)^q e^{-iv_2 \dot{T}} dv_2. \quad (4.4)$$

This expression shows why the moments expansion of the characteristic function is not convenient. One cannot guarantee the existence of these integrals in a usual sense, since v_1^p and v_2^q are not bounded functions.

This pitfall can be avoided when applying *Method 2*, i.e. writing the character-

istic function in terms of its cumulants expansion:

$$M(iv_1, iv_2) \;=\; \exp\left[\sum_{p=0}^{\infty}\,\sum_{q=0}^{\infty}\,\frac{K_{pq}}{p!\,q!}\,(iv_1)^p\,(iv_2)^q\right].\qquad(4.5)$$

where K_{pq} are the bi-variate cumulants of order $p\ q$.

This expansion allows the representation of the joint pdf in a series of Hermite polynomials, which leads to a result very similar to a bi-variate Gram-Charlier series of type-A.

4.2   Method Outline

The starting point for the method presented in this section is the cumulants series expansion of the characteristic function. From this representation, another series is developed which has the coefficients as functions of the cumulants.

Previous attempts by Longett-Higgins [13,14] and by Vinje [24,26] to apply the present method to determine the probability distribution of non-linear stochastic variables resulted basically in the same series representation. However, their methodology to evaluate the coefficients in the resulting series was very cumbersome, i.e. not practical, and could not be automated in a computer program.

In the case of a bi-variate Gaussian distribution, the characteristic function in

terms of the cumulants, is simply:

$$M_g(iv_1, iv_2) = \exp\left[-\frac{K_{20}}{2} v_1^2 - \frac{K_{02}}{2} v_2^2 - K_{11} \sqrt{K_{20} K_{02}}\ v_1\, v_2 \right]. \qquad (4.6)$$

Because we want to relate the joint pdf $f(T, \dot{T})$ of the non-linear tension to the Gaussian distribution, we can rewrite equation (4.5) factoring out the cumulants K_{20} and K_{02} :

$$M(iv_1, iv_2) = \exp\left[-\frac{K_{20}}{2} v_1^2 - \frac{K_{02}}{2} v_2^2 \right] \exp\left[\sum_{p=0}^{\infty} \sum_{q=0}^{\infty} \frac{K_{pq}}{p!\, q!} (iv_1)^p (iv_2)^q \right] \qquad (4.7)$$

where the pairs $(p, q) = (0, 2)\&(2, 0)$ are excluded in the p and q summations above.

Applying the series expansion for the exponential:

$$e^x = \sum_{0}^{\infty} \frac{1}{j!} x^j$$

we get:

$$M(iv_1, iv_2) = \exp\left[-\frac{K_{20}}{2} v_1^2 - \frac{K_{02}}{2} v_2^2 \right] \sum_{j=0}^{\infty} \frac{1}{j!} \left[\sum_{\substack{p=0 \\ (p,q)\, \neq\, (0,2)\&(0,2)}}^{\infty} \sum_{q=0}^{\infty} \frac{K_{pq}}{p!\, q!} (iv_1)^p (iv_2)^q \right]^j.$$

$$(4.8)$$

The expansion of the exponential (j-summation) can be carried out and common

powers $v_1^t \, v_2^s$ grouped such that:

$$M(iv_1, iv_2) = \exp\left[-\frac{K_{20}}{2} v_1^2 - \frac{K_{02}}{2} v_2^2\right] \left[\sum_{t=0}^{\infty} \sum_{s=0}^{\infty} \Psi_{ts} (iv_1)^t (iv_2)^s\right]. \qquad (4.9)$$

Then, performing a Fourier Transform, term by term, in the expression above the joint pdf $f(T, \dot{T})$ can be determined, as suggested in (4.2). The key element in the development is the description of the coefficients Ψ_{ts} in terms of the cumulants. The next steps to be described are:

i - Evaluation of the coefficients Ψ_{ts}.

ii - Integration of equation (4.9) to determine $f(T, \dot{T})$.

4.3 Evaluation of the Coefficients Ψ_{ts}

When performing the series expansion of the exponential in equation (4.8) that results in the equation (4.9) we have:

$$\sum_{t=0}^{\infty} \sum_{s=0}^{\infty} \Psi_{ts} (iv_1)^t (iv_2)^s = \sum_{j=0}^{\infty} \frac{1}{j!} \left[\sum_{\substack{p=0 \\ (p,q) \neq (0,2) \& (0,2)}}^{\infty} \sum_{q=0}^{\infty} \frac{K_{pq}}{p! \, q!} (iv_1)^p (iv_2)^q\right]^j \qquad (4.10)$$

Rewriting in a more convenient way, let:

$$T_j = \frac{1}{j!} \left[\sum_{\substack{p=0 \\ (p,q) \neq (0,2) \& (0,2)}}^{\infty} \sum_{q=0}^{\infty} C_{pq} (iv_1)^p (iv_2)^q\right]^j \quad \text{with} \quad C_{pq} = \frac{K_{pq}}{p! \, q!}. \qquad (4.11)$$

46

Then, according to (4.8):

$$\sum_{j=0}^{\infty} T_j = \sum_{t=0}^{\infty} \sum_{s=0}^{\infty} \Psi_{ts} (iv_1)^t (iv_2)^s . \tag{4.12}$$

To determine the coefficients Ψ_{ts} in terms of the C_{pq}, i.e. the cumulants, common powers $(iv_1)^t (iv_2)^s$ that exist in every term T_j for $j = 1, 2, 3, \ldots$ need to be grouped. The method goes as follows:

STEP 1.

Restrict the j-sum to certain order: m:

$$T_j = \frac{1}{j!} [\sum_{\substack{p=0 \\ (p,q) \neq (0,2) \& (0,2)}}^{m} \sum_{q=0}^{m} C_{pq} (iv_1)^p (iv_2)^q]^j \tag{4.13}$$

STEP 2.

Reorder the coefficients C_{pq} in some new ordering such that the double sum in p and q can be reduced to one:

$$T_j = \frac{1}{j!} [\sum_{k=1}^{(m+1)^2} C_{p_k q_k} (iv_1)^{p_k} (iv_2)^{q_k}]^j \tag{4.14}$$

STEP 3.

To raise the k-sum inside the brackets to the jth-powers one can make use of the

multinomial expansion formula:

$$(x_1 + x_2 + \cdots + x_k)^n = \sum_{\ell} \frac{n!}{r_{\ell_1}! r_{\ell_2}! \ldots r_{\ell_k}!} x_1^{r_{\ell_1}} x_2^{r_{\ell_2}} \ldots x_k^{r_{\ell_k}}$$

where the sum-ℓ is over all possible sets $\{r_\ell\} = \{r_{\ell_1} \ r_{\ell_2} \ \ldots \ r_{\ell_k}\}$ such that $\sum_{i=1}^{k} r_{\ell_i} = n$.

This results in:

$$T_j = \frac{1}{j!} \sum \frac{j!}{r_{\ell_1}! r_{\ell_2}! \ldots r_{\ell_k}!} \prod_{i=1}^{k} C_{p_i q_i} (iv_1)^{p_i r_{\ell_i}} (iv_2)^{q_i r_{\ell_i}} \qquad (4.15)$$

In T_j above, carrying out the product and defining:

$$t \stackrel{\triangle}{=} \sum_{i=1}^{k} p_i \, r_{\ell_i} \quad \text{and} \quad s \stackrel{\triangle}{=} \sum_{i=1}^{k} q_i \, r_{\ell_i}$$

we get the reduced expression for T_j :

$$T_j = \sum_{\ell} \frac{1}{r_{\ell_1}! r_{\ell_2}! \ldots r_{\ell_k}!} \left[\prod_{i=1}^{k} C_{p_i q_i}^{r_{\ell_i}} \right] (iv_1)^t (iv_2)^s \qquad (4.16)$$

Comparing (4.16) above with the equation (4.12) and making $j = 1, 2, \ldots m$

we get the final expression for the coefficients Ψ_{ts}:

$$\Psi_{ts} = \sum_{\ell} \frac{1}{r_{\ell_1}! r_{\ell_2}! \ldots r_{\ell_k}!} \prod_{i=1}^{k} C_{p_i q_i}^{r_{\ell_i}} \qquad (4.17)$$

where the sum is over all possible sets $\{r_{\ell_i}\} = \{r_{\ell_1}, r_{\ell_2}, \ldots, r_{\ell_k}\}$ such that:

- $\sum_{i=1}^{k} r_{\ell_i} = j$ and $j = 1, 2, \ldots (t + s)$, being $k = (m + 1)^2$

with the additional constraints:

- $\sum_{i=1}^{k} p_i\, r_{\ell_i} = t$ - $\sum_{i=1}^{k} q_i\, r_{\ell_i} = s$.

Following these steps, a computer program can be coded to generate automatically the coefficients Ψ_{ts}.

It is structured as follows:

Given a certain order N up to which we want to represent the characteristic function $M(iv_1, iv_2)$:

1. Declare two vectors $\vec{p} = \{\cdots\, p_i\, \cdots\}$ and $\vec{q} = \{\cdots\, q_i\, \cdots\}$ to store the indices of the coefficients C_{pq}. In other words, the elements p_i and q_i are the order of the cumulants. The dimension of these vectors - k is chosen to accommodate all cumulants considered in the $M(iv_1, iv_2)$ series given by the equation (4.5).

2. Determine all possible pairs t, s such that $t + s < N$. This is achieved by an algorithm to evaluate the compositions of N in two elements.

3. For each pair t, s determine all possible l compositions of the integer $j = 1, 2, \ldots, t + s$ into k elements to define the vectors $\vec{r}_\ell = r_{\ell_1}, \ldots, r_{\ell_k}$. The elements of $\vec{r}_\ell$ automatically satisfies $\sum r_{\ell_i} = j$.

49

4. Among all vectors $\vec{r}_\ell$ generated by the composition algorithm save only the ones that satisfy both $\vec{p} \cdot \vec{r}_\ell = t$ and $\vec{q} \cdot \vec{r}_\ell = s$.

5. Collect the products $C_{p_i q_i}^{r \ell_i}$ which, according to the equation (4.17) represent the wanted coefficients Ψ_{ts}.

A typical output of this program for $N = 6$ and $(t, s) = (4, 2)$ would be:

$$
\begin{aligned}
\Psi_{4,2} \;=\; & C_{42} + \frac{1}{2} C_{21}^2 + C_{12} C_{30} + C_{11} C_{31} + C_{10} C_{32} + C_{01} C_{41} + \\[2mm]
& C_{10} C_{11} C_{21} + \frac{1}{2} C_{10}^2 C_{22} + C_{01} C_{11} C_{30} + C_{01} C_{10} C_{31} + \frac{1}{2} C_{01}^2 C_{40} + \\[2mm]
& \frac{1}{4} C_{10}^2 C_{11}^2 + \frac{1}{6} C_{10}^3 C_{12}^2 + \frac{1}{2} C_{01} C_{10}^2 C_{21}^2 + \frac{1}{2} C_{01}^2 C_{10} C_{30} + \\[2mm]
& \frac{1}{6} C_{01} C_{10}^3 C_{11} + \frac{1}{48} C_{01}^2 C_{10}^4 .
\end{aligned}
$$

4.4 The Hermite Polynomials Series for $f(T, \dot{T})$

In the previous section it was shown that the equation (4.9) can express the characteristic function of the joint distribution up to any desired order N.

The joint pdf $f(T, \dot{T})$, is then determined by a two-dimensional Fourier Transform operation on the characteristic function, as shown in the equation (4.2).

This process results in the following integral:

$$
f(T, \dot{T}) = \frac{1}{(2\pi)^2} \sum_{t=0}^{\infty} \sum_{s=0}^{\infty} \Psi_{ts} \int_{-\infty}^{\infty} (iv_1)^t e^{-K_{20} \frac{v_1^2}{2}} e^{-iv_1 T} dv_1 \int_{-\infty}^{\infty} (iv_2)^s e^{-K_{02} \frac{v_2^2}{2}} e^{iv_2 \dot{T}} dv_2
$$

(4.18)

50

In the above, the integrals in the variables v_1 and v_2 can be related to Hermite polynomials $He_n(x)$ generated by [29]:

$$(-1)^n \frac{d^n}{dx^n} \alpha(x) = He_n(x) \, \alpha(x) \quad \text{with} \quad \alpha(x) = \frac{1}{2\pi} e^{-\frac{x^2}{2}} \tag{4.19}$$

Defining:

$$I_t(T) \triangleq \int_{-\infty}^{\infty} (iv_1)^t e^{-K_{20}\frac{v_1^2}{2}} e^{-iv_1 T} dv_1 \quad \text{and} \quad I_s(\dot{T}) \triangleq \int_{-\infty}^{\infty} (iv_1)^s e^{-K_{02}\frac{v_2^2}{2}} e^{-iv_2 \dot{T}} dv_2$$

$$\tag{4.20}$$

the equation for the joint pdf (4.18) can be rewritten as:

$$f(T,\dot{T}) = \frac{1}{(2\pi)^2} \sum_{t=0}^{\infty} \sum_{s=0}^{\infty} \Psi_{ts} I_t(T) I_s(\dot{T}) \tag{4.21}$$

To perform the integrals $I_t(T)$ and $I_s(\dot{T})$ the following change of variables is convenient:

$$x_1 \triangleq \sqrt{K_{20}} \, v_1 \quad \text{and} \quad \overline{T} \triangleq \frac{T}{\sqrt{K_{20}}} \tag{4.22}$$

$$x_2 \triangleq \sqrt{K_{02}} \, v_2 \quad \text{and} \quad \overline{\dot{T}} \triangleq \frac{\dot{T}}{\sqrt{K_{02}}} \tag{4.23}$$

such that:

$$I_t(\overline{T}) = (\frac{1}{K_{20}})^{\frac{t+1}{2}} \int_{-\infty}^{\infty} (ix_1)^t e^{-\frac{x_1^2}{2}} e^{-ix_1 \overline{T}} dx_1$$

and

$$I_s(\overline{\dot{T}}) = \left(\frac{1}{K_{02}}\right)^{\frac{s+1}{2}} \int_{-\infty}^{\infty} (ix_2)^s \, e^{-\frac{x_2^2}{2}} \, e^{-ix_2\overline{\dot{T}}} \, dx_2 \tag{4.24}$$

Knowing that:

$$\int_{-\infty}^{\infty} e^{-\frac{x^2}{2}} \, e^{-ixw} \, dx = \sqrt{2\pi} \, e^{-\frac{w^2}{2}} \tag{4.25}$$

and using the derivative property of Fourier Transforms:

$$\int_{-\infty}^{\infty} (ix)^n \, e^{-\frac{x^2}{2}} \, e^{-ixw} \, dx = \sqrt{2\pi} \, (-1)^n \, \frac{d^n}{dw^n} \, e^{-\frac{w^2}{2}} \tag{4.26}$$

The integrals (4.24), give results for $I_t(\overline{T})$ and $I_s(\overline{\dot{T}})$ as:

$$I_t(\overline{T}) = \left(\frac{1}{K_{20}}\right)^{\frac{t+1}{2}} e^{-\frac{\overline{T}^2}{2}} He_t(\overline{T}) \quad \text{and} \quad I_s(\overline{\dot{T}}) = \left(\frac{1}{K_{02}}\right)^{\frac{s+1}{2}} e^{-\frac{\overline{\dot{T}}^2}{2}} He_s(\overline{\dot{T}}) . \tag{4.27}$$

Substituting the above into the equation (4.21), the final expression for $f(T,\dot{T})$ is

obtained, as a Hermite polynomials series very similar to the Gram-Charlier result:

$$f(T,\dot{T}) = \frac{1}{2\pi} \sum_{t=0}^{\infty} \sum_{s=0}^{\infty} \Psi_{ts} \left(\frac{1}{K_{20}}\right)^{\frac{t+1}{2}} \left(\frac{1}{K_{02}}\right)^{\frac{s+1}{2}} e^{-\frac{\overline{T}^2}{2}} He_t(\overline{T}) \, e^{-\frac{\overline{\dot{T}}^2}{2}} He_s(\overline{\dot{T}}) . \tag{4.28}$$

where $\overline{T}$ and $\overline{\dot{T}}$ are the normalized tension and tension derivative:

$$\overline{T} \triangleq \frac{T}{\sqrt{K_{20}}} \quad \text{and} \quad \overline{\dot{T}} \triangleq \frac{\dot{T}}{\sqrt{K_{02}}} \tag{4.29}$$

This equation can be rewritten in a more convenient form to allow a direct comparison with the Gaussian bi-variate distribution:

$$f(T,\dot{T}) = \frac{1}{2\pi\sqrt{K_{20}K_{02}}} \sum_{t=0}^{\infty} \sum_{s=0}^{\infty} \Psi_{ts}\ e^{-\frac{\overline{T}^2}{2}}\ e^{-\frac{\overline{\dot{T}}^2}{2}}\ \left(\frac{1}{\sqrt{K_{20}}}\right)^t \left(\frac{1}{\sqrt{K_{02}}}\right)^s He_t(\overline{T})\ He_s(\overline{\dot{T}}).$$

(4.30)

4.5 The Number of Crossings at Tension Level T_0

The equation (4.28) or (4.30) can be used with equation (4.1) to determine the expression for $N(T_0)$.

Defining:

$$I_s \triangleq \int_0^{\infty} \overline{\dot{T}}\ e^{-\frac{\overline{\dot{T}}^2}{2}}\ He_s(\overline{\dot{T}})\ d\overline{\dot{T}}$$

(4.31)

and the normalized coefficients $\overline{\Psi}_{ts}$:

$$\overline{\Psi}_{ts} \triangleq \frac{\Psi_{ts}}{\sqrt{K_{20}^t\ K_{02}^s}}$$

(4.32)

Under the present approach, the number of crossings is given by:

$$N(T_0) = \frac{1}{2\pi} \sqrt{\frac{K_{02}}{K_{20}}}\ e^{-\frac{\overline{T}_0^2}{2}} \sum_{t=0}^{\infty} \sum_{s=0}^{\infty} \overline{\Psi}_{ts}\ He_t(\overline{T}_0)\ I_s.$$

(4.33)

where the integrals I_s are constants that can be evaluated using properties of the

Hermite polynomials:

$$
I_s = \begin{cases} 1 & \text{if } s = 0 \\ \sqrt{\frac{\pi}{2}} & \text{if } s = 1 \\ He_{s-2}(0) & \text{if } s \geq 2 \end{cases}
\tag{4.34}
$$

4.6 The Probability of Extremes

Given the number of crossings at certain level T_0 , the probability of having one extreme T , bellow this level can be given by:

$$
P_T(T \leq T_0) = 1 - \frac{N(T_0)}{N(0)}
\tag{4.35}
$$

The probability density function is then:

$$
p_T(T \leq T_0) = -\frac{1}{N(0)} \frac{d}{dT_0} N(T_0)
\tag{4.36}
$$

According to the equation (4.33) we have for the number of zero-crossings:

$$
N(0) = \frac{1}{2\pi} \sqrt{\frac{K_{20}}{K_{02}}} \sum_{t=0}^{\infty} \sum_{s=0}^{\infty} \overline{\Psi}_{ts} \; He_t(0) \; I_s
\tag{4.37}
$$

Also, the derivative $\frac{d}{dT} N(T)$ gives:

$$
\frac{d}{dT} N(T) = -\frac{\sqrt{K_{02}}}{2\pi K_{20}} e^{-\frac{1}{2}\overline{T}^2} \sum_{t=0}^{\infty} \sum_{s=0}^{\infty} \overline{\Psi}_{ts} \; I_s \; He_{t+1}(\overline{T})
\tag{4.38}
$$

Such that, for the probability density function of the extremes:

$$p_T(T \leq T_0) = \frac{1}{\sqrt{K_{20}}} e^{-\frac{1}{2}\overline{T}_0^2} \frac{\sum_{t=0}^{\infty} \sum_{s=0}^{\infty} \overline{\Psi}_{ts} I_s He_{t+1}(\overline{T}_0)}{\sum_{t=0}^{\infty} \sum_{s=0}^{\infty} \overline{\Psi}_{ts} I_s He_t(0)} \qquad (4.39)$$

Restricting the sum in (4.39) above to the order N :

$$p_T(T \leq T_0) = \frac{1}{\sqrt{K_{20}}} e^{-\frac{1}{2}\frac{T_0^2}{K_{20}}} \frac{\sum_{t=0}^{N} \sum_{s=0}^{N} \overline{\Psi}_{ts} I_s He_{t+1}\left(\frac{T_0}{\sqrt{K_{20}}}\right)}{\sum_{t=0}^{N} \sum_{s=0}^{N} \overline{\Psi}_{ts} I_s He_t(0)} \qquad (4.40)$$

Taking into account that $\overline{\Psi}_{00} = 1$, the pdf for the maxima can be rewritten (to order N):

$$p_T(T \leq T_0) = \frac{T_0}{K_{20}} e^{-\frac{1}{2}\frac{T_0^2}{K_{20}}} \left[1 + \frac{\sum_{\substack{t=0 \\ (t,s)\neq(0,0)}}^{N} \sum_{\substack{s=0}}^{N} \overline{\Psi}_{ts} I_s He_{t+1}\left(\frac{T_0}{\sqrt{K_{20}}}\right)}{\sum_{\substack{t=0 \\ (t,s)\neq(0,0)}}^{N} \sum_{\substack{s=0}}^{N} \overline{\Psi}_{ts} I_s He_t(0)} \right] \qquad (4.41)$$

In the above the multiplying factor outside the brackets:

$$\frac{T_0}{K_{20}} e^{-\frac{1}{2}\frac{T_0^2}{K_{20}}}$$

is recognized as the Rayleigh pdf, obtained in the linear analysis of extremes (section

3.2). Therefore, the non-linear statistics of extremes under the Gram-Charlier series

approach, shows how much the pdf for the maxima departs from the linear results,

55

with this amount given by term inside the brackets in equation (4.41).

4.7 Numerical Results

In this section numerical results for extreme tensions determined by the Gram-Charlier approach are presented.

The input to these calculations are the cable elongations which are determined by the equivalent linearization of the twelve degrees of freedom dynamic problem, as outlined in Chapter 2. The ships are the Tug ARS50 and the Frigate PAGE with main characteristics given in Table 3.1. The towing speed is 3 knots and the wind speed is 30 knots.

The two cases presented in this section differ by the towline connecting the ships. In Case I the hawser is the same studied under the linear theory of extremes (section 3.3); it represents a relatively short wire hawser, but in the usual length range applied during actual tow operations. In Case II the hawser is longer and heavier, therefore "softer" than the previous one, which causes less restriction to the ships' motions and thus giving larger cable elongations.

		HAWSER I	HAWSER II
Diameter	(in)	2.0	2.25
Length	(ft)	1200	1800
Weight	(lbs/ft)	6.0	3.4
Static Tension	(kips)	20.0	20.0

Table 4.1: Characteristics of Hawser I and Hawser II

The numerical calculations consist in:

- The joint moments of the tension and its time derivative are evaluated using either the polynomial tension representation or a random input simulation with the cable dynamics program;

- Once the moments are evaluated, the joint cumulants are obtained through a computer coded look-up table, as given in David, Kendall and Barton [23];

- The procedure outlined in section 4.3 is then applied to the evaluation of the coefficients Ψ_{ts} and the probability density function for the extremes, $p_T(T \leq T_{ext})$, is determined according to (4.41);

- The extreme tension, T_{ext}, which is the tension level that has a probability of 0.1% of being exceeded in 24 hours ($\alpha = 0.001$ and $\Delta t = 24$ hs), is then calculated using the above pdf, with the same numerical method described in section 3.3 for the linear analysis.

4.7.1 Results for Hawser I

To order $N = 6$, the moments are evaluated for $(m, n) = \{0, \cdots 6\}$ and $(m + n) \leq 6$. The resulting matrix, obtained from a 30.0 minutes long random

input simulation with the cable dynamics program is:

$$
\mathcal{M}_{nm} =
\begin{bmatrix}
\cdots & 0.025 & 5.81E+02 & 6.36E+03 & 1.10E+07 & 1.47E+09 & 8.56E+11 \\
4.87 & 0.95 & 4.23E+03 & -2.57E+05 & -7.91E+07 & -1.71E+10 & \cdots \\
6.42E+02 & 1.56E+01 & 4.23E+05 & -3.37E+06 & 2.33E+09 & \cdots & \cdots \\
3.12E+04 & 1.43E+03 & 0.23E+07 & -3.37E+08 & \cdots & \cdots & \cdots \\
2.53E+06 & 9.61E+04 & 1.77E+09 & \cdots & \cdots & \cdots & \cdots \\
2.11E+08 & 8.93E+06 & \cdots & \cdots & \cdots & \cdots & \cdots \\
1.96E+10 & \cdots & \cdots & \cdots & \cdots & \cdots & \cdots
\end{bmatrix}
$$

The cumulants matrix obtained by the "computerized" look-up table is:

$$
K_{nm} =
\begin{bmatrix}
0.0 & 2.47E-02 & 5.82E+02 & 6.32E+03 & 9.96E+06 & 1.43E+09 & 7.65E+11 \\
4.87 & 8.27E-01 & 1.40E+03 & -2.89E+05 & -1.37E+08 & -2.27E+10 & \cdots \\
6.17E+03 & -8.21 & 3.58E+04 & -4.68E+06 & -3.56E+09 & \cdots & \cdots \\
2.21E+04 & -8.14E+02 & 1.67E+06 & 8.73E+07 & \cdots & \cdots & \cdots \\
8.64E+05 & -2.22E+04 & -5.03E+07 & \cdots & \cdots & \cdots & \cdots \\
1.92E+07 & 1.60E+06 & \cdots & \cdots & \cdots & \cdots & \cdots \\
-2.15E+09 & \cdots & \cdots & \cdots & \cdots & \cdots & \cdots
\end{bmatrix}
$$

The matrix of the coefficients Ψ_{ts} for the pdf series representation (to order 6):

$$
\Psi_{ts} =
\begin{bmatrix}
1.00 & 2.47E-02 & 6.10E-04 & 1.05E+03 & 4.15E+05 & 1.19E+07 & 1.06E+09 \\
4.87 & 9.48E-01 & 6.99E+02 & -4.31E+04 & -3.70E+06 & -1.30E+08 & \cdots \\
11.86 & 2.15E-01 & 1.24E+04 & -5.96E+05 & -9.17E+07 & \cdots & \cdots \\
3.70E+03 & -54.41 & 1.91E+05 & 3.88E+06 & \cdots & \cdots & \cdots \\
5.39E+04 & 2.76E+03 & 2.33E+06 & \cdots & \cdots & \cdots & \cdots \\
3.79E+05 & 4.60E+04 & \cdots & \cdots & \cdots & \cdots & \cdots \\
5.07E+06 & \cdots & \cdots & \cdots & \cdots & \cdots & \cdots
\end{bmatrix}
$$

For the shorter hawser, the resultant extreme tension, T_{ext}, is:

$$T_{ext_{GC}} = 173.0 \text{ kips}$$

In Figure 4.1 the Gram-Charlier pdf for the extreme tension with $N=6$ is shown together with the linear one (Figure 3.1) for comparison. It can be seen they are far apart, explaining the different values obtained for the extreme tension: 84.5 kips in the linear analysis and 173.0 kips here.

Figure 4.2 shows the same curves in a log-scale such that the behavior of the these pdf's for larger tensions can be observed.
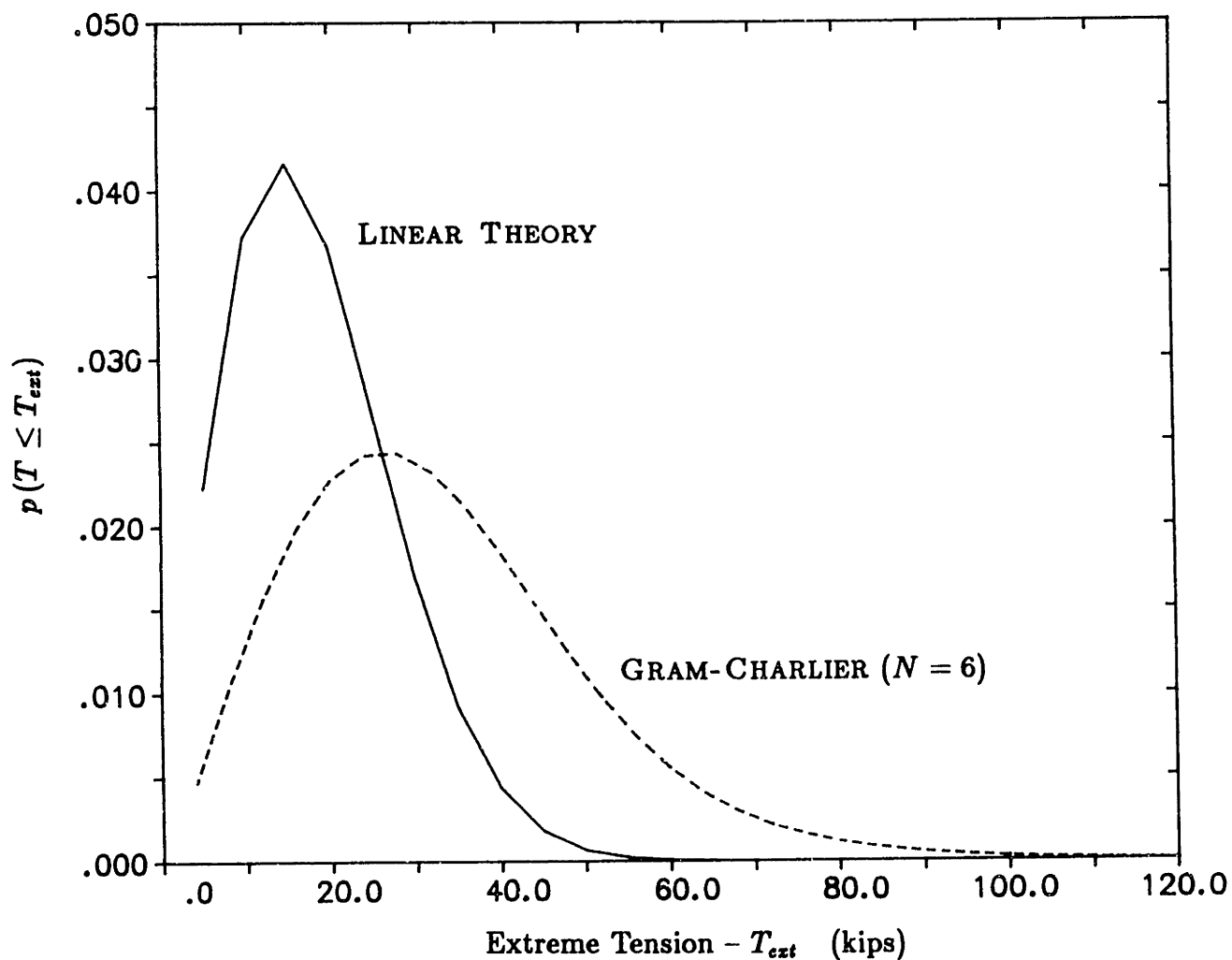
Figure 4.1: HAWSER I - Probability Density Functions
Gram-Charlier Series ($N = 6$) and Linear Analysis
ARS-50 Towing Frigate PAGE at 3 knots
Wind Speed: 30 knots.
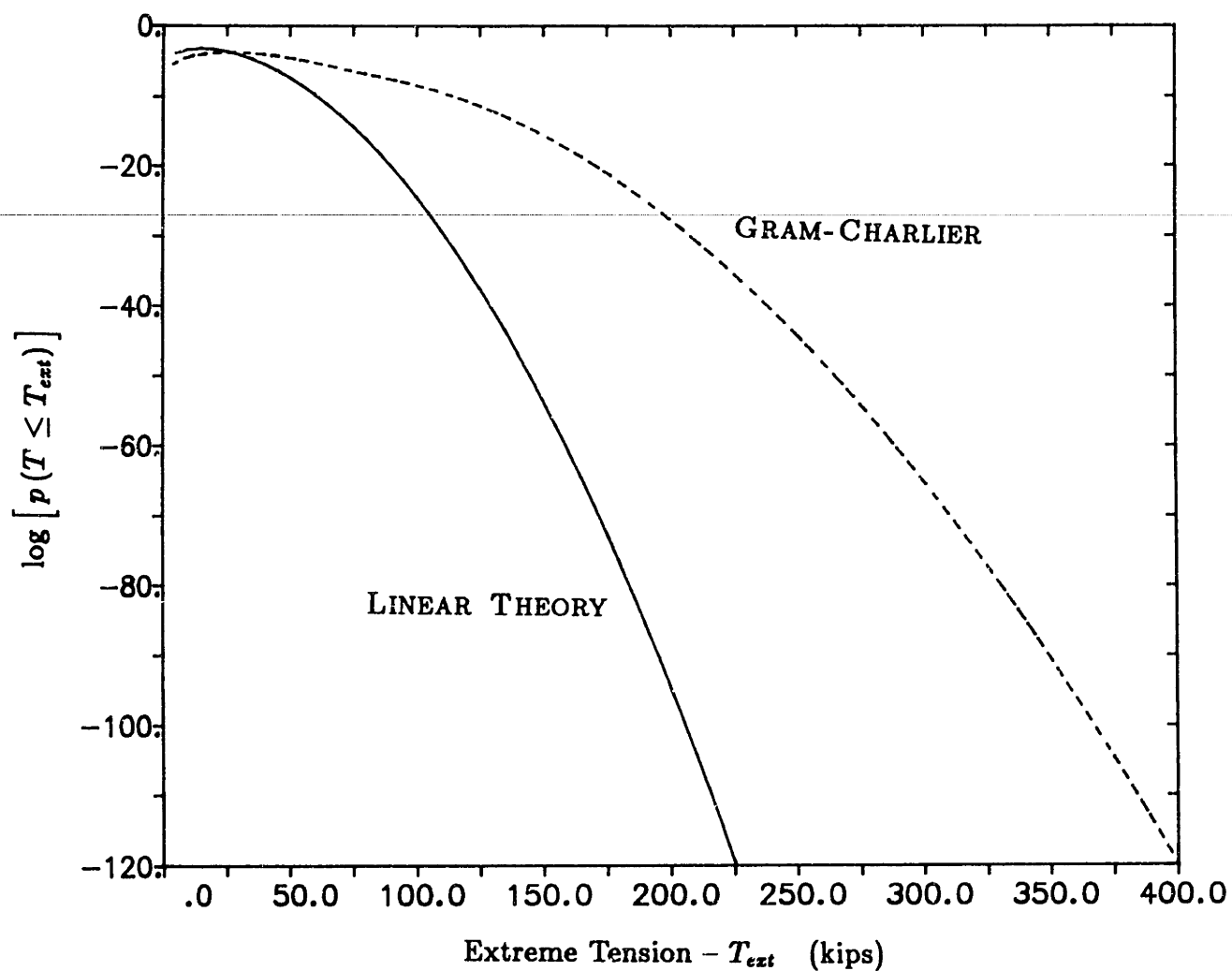
Figure 4.2: HAWSER I - Probability Density Functions
Gram-Charlier Series $(N = 6)$ and Linear Analysis
ARS-50 Towing Frigate PAGE at 3 knots
Wind Speed: 30 knots.

4.7.2 Results for Hawser II

In this case the joint moments of the tensions and its derivative, $\mathcal{M}_{nm}$, are determined from the coefficients of the tension polynomial approximation, equation (2.1), which for HAWSER II are:

$$a_{10} = 249.55 \quad a_{20} = -0.738 \quad a_{30} = -0.591$$

$$a_{01} = 1064.71 \quad a_{02} = 59.24 \quad a_{03} = 2.49$$

$$a_{11} = 59.43 \quad a_{21} = 3.07 \quad a_{12} = 6.47$$

where these coefficients have proper dimensions considering the units for tension in *lbs*, elongation in *ft* and elongation time derivative in *ft/sec*.

The cable elongation spectral moments, resulting from the solution of the equations of motion, are:

$$m_{0_x} = 24.726 \text{ ft}^2 \qquad m_{2_x} = 11.090 \text{ ft}^2/\text{sec}^2 \qquad m_{4_x} = 5.804 \text{ ft}^2/\text{sec}^4$$

Once the elongation spectral moments are determined and the polynomial tension model is known, a computer program evaluates the joint moments for the

tension and its derivative. The resulting moments matrix is (to order $N = 6$):

$$
M_{nm} = \begin{bmatrix}
\cdots & 0.00 & 1.56E+01 & -3.05E+01 & 9.85E+02 & -5.87E+03 & 1.09E+05 \\
3.05E\text{-}01 & 1.91E\text{-}21 & 3.54E+01 & -5.23E+01 & 3.72E+03 & -1.36E+04 & \cdots \\
2.86E+01 & 2.13E\text{-}15 & 5.78E+02 & -1.09E+03 & 4.18E+04 & \cdots & \cdots \\
1.05E+02 & 6.23E\text{-}14 & 4.84E+03 & -5.48E+03 & \cdots & \cdots & \cdots \\
2.94E+03 & 8.24E\text{-}13 & 7.26E+04 & \cdots & \cdots & \cdots & \cdots \\
2.90E+04 & 2.19E\text{-}11 & \cdots & \cdots & \cdots & \cdots & \cdots \\
5.89E+05 & \cdots & \cdots & \cdots & \cdots & \cdots & \cdots
\end{bmatrix}
$$

The look-up table program evaluates the cumulants matrix from these moments:

$$
K_{nm} = \begin{bmatrix}
0.00 & 0.00 & 1.56E+01 & -3.05E+01 & 2.58E+02 & -1.13E+03 & -1.77E+04 \\
3.05E\text{-}01 & 1.91E\text{-}21 & 3.07E+01 & -4.30E+01 & 5.57E+02 & 4.19E+03 & \cdots \\
2.85E+05 & 2.13E\text{-}15 & 1.14E+02 & -1.95E+02 & -4.74E+03 & \cdots & \cdots \\
7.87E+01 & 6.03E\text{-}14 & 4.78E+02 & 1.58E+03 & \cdots & \cdots & \cdots \\
3.95E+02 & 3.85E\text{-}13 & -6.24E+03 & \cdots & \cdots & \cdots & \cdots \\
2.15E+03 & 1.87E\text{-}12 & \cdots & \cdots & \cdots & \cdots & \cdots \\
-3.79E+04 & \cdots & \cdots & \cdots & \cdots & \cdots & \cdots
\end{bmatrix}
$$

Finally, the matrix of the coefficients Ψ_{ts} for the Gram-Charlier Series is obtained according to the procedure outlined in Section 4.3.

$$
\Psi_{ts} = \begin{bmatrix}
1.00 & 0.00 & 0.00 & -5.08 & 1.08E+01 & -9.41 & 1.28 \\
3.05E\text{-}01 & 1.91E\text{-}21 & 1.53E+01 & -8.71 & 2.65E+01 & -4.59E+01 & \cdots \\
4.64E\text{-}02 & 1.07E\text{-}15 & 3.32E+01 & -1.89E+0 & 1.45E+02 & \cdots & \cdots \\
1.31E+01 & 1.04E\text{-}14 & 4.86E+01 & -2.82E+01 & \cdots & \cdots & \cdots \\
2.04E+01 & 1.92E\text{-}14 & 8.47E+01 & \cdots & \cdots & \cdots & \cdots \\
2.36E+01 & 3.49E\text{-}14\cdots & \cdots & \cdots & \cdots & \cdots & \cdots \\
3.97E+01 & \cdots & \cdots & \cdots & \cdots & \cdots & \cdots
\end{bmatrix}
$$

In the present case, the extreme tension, T_{ext}, determined by the Gram-Charlier series is:

$$T_{ext_{GC}} = 55.0 \text{ kips}$$

while the linear analysis procedure gives:

$$T_{ext_L} = 44.2 \text{ kips}$$

In Figure 4.3 both extreme tension pdf's are shown in a log-scale plot. The Gram-Charlier pdf is for $N=6$ and the linear one is a Rayleigh pdf given by equation (3.9) with $m_{0_T} = 18.76 \text{ lbs}^2$.
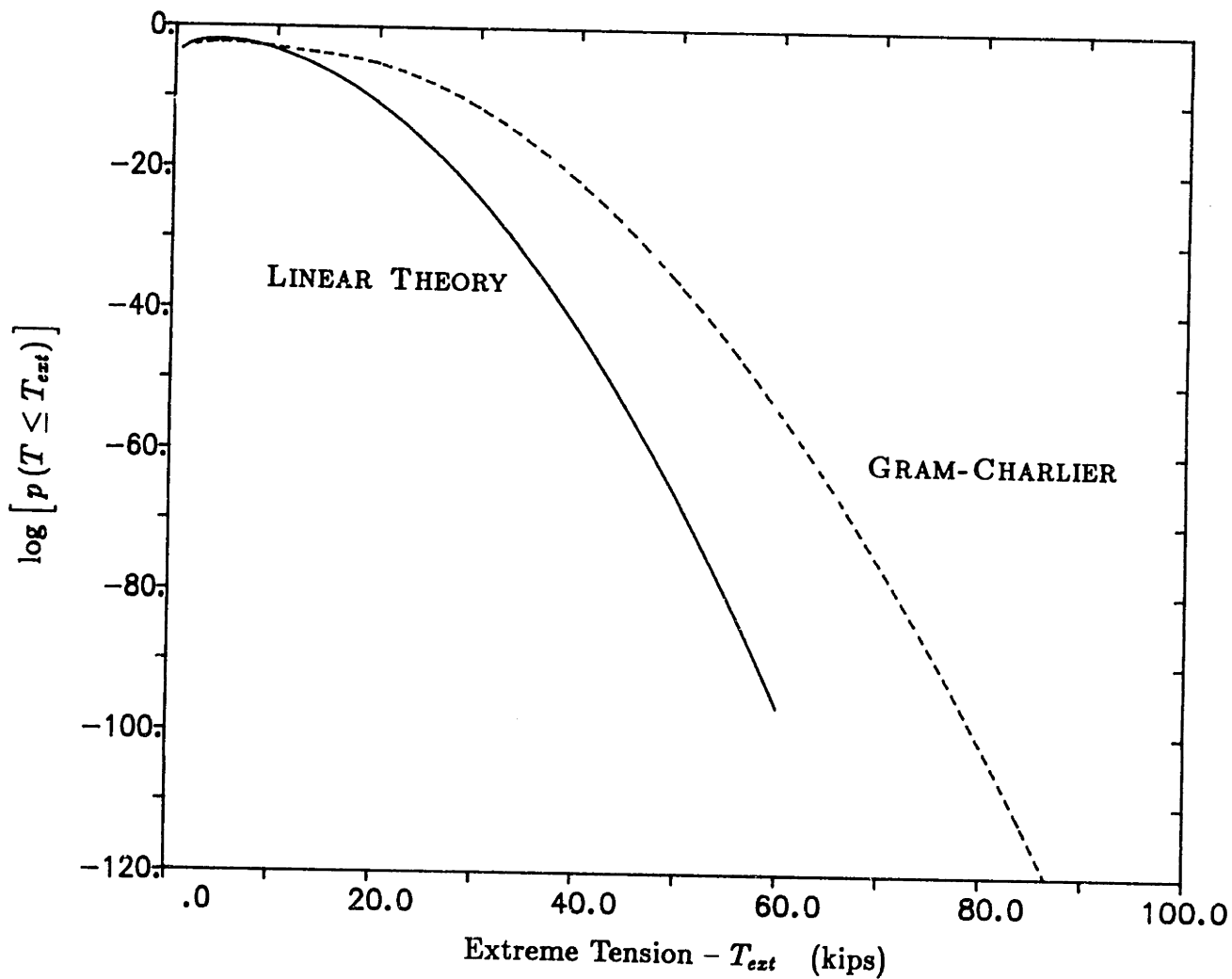
Figure 4.3: HAWSER II - Probability Density Functions
Gram-Charlier Series $(N = 6)$ and Linear Analysis
ARS-50 Towing Frigate PAGE at 3 knots
Wind Speed: 30 knots.

4.7.3   Comments on Gram-Charlier Extremes

The table 4.2 summarizes the results obtained thus far for hawsers I and II. The extreme tensions designated as "linear," are determined by the linear statistical theory (Chapter 3), where the hawser is approximated by the equivalent linearized coefficients. The ones designated as "Gram-Charlier" are determined according to the procedures introduced in this chapter. Also included in the table are the extreme values for the cable elongation, which are the result of the linear extreme statistics applied to the elongation spectra.

To be able to analyze the effectiveness of the present method, these results are marked on the static tension curves (tension $\times$ change in span) for Hawsers I and II, Figures 4.4 and 4.5, respectively. The zero span in these curves represent the static configurations of the hawsers, i.e. the span for the static tension of 20 kips.

The fourth entry in table 4.2, labeled "static," is the tension value obtained from the static curves with the change in span caused by the extreme elongations.

		HAWSER I	HAWSER II
Linear T_{ext_L}	(kips)	84.5	44.2
Gram-Charlier $T_{ext_{GC}}$	(kips)	173.0	55.0
Elongation x_{ext}	(ft)	24.82	28.22
Static $T_{ext_{St}}$	(kips)	$\sim 280.$	$\sim 36.$

Table 4.2: Extreme Values for Hawser I and Hawser II

The "static" extreme tension, $T_{ext_{St}}$, can be interpreted as a physical measure for the accuracy of the extreme tension calculations. This is so, because when the

span changes, to accommodate the cable's extreme elongation, the tension should increase <u>at least</u> the amount given by the static curve. Any other effect that would contribute to the tension build up, like the dynamics of the hawser motion, would add to this minimum extreme tension value.

For the Hawser II, the extreme tension results seem reasonable under this consideration. The Gram-Charlier series gives a slightly higher extreme tension compared to the linear analysis result, and both methods retrieve some dynamic effects (of the hawser motion) in the extreme tension since they are larger than the "static" extreme value (see Figure 4.5).

For Hawser I this does not happen. Although the extreme determined with the Gram-Charlier series represents a large improvement over the linear analysis result, it is still too small when compared with the "static" extreme tension (see Figure 4.4).

According to equation (4.41), the first term in the Gram-Charlier series represents the Rayleigh probability density function, which is the resultant pdf for the extremes in the linear statistical theory. All the other terms in the series can be reduced to a single factor that modifies this linear result in order to conform the pdf with the non-linearities inherent to the process being analyzed, which are embedded in the moments.

Figure 4.6 presents two probability density functions. The first one is the multiplying factor outside the brackets in equation (4.41), which is the Rayleigh pdf
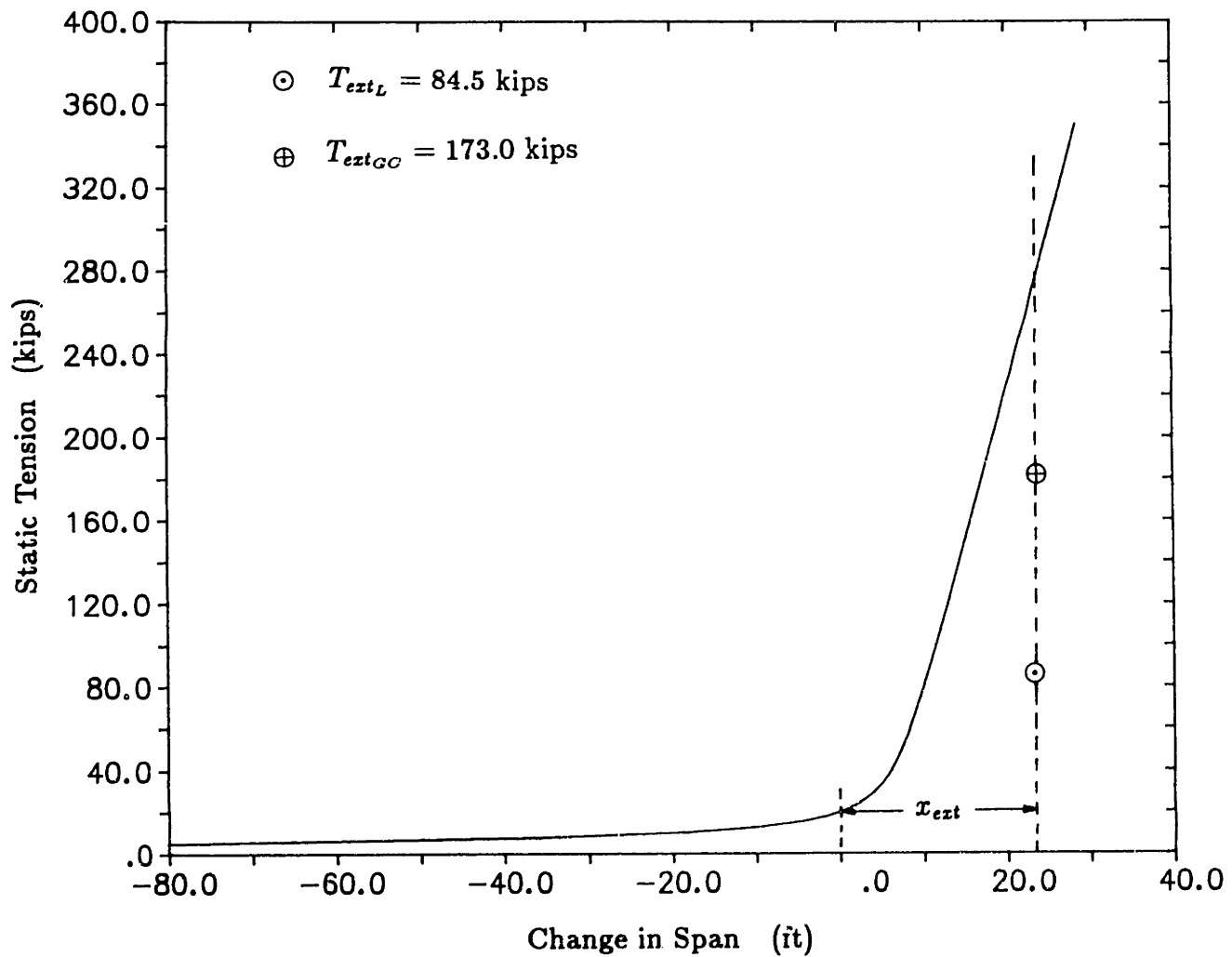
Figure 4.4: Hawser I Static Curve - Tension × Change in Span
Extreme Tension Predictions
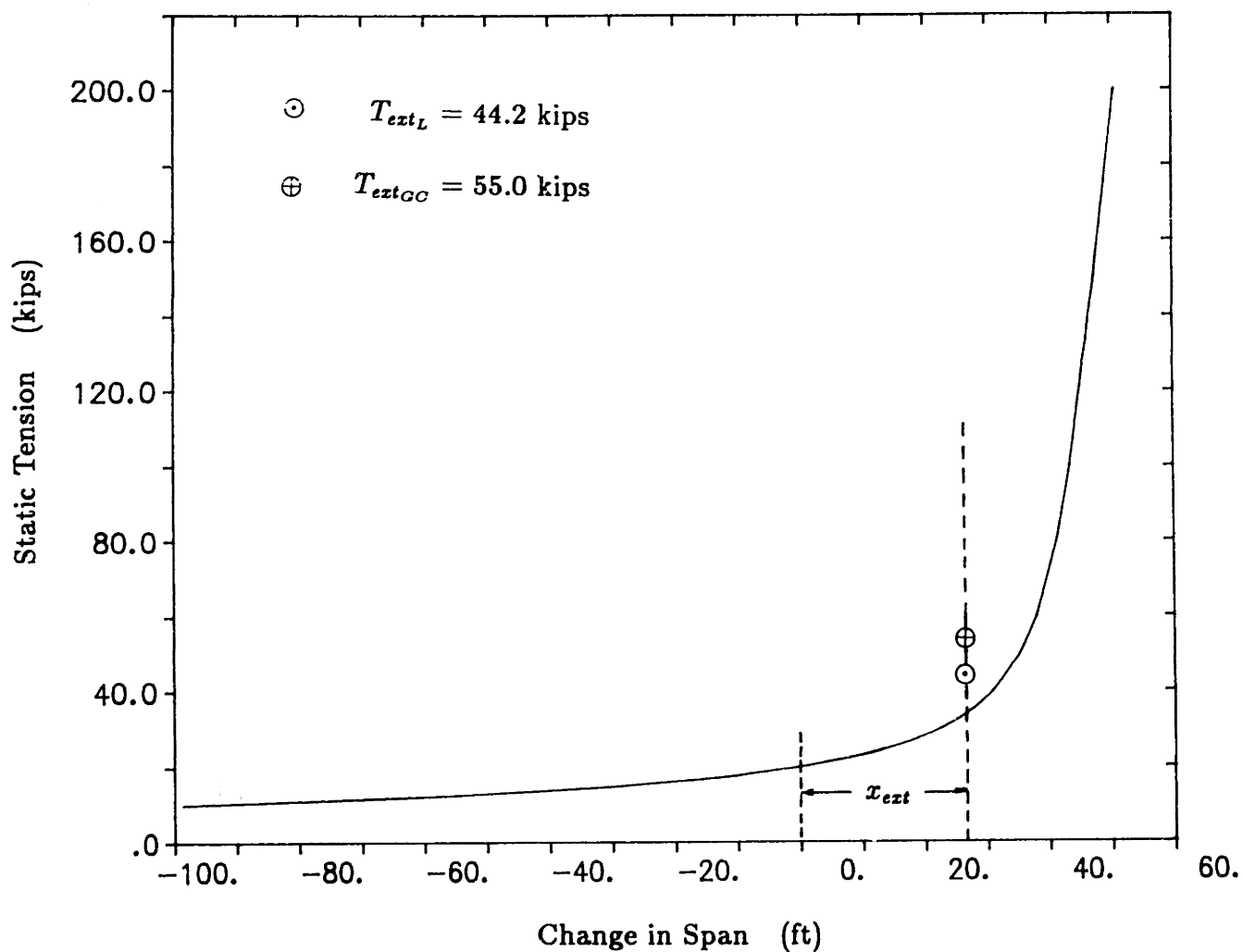
Figure 4.5: Hawser II Static Curve - Tension × Change in Span
Extreme Tension Predictions

with $m_{0_T} = \mathcal{M}_{20}$, i.e. the Gram-Charlier series with $N = 0$. The second one is the complete Gram-Charlier series to order $N = 6$. As shown in this Figure, the effect of all additional terms on the first one is the small shift to right. These terms skew the Rayleigh pdf but not largely enough to account for the severe non-linearity presented by this hawser static curve.

The static curve of wire hawsers present a very strong non-linear behavior. In general, these curves show two dominant slopes. In the small slope region, large changes in span cause small changes in the tension; in this case the static tension increases to accommodate the geometric changes on the hawser catenary configuration. In the steep slope region, small changes in span produce large increases in tension; which happens because the catenary configuration is already very shallow, and any increase in span is accommodated by the stretching of the cable.

The fact that the Gram-Charlier Series represents well the probability structure of slightly non-linear random variables is well established in the literature [16,10,13,24,26]. This conclusion is reinforced by the results obtained thus far. In the case of Hawser II, the extreme elongation is such that it does not go very far in the high slope (stretching) region of the static curve, therefore the results obtained are reasonable. For Hawser I the same does not happen. The extreme elongation goes well into this stretching region and the predicted extreme tensions are not accurate enough.
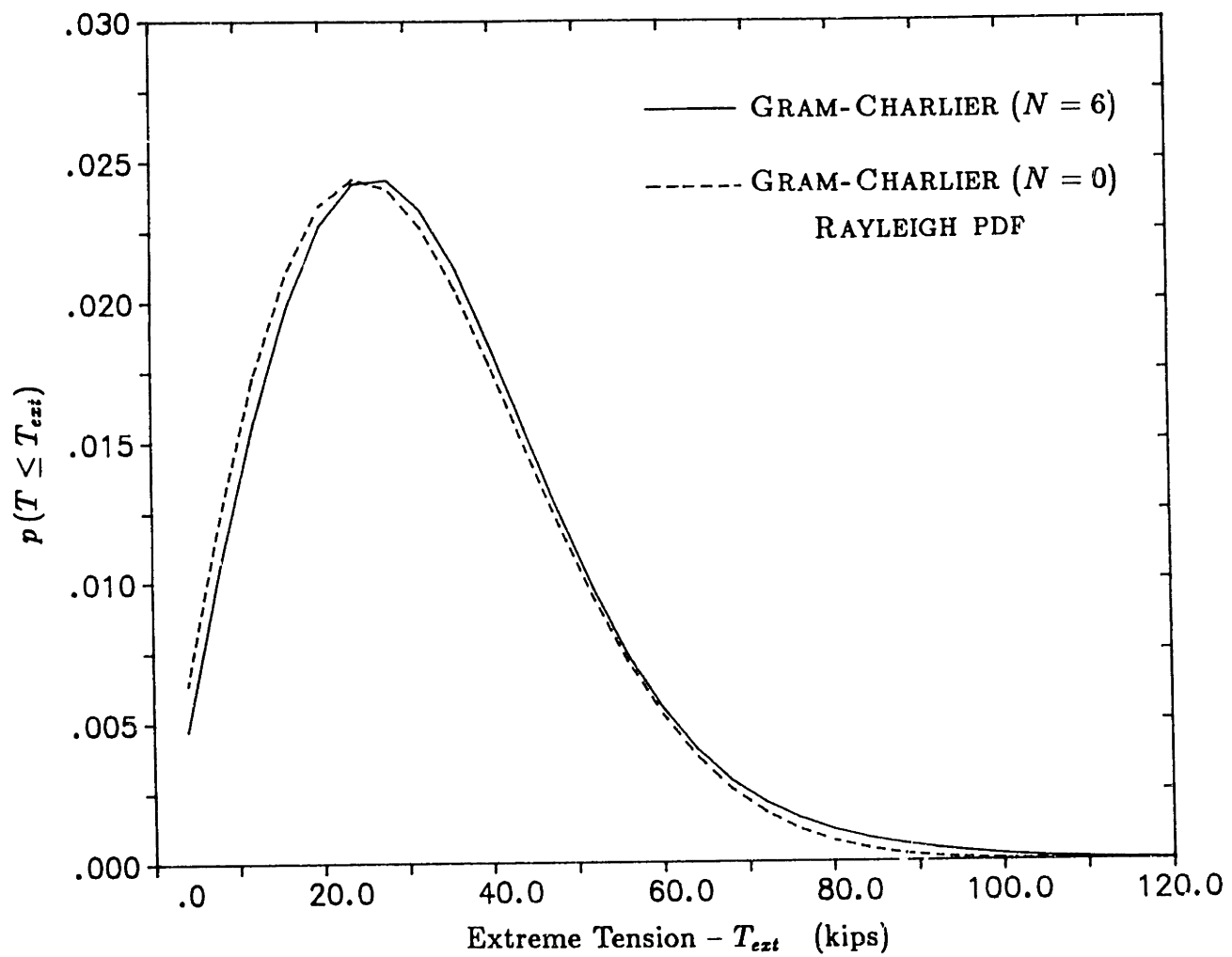
Figure 4.6: HAWSER I - Gram Charlier Series pdf
$N=0$ and $N=6$

Even with the automated method to evaluate the coefficients of the series, it is not practical to consider very large order series. It is worth noting that increasing the order of the series does not guarantee a better representation of the statistical properties of the non-linear tension. As pointed out by Wallace [30], the convergence property of the Gram-Charlier series means that for a sufficiently large N the addition of one more term to the series will improve the approximation. However this is not necessarily true for small N as considered here. In this case, only the first few terms can be improvements. This fact was confirmed in the course of extreme tension calculations for several different hawsers. In some instances, the Gram-Charlier series with $N = 3$ was reasonable, but when higher order series $N = 4, 5, 6$ were considered the resulting pdf presented negative probabilities in the tail region, therefore being inconsistent.

The main conclusion of this chapter is the fact, leaving all possible dynamic effects aside, the relationship between static tension and change in span (cable elongation) represents a very strong non-linearity, which in some cases is too non-linear to be practically analyzed under the Gram-Charlier series approach. Although the joint moments of the tension and its time derivative bring this static curve non-linearity into the analysis, when the extreme elongation is large enough to go into the steep slope region of the static curve, the Gram-Charlier series either does not converge with a reasonable number of terms or it is not able to represent well the probability structure of such hawsers, thus underestimating the extreme tensions.

Chapter 5

Direct Integration Approach

5.1 Method Outline

In this chapter a second method to evaluate the number of crossings of certain level T_0 is developed. This method proved more appropriate for the predictions of extreme towline tension.

It consists of performing the integration for $N(T_0)$ directly, using the concepts of calculus of expectations.

For the frequency of crossings, as in (4.1) we have:

$$N(T_0) = \int_0^\infty \dot{T}\, f(T_0, \dot{T})\, d\dot{T} \tag{5.1}$$

This integral can be interpreted as an expectation operation. For this purpose,

the following singularity functions are used:

− the delta function:

$$\delta(t) = \begin{cases} 1 & \text{if } t = 0 \\ 0 & \text{if otherwise.} \end{cases} \tag{5.2}$$

− the unit step function:

$$u(t) = \begin{cases} 1 & \text{if } t \geq 0 \\ 0 & \text{if } t < 0 \end{cases} \tag{5.3}$$

Equation (4.1) can be rewritten as:

$$N(T_0) = \int_{-\infty}^{\infty} \int_{-\infty}^{\infty} \dot{T} \, u(\dot{T}) \, \delta(T_0 - T) \, f(T, \dot{T}) \, dT \, d\dot{T} \tag{5.4}$$

In the equation above $N(T_0)$ is an expectation. It represents the expected value of the function $g(T, \dot{T}) = \dot{T} \, u(\dot{T}) \, \delta(T_0 - T)$, i.e.:

$$N(T_0) = E\left[\dot{T} \, u(\dot{T}) \, \delta(T_0 - T)\right]. \tag{5.5}$$

The tension on the cable is directly related to the extension at the ends, which has a known probability distribution. Therefore, the above integral can then be evaluated in the extension domain instead of in the $(T, \dot{T})$–plane as the equation (5.4) suggests.

Assuming the tension to be a function of the extension and extension rate of change at the ends of the hawser, the time derivative of the tension would also be

dependent on the extension second time derivative (extension "acceleration"), i.e.:

$$T = T(x, \dot{x}) \quad \text{and} \quad \dot{T} = \dot{T}(x, \dot{x}, \ddot{x})$$

Using these relationships in (5.4), the resulting expression for the number of crossings is:

$$N(T_0) = \int_{-\infty}^{\infty} \int_{-\infty}^{\infty} \dot{T}(x, \dot{x}, \ddot{x}) \, u\big(\dot{T}(x, \dot{x}, \ddot{x})\big) \, \delta\big(T_0 - T(x, \dot{x}, \ddot{x})\big)$$
$$f\big(T(x, \dot{x}, \ddot{x}), \, \dot{T}(x, \dot{x}, \ddot{x})\big) dT \, d\dot{T} \qquad (5.6)$$

which can be carried out in the $(x, \dot{x}, \ddot{x})$ domain as:

$$N(T_0) = \int_{-\infty}^{\infty} \int_{-\infty}^{\infty} \int_{-\infty}^{\infty} \dot{T}(x, \dot{x}, \ddot{x}) \, u(\dot{T}(x, \dot{x}, \ddot{x})) \, \delta(T_0 - T(x, \dot{x}, \ddot{x})) \, p(x, \dot{x}, \ddot{x}) \, dx \, d\dot{x} \, d\ddot{x}$$

$$(5.7)$$

In this work, $p(x, \dot{x}, \ddot{x})$ is the joint Gaussian pdf of the cable's end point elongation and its derivatives, given by:

$$p(x, \dot{x}, \ddot{x}) = \frac{1}{(2\pi)^{\frac{3}{2}} \sqrt{m_{2x} \Delta}} \exp\left[-\frac{1}{2\Delta}(m_{4x} \, x^2 + \frac{\Delta}{m_{2x}} \dot{x}^2 + m_{0x} \, \ddot{x}^2 + 2\, m_{2x} \, x\ddot{x})\right] \quad (5.8)$$

with $\Delta = m_{0x} m_{4x} - m_{2x}^2$

and m_{0x}, m_{2x}, m_{4x} are respectively the expected values $E[x^2]$, $E[\dot{x}^2]$, $E[\ddot{x}^2]$.

In the next sections the following steps are described:

i - The tension end-motion relationship

ii - The transformation of the $N(T_0)$ integral to the "extensions" domain

iii - The scheme for numerical integration.

5.2   The Tension-Extension Relationship

The main idea behind the present approach is to assume that the tension end-motion relationship is known.

As discussed in the Appendix A and section 2.2, through time simulations of the cable non-linear dynamic equations, it is found that the cable dynamic tension can be well represented by a third order polynomial in the cable's end-point elongation and elongation rate of change. Thus, according to equation (2.1) the following model for the dynamic cable tension is adopted:

$$T(x, \dot{x}) = \sum_{m=0}^{3} \sum_{n=0}^{3} a_{mn} \, x^m \, \dot{x}^n \tag{5.9}$$

Taking the time derivative, we obtain for $\dot{T}$:

$$\dot{T}(x, \dot{x}, \ddot{x}) = \sum_{m=0}^{3} \sum_{n=0}^{3} a_{mn} \left(m \, x^{m-1} \, \dot{x}^{n+1} + n \, x^m \, \dot{x}^{n-1} \, \ddot{x} \right) \tag{5.10}$$

where, x , $\dot{x}$, $\ddot{x}$ are respectively, the elongation, the elongation velocity and the elongation acceleration at the cable's end.

5.2.1   The Constant Tension Curves

Performing the integrals in the equation (5.6) will be facilitaded by defining curves $T(x, \dot{x}) = T_0$ (a constant), in the $(x, \dot{x})$ –plane, with $T(x, \dot{x})$ given by the polynomial model in equation (5.9).

To determine these curves, a new function $G(x, \dot{x})$ is introduced:

$$G(x, \dot{x}) = T(x, \dot{x}) - T_0 \qquad (5.11)$$

$G(x, \dot{x}) = 0$ represents the constant tension curve $T(x, \dot{x}) = T_0$.

Defining the unit vectors $\vec{i}, \vec{j}, \vec{k}$ along the coordinates $x, \dot{x}, T$ respectively, the tangent vector to the curves $T(x, \dot{x}) = T_0$ is given by:

$$\vec{t} = \vec{k} \times \frac{\vec{\nabla} G}{|\vec{\nabla} G|} \qquad (5.12)$$

Therefore, solving $G(x, \dot{x}) = 0$ numerically, at least one point in the curve $T = T_0$ can be determined. Knowing the direction of the tangent $\vec{t}$ given by (5.12) the next point on the curve can be inferred, such that these curves are determined for each tension level T_0, as shown in figure 5.1 for Hawser I.
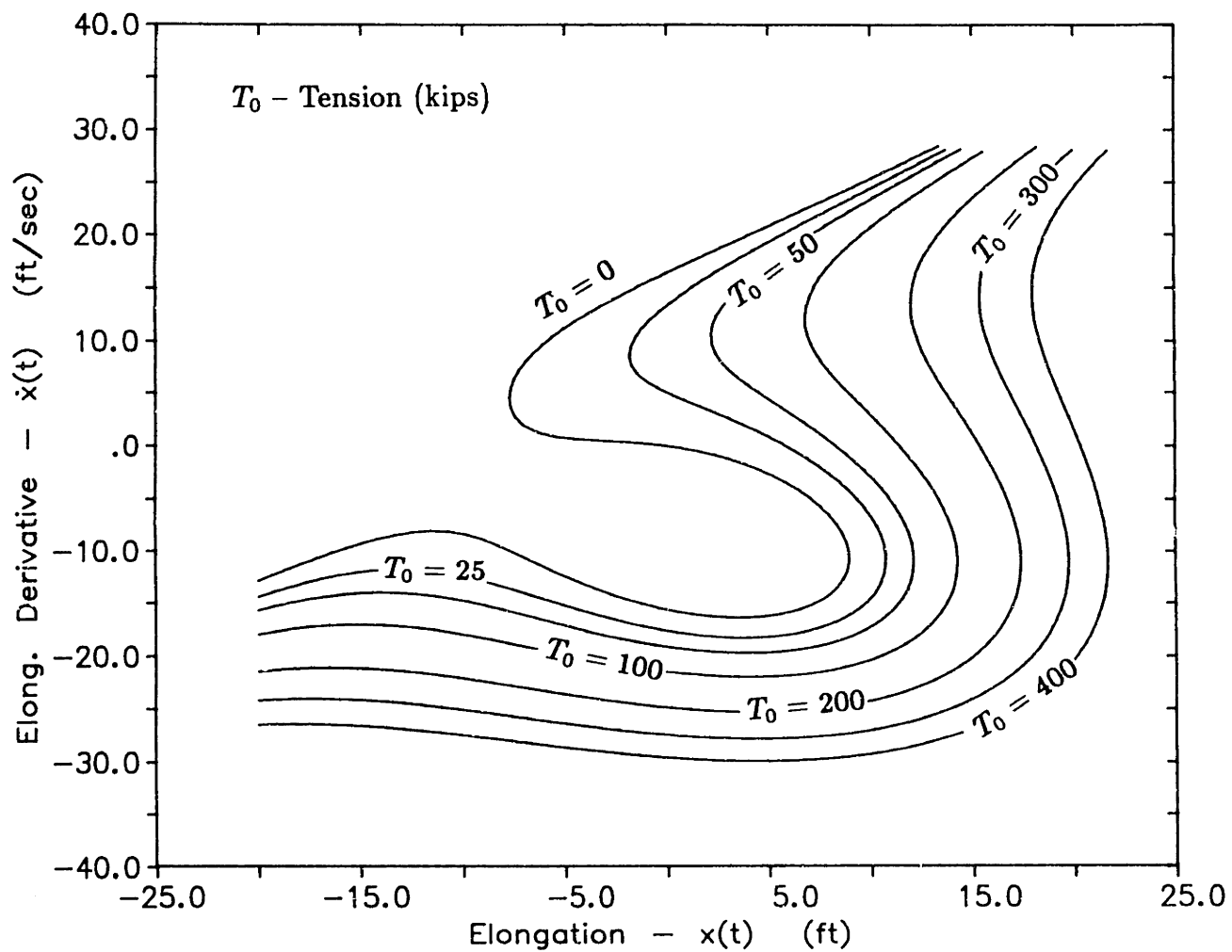
Figure 5.1: Constant Tension Curves for Hawser I
Hawser Length: 1200 ft – Diameter: 2 in.

5.3 The evaluation of $N(T_0)$

Once the model for the tension is established, as given by (5.9), the integral for the number of crossings, equation (5.6), can be evaluated.

According to the equation (5.6) the number of crossings $N(T_0)$ can be interpreted as:

$$N(T_0) = E\left[\dot{T}(x,\dot{x},\ddot{x})\; u\!\left(\dot{T}(x,\dot{x},\ddot{x})\right)\; \delta\!\left(T_0 - T(x,\dot{x},\ddot{x})\right)\right] \tag{5.13}$$

Considering equation (5.7), and the tension mathematical model (shown in Appendix A and described in section 5.2) which gives T as a function of x and $\dot{x}$ (not $\ddot{x}$) only:

$$N(T_0) = \int_{-\infty}^{\infty}\int_{-\infty}^{\infty}\int_{-\infty}^{\infty} \dot{T}(x,\dot{x},\ddot{x})\; u(\dot{T}(x,\dot{x},\ddot{x}))\; \delta(T_0 - T(x,\dot{x}))\; p(x,\dot{x},\ddot{x})\; dx\; d\dot{x}\; d\ddot{x}$$

$$\tag{5.14}$$

5.3.1 The Integration Scheme

In equation (5.14) the effect of the delta function is to preserve only the points $(x_0, \dot{x}_0)$ in the $(x, \dot{x})$ plane for which $T(x, \dot{x}) = T_0$, i.e. the points on the constant tension curves.

For a prescribed T_0, the integrand in equation (5.14) is zero in the $(x, \dot{x})$-plane, except along the constant tension curve for that value of T_0. Thus the $x, \dot{x}$

integration can be carried out as a line integral in this plane.

Defining a coordinate s along these paths (the constant tension curves), locally at the points $s_0 \overset{\Delta}{=} (x_0, \dot{x}_0)$ the equation (5.14) can be written as:

$$N_{T_0}(s_0) = \int_{-\infty}^{\infty} \dot{T}(x_0, \dot{x}_0, \ddot{x}) \ u\Big(\dot{T}(x_0, \dot{x}_0, \ddot{x})\Big) \ p(x_0, \dot{x}_0, \ddot{x}) \ I_\square(s_0) \ d\ddot{x} \qquad (5.15)$$

where:

$$I_\square(s_0) = \int_{-\Delta x_0}^{+\Delta x_0} \int_{-\Delta \dot{x}_0}^{+\Delta \dot{x}_0} \delta\Big(T(x, \dot{x}) - T_0\Big) \ dx \ d\dot{x} \qquad (5.16)$$

and $(\pm\Delta x_0, \pm\Delta \dot{x}_0)$ define a small neighborhood about the point $(x_0, \dot{x}_0)$.

In (5.16) above, the double integral of the delta function can be easily evaluated with a change of variables. Instead of integrating in the $(x, \dot{x})$ coordinates, the integral can be carried out in the variables (T, s), as follows:

Let $(\pm\Delta T, \pm\Delta s)$ be a small region around a point on the path (T_0, s_0) :

$$I_\square(s_0) = \int_{-\Delta T}^{+\Delta T} \int_{-\Delta s}^{+\Delta s} \delta\Big(T(x, \dot{x}) - T_0\Big) \left|\frac{\partial(x, \dot{x})}{\partial(T, s)}\right| dT \ ds \qquad (5.17)$$

The term $\left|\frac{\partial(x, \dot{x})}{\partial(T, s)}\right|$ is the determinant of the Jacobian of the transformation $(x, \dot{x}) \iff (T, s)$, given by:

$$\frac{\partial(x, \dot{x})}{\partial(T, s)} = \begin{bmatrix} \frac{\partial x}{\partial T} & \frac{\partial x}{\partial s} \\ \\ \frac{\partial \dot{x}}{\partial T} & \frac{\partial \dot{x}}{\partial s} \end{bmatrix} \qquad (5.18)$$

80

Actually, for any point on the constant tension curve, the transformation $(x, \dot{x}) \iff (T, s)$ represents a rotation by an angle $\theta(s)$.

Using $\vec{\nabla} T(s)$, the gradient of tension in the $(x, \dot{x})$ plane, the Jacobian can be evaluated:

$$\frac{\partial(x, \dot{x})}{\partial(T, s)} = \begin{bmatrix} \frac{\cos\theta(s)}{|\vec{\nabla} T(s)|} & -\sin\theta(s) \\ \frac{\sin\theta(s)}{|\vec{\nabla} T(s)|} & -\cos\theta(s) \end{bmatrix} \tag{5.19}$$

Such that:

$$\left| \frac{\partial(x, \dot{x})}{\partial(T, s)} \right| = \frac{1}{|\vec{\nabla} T(s)|} \tag{5.20}$$

Using this result in the equation (5.17) the contribution of every point on the path of integration to the number of crossings is given by:

$$I_\square(s_0) = \frac{1}{|\vec{\nabla} T(s_0)|} \Delta s \tag{5.21}$$

Summing up the contributions of all points in the path to the number of crossings:

$$N(T_0) = \int_{s_0} N_{T_0}(s_0)\, ds_0 \tag{5.22}$$

The final expression for the number of crossings at the level T_0, under the current approach is given by:

$$N(T_0) = \int_{s_i}^{s_f} \int_{-\infty}^{\infty} \dot{T}(s, \tilde{x})\, u\!\left(\dot{T}(s, \tilde{x})\right) p(s, \tilde{x}) \frac{1}{|\vec{\nabla} T(s)|}\, d\tilde{x}\ ds \tag{5.23}$$

where $s \iff (x_0, \dot{x}_0)$ are the points along the constant tension curve $T = T_0$, and s_i, s_f indicate the initial and final value to be considered in the integration.

5.4   Numerical Calculations

In this section some computations of extreme tensions with the direct integration approach are presented.

The ships included in the towing dynamic calculations are the same introduced in earlier Chapters: the Tug ARS50 and the Frigate PAGE (Table 3.1). The towing speed is 3 knots and the sea conditions determined by 30 knots wind.

Three hawsers are considered: Hawser I and II which were introduced in Chapter 4, and Hawser III which is a longer version of Hawser II. Their main characteristics are summarized in Table 5.1.

The coefficients of the polynomial tension model (5.9) for these three hawsers are given in Table 5.2.

The main results from the linearized dynamic towing problem, which gives the cable elongation statistical properties that are input to the extreme tension calculation under the direct integration approach are presented in table 5.3.

		HAWSER I	HAWSER II	HAWSER III
Diameter	(in)	2.0	2.25	2.25
Length	(ft)	1200	1800	2100
Weight	(lbs/ft)	6.0	8.4	8.4
Static Tension	(kips)	20.0	20.0	20.0

Table 5.1: Characteristics of Hawsers I, II and III

Coefficients	HAWSER I	HAWSER II	HAWSER III	Units
a_{10}	785.54	249.55	165.92	lbs/ft
a_{20}	145.29	-0.74	-1.07	lbs/ft^2
a_{30}	13.47	-0.59	-0.43	lbs/ft^3
a_{01}	4079.8	1064.7	837.06	lbs·sec/ft
a_{02}	49.99	59.24	51.29	lbs·sec^2/ft^2
a_{03}	-16.11	2.49	2.94	lbs·sec^3/ft^3
a_{11}	478.46	59.43	35.78	lbs·sec/ft^2
a_{21}	17.96	3.07	2.19	lbs·sec/ft^3
a_{12}	47.91	6.47	4.43	lbs·sec^2/ft^3

Table 5.2: Polynomial Tension Model Coefficients

		HAWSER I	HAWSER II	HAWSER III
Elongation Moments				
m_{0x}	ft^2	19.203	24.726	26.984
m_{2x}	ft^2/sec^2	8.716	11.090	11.787
m_{4x}	ft^2/sec^4	4.823	5.804	5.893
Linearized Tension Coefficients				
k_{eq}	lbs/ft	1937.3	277.52	183.18
b_{eq}	lbs·sec/ft	4003.4	1223.4	999.88
Extreme Cable Elongation				
x_{ext}	ft	24.82	28.16	29.41

Table 5.3: Results from Towing Dynamics

The extreme tension calculations, under the direct integration approach, consist in:

- Evaluation of the curves of constant tension, based on the polynomial tension model: equation (5.9);

- Numerical integration of equation (5.23) along these constant tension curves to determine the number of level crossings;

- According to equation (3.8), the probability density function for the tension extremes, T_{ext}, can be expressed as:

$$p(T \leq T_{ext}) = -\frac{1}{N(0)} \frac{d}{dT_{ext}} N(T_{ext}) \qquad (5.24)$$

thus, through the numerical differentiation of the number of level crossings, the probability density function for the tension extremes is evaluated.

- The extreme tension, defined as the tension level which has the probability of 0.1% of being exceeded in 24 hours, is then calculated numerically, according to the procedure suggested in section 3.3.

5.4.1 Validation of the Numerical Scheme

In order to verify the accuracy of the integration scheme proposed in section 5.3.1, the number of crossings and the extreme tension pdf are evaluated for the

84

linear hawser presented in section 3.3.1. This hawser constitutes the equivalent linearized version of Hawser I, where the tension elongation relationship is given by equation (2.2):

$$T(x, \dot{x}) = k_{eq} \, x(t) \, + \, b_{eq} \, \dot{x}(t)$$

with: $k_{eq} = 1.937$ kips/ft and $b_{eq} = 4.003$ kips $\cdot$ sec/ft, as given in Table 5.3.

Under the scope of linear theory the number of crossings and thus the pdf for the extremes can be evaluated analytically. As shown in section 3.2, for Gaussian distributed random variables, as the linearized hawser tension, the extremes are Rayleigh distributed (equation 3.9):

$$p(T \leq T_{ext}) = \frac{T_{ext}}{m_{0_T}} \, \exp[-\frac{1}{2} \frac{T^2_{ext}}{m_{0_T}}] \tag{5.25}$$

where m_{0_T}, given by equation (3.10), is 211.7 Kips^2.

The constant tension curves for this linearized hawser are shown in Figure 5.2. The numerical integration of equation (5.23) is performed and the number of crossings differentiated, as in equation (5.24), in order to determine the pdf for the extremes.

The resulting probability density function for the extremes is compared to the analytic solution, given by the Rayleigh pdf, in Figure 5.3. As shown, the numerical scheme proves very accurate.
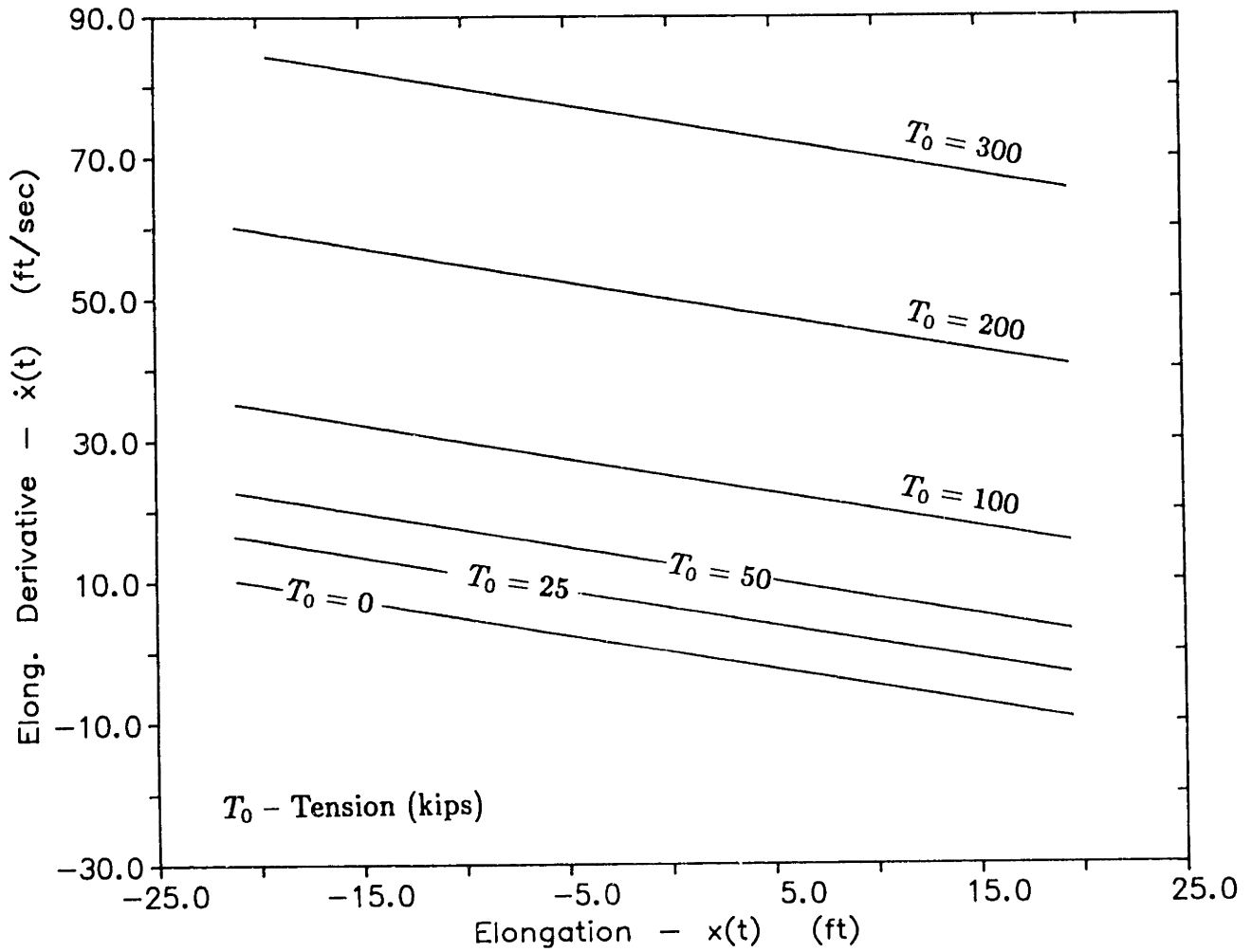
Figure 5.2: Constant Tension Curves for Linearized Hawser I
$$T(x, \dot{x}) = k_{eq}\, x(t) \;+\; b_{eq}\, \dot{x}(t)$$
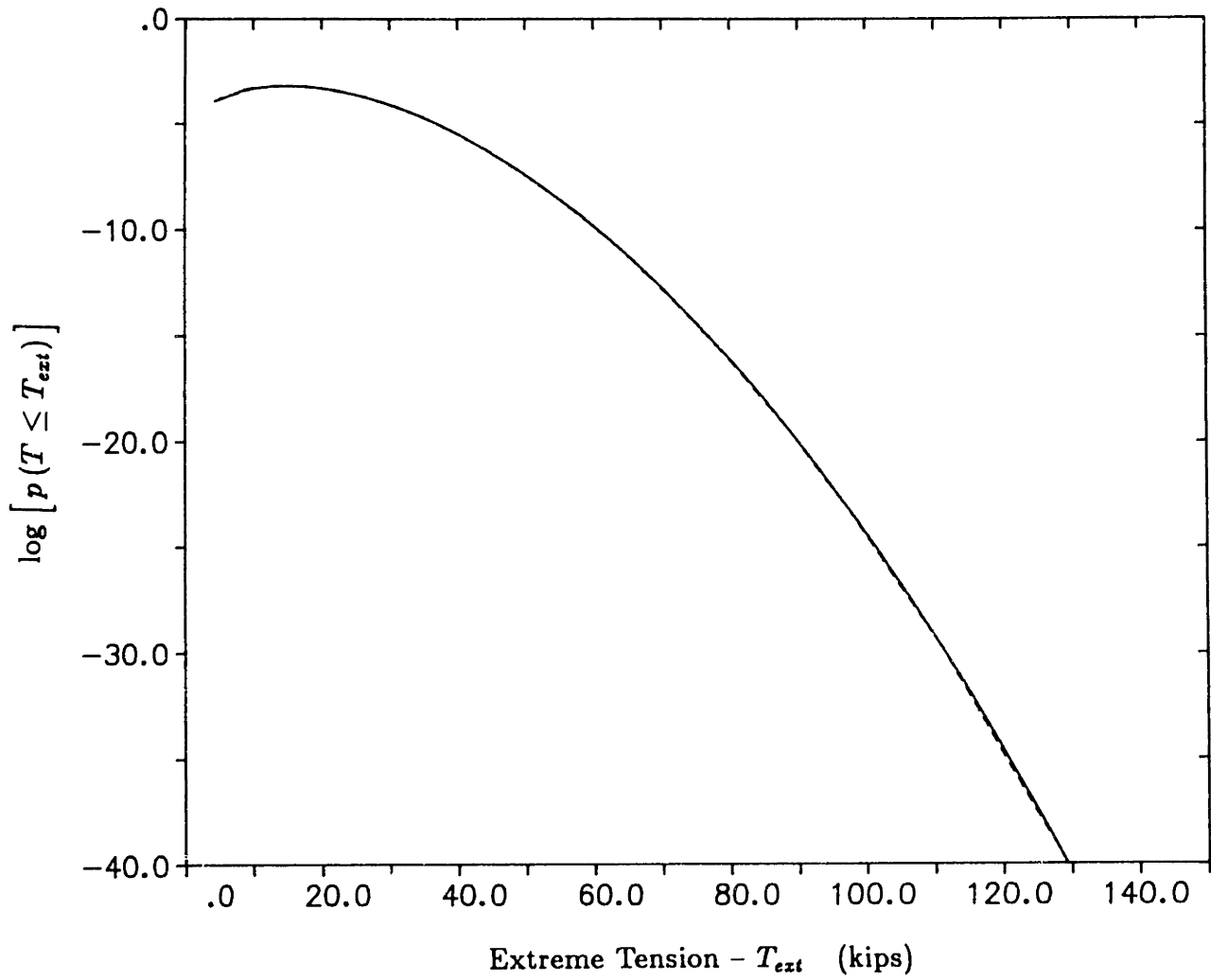$k_{eq} = 1.937$ kips/ft and $b_{eq} = 4.003$ kips · sec/ft.

Figure 5.3: Probability Density Functions - $p(T \leq T_{ext})$
Direct Integration and Exact Linear Solution
Linearized Version Hawser I

5.4.2 Extreme Tensions Results

The numerical calculations for the extreme tensions under the present approach, $T_{ext_{DI}}$, result for Hawsers I, II and III:

HAWSER I .... 369 kips,

HAWSER II .... 101 kips,

HAWSER III .... 99 kips.

In order to compare this results to the values obtained previously, according to the linear theory and to the Gram-Charlier approach, Table 5.4 presents all tension extremes obtained thus far, which are also plotted in Figures 5.4, 5.5 and 5.6 on the static curves (static tension × change in span) of hawsers I, II and III.

EXTREME TENSION (kips)		HAWSER I	HAWSER II	HAWSER III
Linear	T_{ext_L}	84.5	44.2	40.1
Gram-Charlier	$T_{ext_{GC}}$	173.0	55.0	44.3
Direct Integration	$T_{ext_{DI}}$	369.0	101.0	99.0
Static	$T_{ext_{St}}$	$\sim 320.$	$\sim 36.$	$\sim 30.$

Table 5.4: Extreme Tensions for Hawsers I, II and III

5.4.3 Comments on the D.I. Extremes

As shown in Table 5.4, as well as in Figures 5.4, 5.5 and 5.6, the Direct Integration approach is able to retrieve the complete non-linear behavior of the static

tension curve and the hawser dynamics, even for Hawser I, that presents the extreme change in span well into the steep slope region.

Numerically, these extreme tension predictions are justified by the behavior of the extremes' probability density function for large tensions (tails). The direct integration extremes are larger than the previous ones, because the probabilities determined by this approach exceed the others in that region. This is shown in Figures 5.7, 5.8 and 5.9 where the pdfs are plotted in log-scale for the three hawsers.

Physically, these results are explained by the dynamic effects of the cable motion in water, caused by the cross-flow hydrodynamic drag. As shown by Bliek [9] and Burgess [8], when the hawser oscillates in water, excited by the motions of the ships, the drag force increases with the frequency of the exciting end motion. At some point the balance of forces is such that the average horizontal and vertical (drag + weight) forces along the length "lock" the hawser into a new geometric configuration, and any excitation at the ends is accommodated by the cable stretch.

Therefore, due to the dynamic effects of the hydrodynamic drag on motion of the cable in water, the steep slope of the static curve is applied to smaller elongations than it would be otherwise, when the end motion is quasi-static (low-frequency). In other words, if a curve for dynamic tension × change in span were drawn, it would present the steep slope for smaller elongations that the static one. However, since this kind of plot cannot be drawn in a straight forward manner, because of the frequency dependence embedded into it, the static curve is used as the basis

reference.

Hawsers II and III present larger elongations, as shown by the elongation statistics in Table 5.3. In these circumstances the effects of the cross-flow drag are accentuated because these hawsers oscillate more. Thus, extreme tensions should show the influences of these cables operating in theirs elastic regime (when stretching occurs), which is obtained with the direct integration approach.
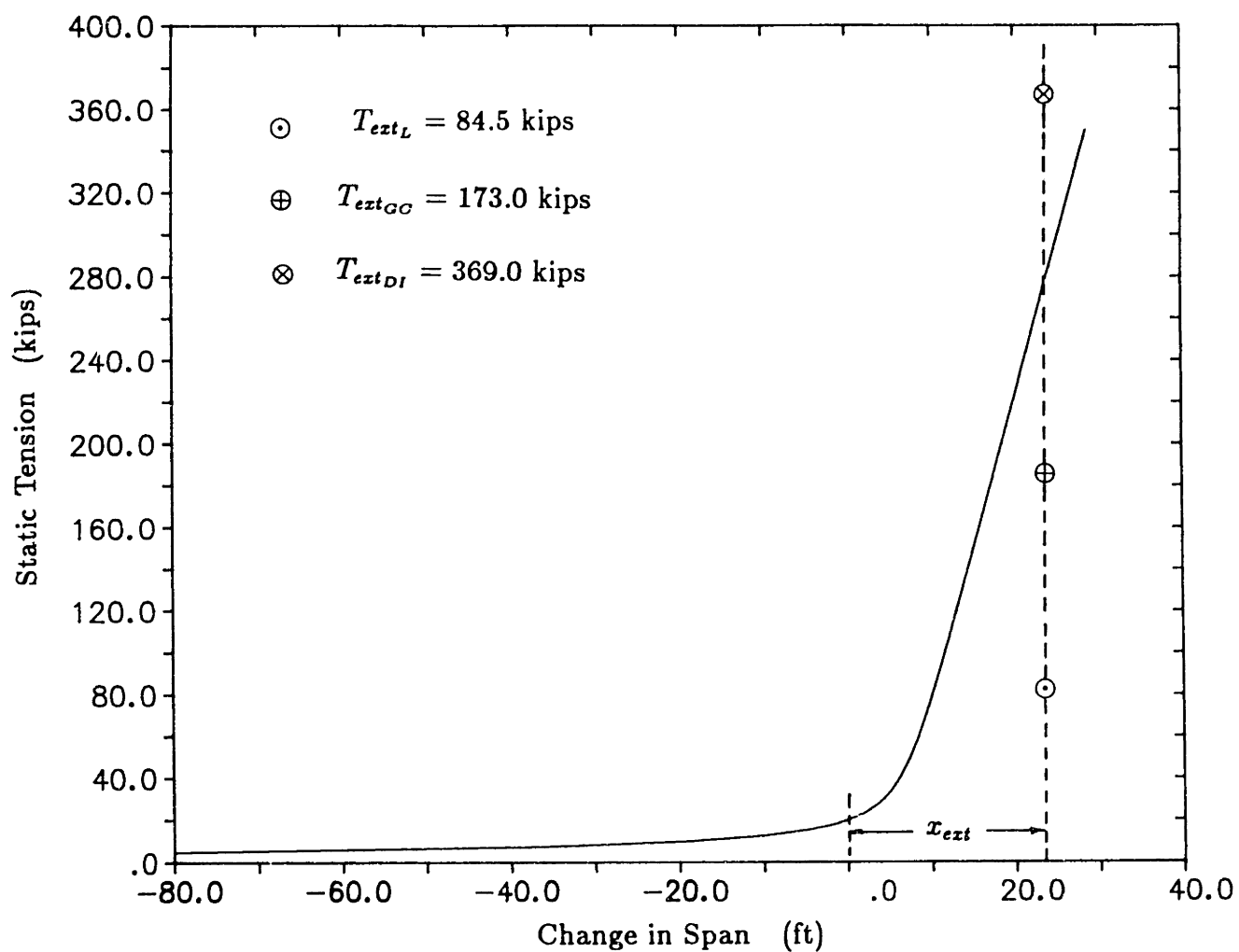
Figure 5.4: Hawser I Static Curve - Tension × Change in Span
Extreme Tension Predictions
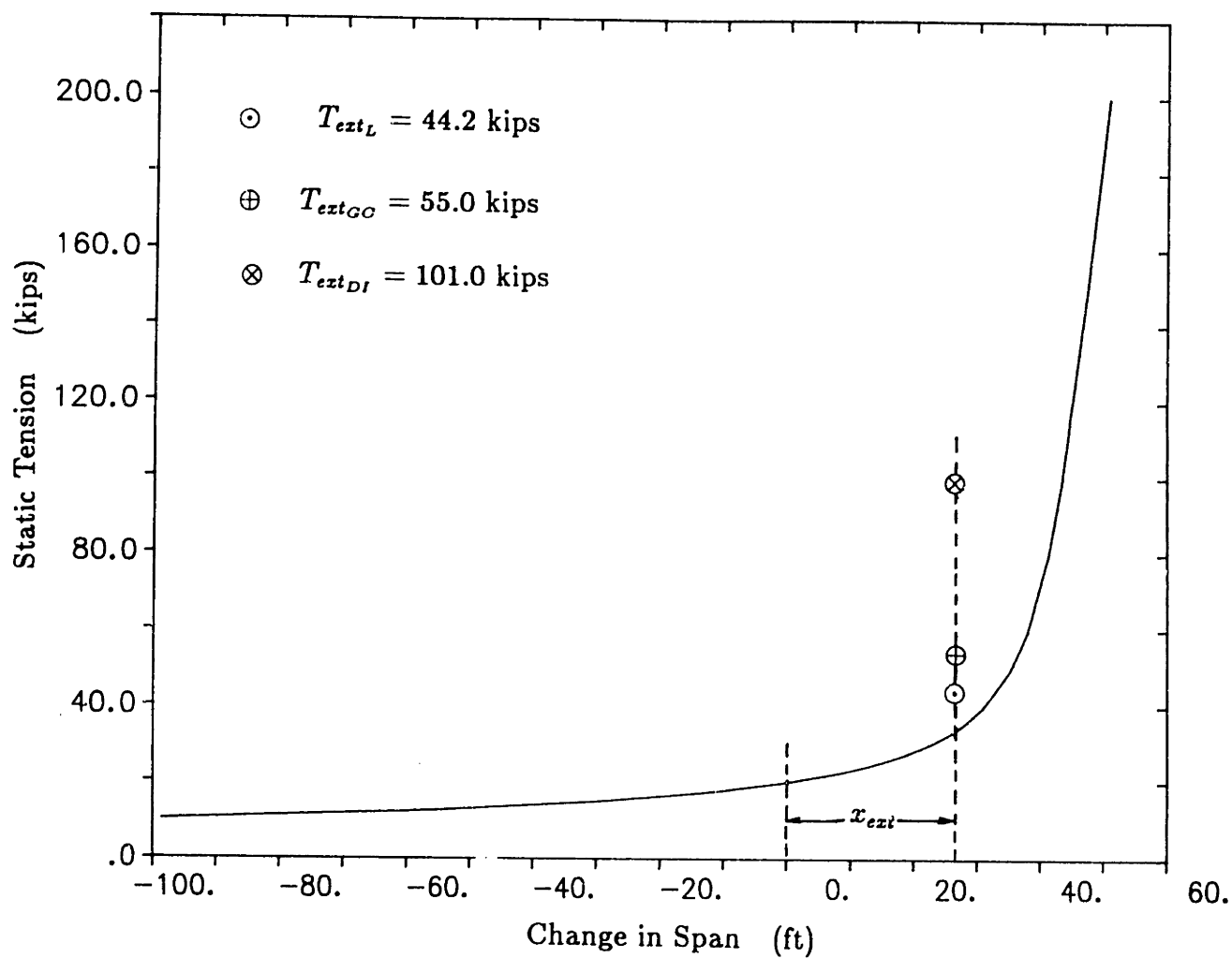
Figure 5.5: Hawser II Static Curve - Tension × Change in Span
Extreme Tension Predictions
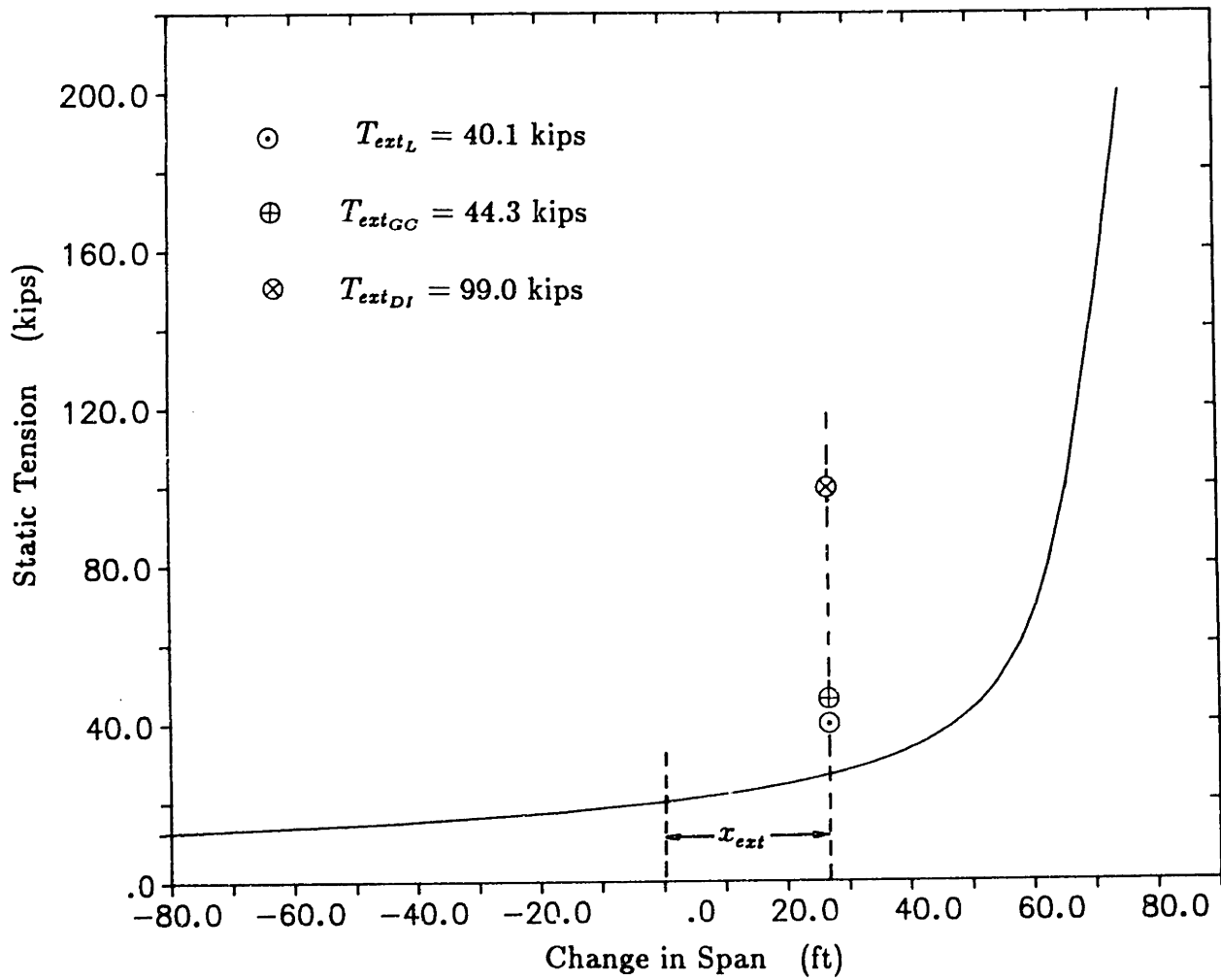
Figure 5.6: Hawser III Static Curve - Tension × Change in Span
Extreme Tension Predictions
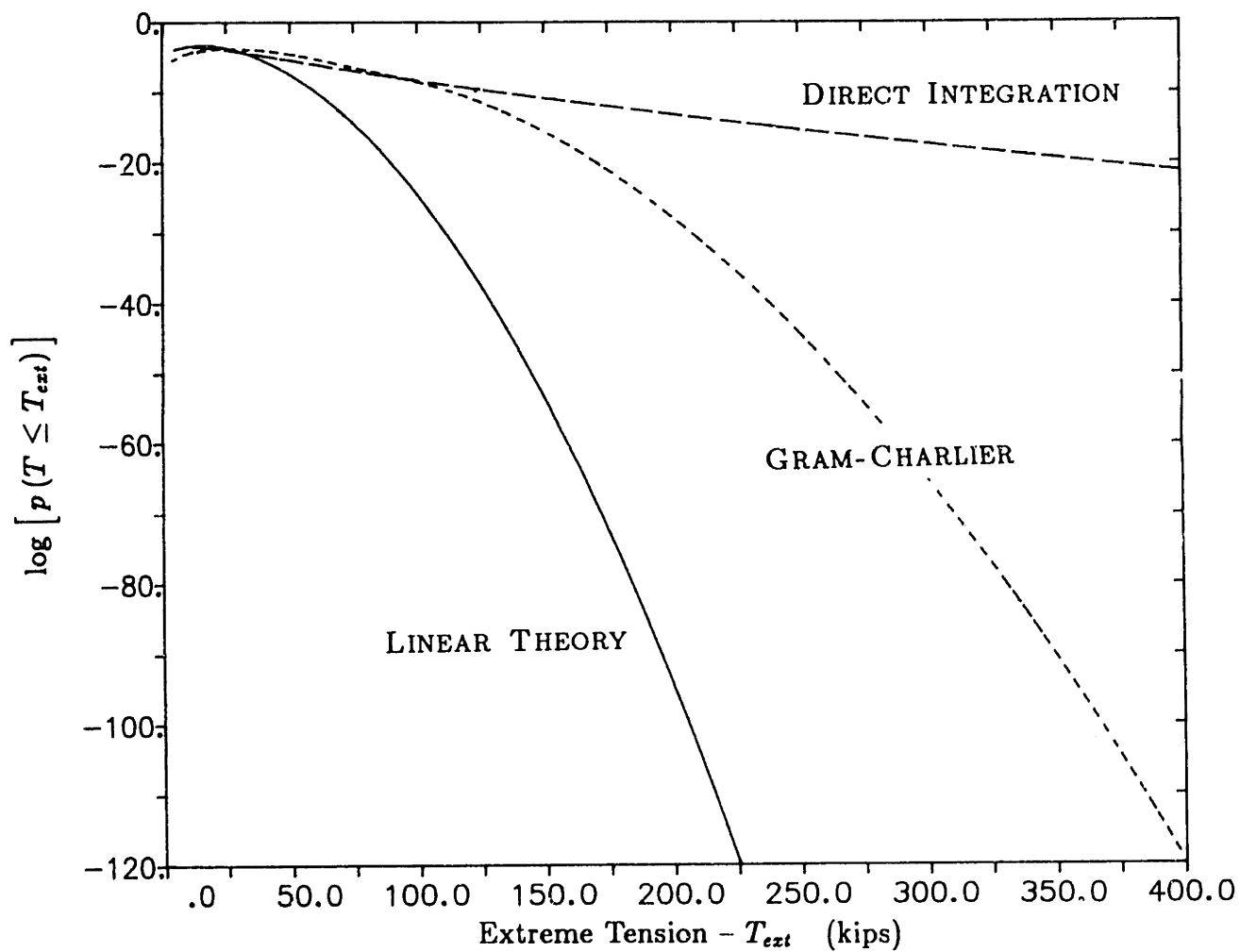
Figure 5.7: HAWSER I - Probability Density Functions
Gram-Charlier Series $(N = 6)$,
and Direct Integration,
and Linear Analysis.
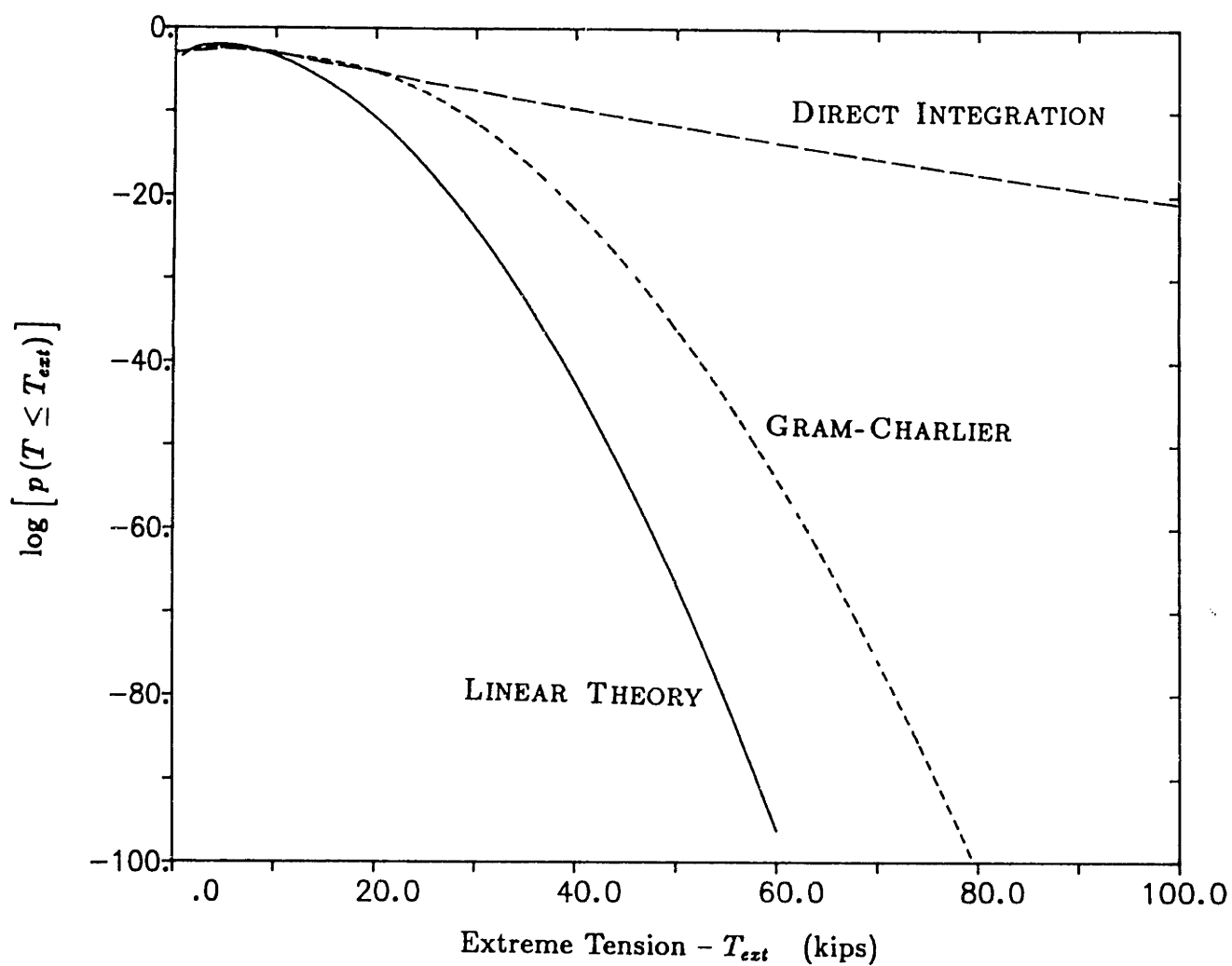
Figure 5.8: HAWSER II - Probability Density Functions
Gram-Charlier Series $(N = 6)$,
and Direct Integration,
and Linear Analysis.
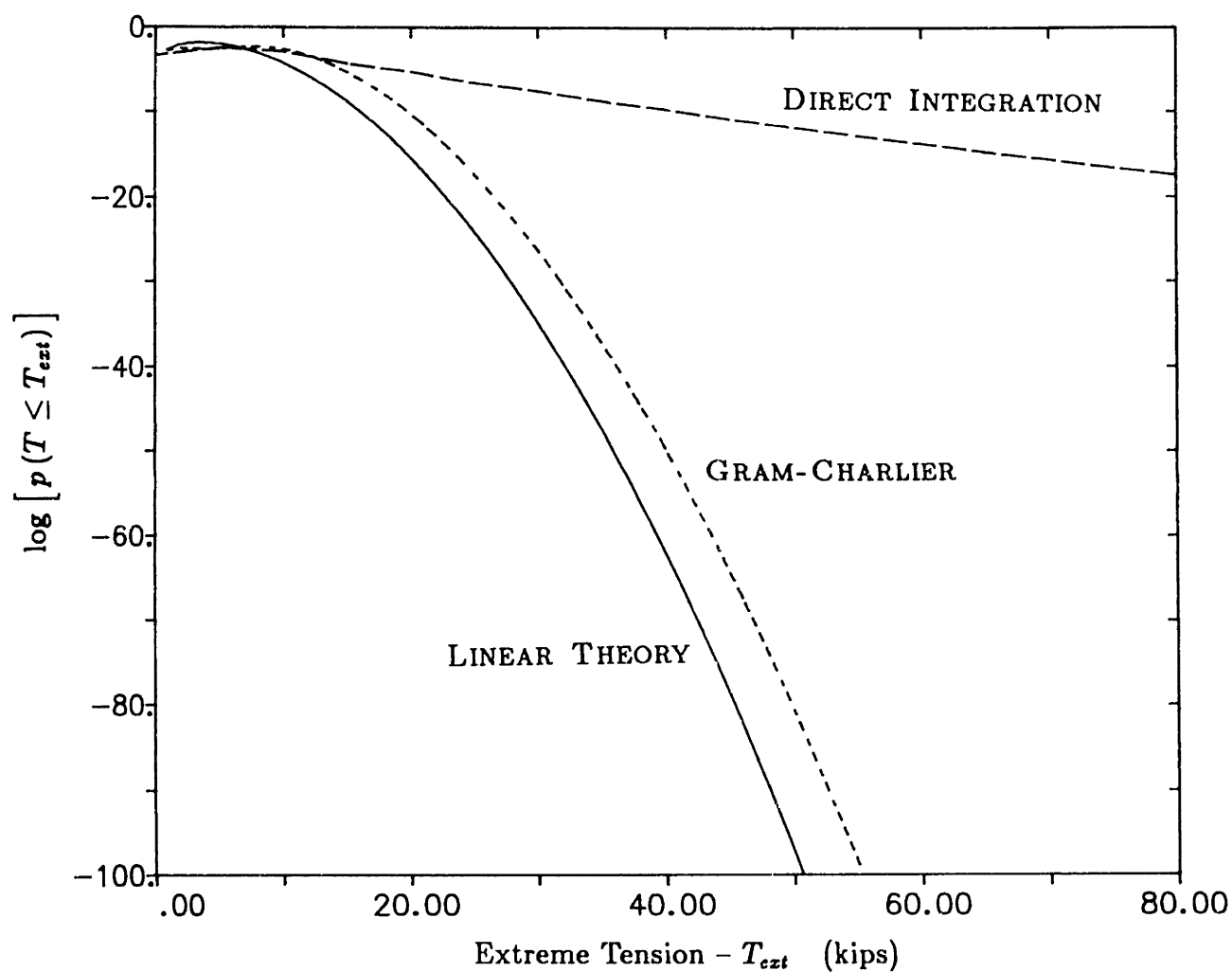
Figure 5.9: HAWSER III - Probability Density Functions
Gram-Charlier Series $(N = 3)$,
and Direct Integration,
and Linear Analysis.

Chapter 6

Conclusions

6.1 Summary

Significant advances in the study of towing systems were accomplished within this work. The analysis of the towing problem as a twelve degrees of freedom dynamic system, formed by the tug and tow vessels connected with the hawser, allows the explicit consideration of the dynamic loads when predicting extreme towline tensions. With it, towing operations can be undertaken with increased safety and confidence under a whole range of conditions.

The understanding of the hawser forces, and their effects on the motion of the ships are important elements in the present analysis. The hawser, as the dynamic coupling element between the two vessels, presents a particularly non-linear behavior. Just on a quasi-static basis, the mechanical properties (tension vs. elongation)

of a wire rope towline is highly non-linear. Therefore, at low frequencies small elongations (caused by the ship motions) are accommodated by the cable catenary becoming shallower, which generates small dynamic tensions. For larger motion amplitudes, the resulting cable extension is accommodated by stretching the cable itself, which causes very large tensions. Dynamically, as the cable catenary changes its shape in the water, the transverse hydrodynamic drag force causes even more non-linearity. In fact, at intermediate and high frequencies, the drag force can be large enough to nearly immobilize the cable, causing stretching of the cable even for small extensions. Besides all this, the cable attains more tension during extension and actually can become slack when the distance between vessels is reduced, which is another strong non-linearity.

A computer program for computing time simulations of the cable tension, for dynamic excitations at the ends, plays a major role in this work. To gain confidence in this time-domain model several experiments were compared with its results.

Although central to this work, the time domain simulations are not practical for determining statistics of extreme tensions due to the computer time required. Typically, for specified vessels, towline geometry and sea state; the extreme tension is determined as the tension that has a probability of occurrence of 0.1% in one day of towing. To determine this tension, simulations would need to be done for <u>at least</u> 1000 days actual time. Since the simulations take about 50 times the real time in a medium power computer, the computing time required is clearly prohibitive.

To do the problem, a non-linear mathematical model for the cable tension is developed. It consists in a polynomial relationship between the tension and the cable elongation (or extension) and the elongation time-derivative. The coefficients of this polynomial model are determined by fitting it to time simulations, with weights adjusted, such that tension is accurate for high loads.

The next step in the developed methodology is the evaluation of the ship motions at the ends of the towline, which cause the cable elongation. This is done under the scope of linear seakeeping theory considering the linearized hawser forces on the vessels, which are determined with the equivalent linearization method.

Once the motions are determined, the cable elongation RAO is computed and used as the input to the polynomial tension relation for the non-linear statistical prediction of extreme tensions. The extremes thus obtained are conservative. The dominant contribution to the elongation comes from the ships' surge motion, for which the hawser forces are the only restoring forces present. Therefore, using the equivalent linearized forces leads to somewhat larger extreme elongations, thus conservative extreme tension estimates.

Two methods are developed for the non-linear statistical calculations of the extreme tensions. In the first one, the frequency of crossings at a certain tension level is determined using an approximate joint probability density function of the tension and its time derivative, $p(T, \dot{T})$, obtained from its Gram-Charlier Series. It was found that the towline characteristics were so non-linear that the series did

99

not give a good approximation with a reasonable number of terms.

The second method is fully non-linear. There, the polynomial tension model is integrated with the known (from the equivalently linearized analysis of the ship motions) joint probability density function of the elongation and its first two time-derivatives. The integration results in a non-linear mapping from tension values to the frequency of crossings, such that the probability density function for the extremes is obtained. This method proved successful, and the results include the complete non-linear behavior of the towline.

6.2   Conclusions on the Extremes Calculations

The statistical analysis of extreme tensions in cable systems is not a simple task because of its extremely non-linear dynamic behavior.

The hawser dynamic response to the exciting ship motions at the ends is a strongly non-linear phenomenon. Since the motions are assumed linear, they are Gaussian distributed and so is the cable elongation. Therefore, the extreme elongation can be obtained by the conventional methods of the linear statics of extremes. This extreme elongation determines in the static characteristic of the hawser (tension vs. elongation curve), a minimum estimate for the extreme tension that constitutes a "physical measure" for the accuracy of the extreme tension predictions by any other method. This is so because, besides any dynamic effect, when the cable

100

elongates a certain amount the tension should increase <u>at least</u> to the value given in the static curve for that elongation.

The results obtained with the Gram-Charlier series do not follow this physical property of the hawsers. In some cases, the extreme tensions are much smaller than the mentioned "static" extreme. In other circumstances, when the extreme is reasonable under this criteria, the estimate obtained does not differ much from the one determined linearly, with the equivalent linearized hawser model. Thus, the method does not accurately reflect the non-linear dynamic behavior of hawsers due to the hydrodynamic cross-flow drag.

Although the Gram-Charlier series was not appropriate for the statistical analysis of extreme tensions, because towing hawsers are too non-linear, the methodology developed for its application in Chapter 4 constitutes an important contribution. The procedures introduced systematize and automate the evaluation of the coefficients in the series, making its application much more straight forward. It is the author's belief that this method is useful for the analysis of slightly non-linear phenomena.

The extreme tension estimates with the Direct Integration approach were much more accurate. Because the method is fully non-linear, the static and dynamic non-linear tension behavior are completely embedded in it. Therefore the methodology gives results for extreme tensions, that translates all non-linearities of the hawser tension, not only the static curve non-linearity, but also the drag force effects.

6.3   Further Studies

The analysis done so far constitutes a large step in the study of towing dynamics. Nevertheless some important points could be studied more deeply or extended into new developments.

In this work, the motions were determined from linear seakeeping theory, considering the equivalent linearized hawser forces acting on the ships. One immediate further development could be the inclusion of the non-linear motions in the analysis, specifically the non-linear surge, since this is the motion that most contributes to the cable elongation. Gains in accuracy of the extreme tension predictions could be achieved by determining the surge motion response due to the actual non-linear towline forces. This is so, because for the surge motions the hawser forces are the only restoring force present and a significant damping contribution. For the other motions, the equivalently linearized hawser force already does a good job in determining them, mainly because the hawser forces are small when compared to the hydrostatic ones.

Although the hawser forces are highly non-linear; due to the fact that the inertial forces are dominant, the resulting surge motion is only slightly non-linear. Therefore, there is a good chance that the probability density function for non-linear the surge (and thus the cable elongation) and its time derivatives, can be well approximated by a tri-variate Gram-Charlier Series. Extending the analysis in Chapter 4

to three variables, the joint pdf of the elongation and its first and second derivatives could be determined taking into account the non-linear surge. This pdf could then be used in the Direct Integration approach for the extreme tension predictions.

In the present study only wire ropes towlines were considered. Further developments, mainly applications of these methodologies for fiber rope towlines could be undertaken. Fiber rope towlines are much lighter and softer than their wire counterparts, and the tension-extention behavior should be much less non-linear than the one presented by wire ropes. In this case, the Gram-Charlier Series may well give adequate accuracy in the extreme tension predictions. Besides that, the procedures developed are also useful for determining the complete probability distribution of extremes which is necessary for fatigue analysis; very important for fiber rope towlines.

Bibliography

[1] Naval Sea Systems Command, U. S. Navy, *Tow Manual*, 1987

[2] ABKOWITZ, M. *Stability and Motion Control of Ocean Vehicles.* MIT Press, Cambridge, MA. 1969

[3] BERNITSAS, M. M. & LATORRE, R. & KEKRIDIS, N. *Linear Simulation of Time Dependent Towing of Ocean Vehicles.* Report 286, Dept. Of Naval Arch. and Marine Eng., The University of Michigan, September 1983.

[4] BERNITSAS, M. M. & KEKRIDIS, N.S.& PAPOULIAS, A.P. "Solution of the Problem of Ship Towing by Elastic Rope Using Perturbation." *Journal of Ship Research*, SNAME, Vol. 30, N. 1:51-68, 1986.

[5] MILLER, E.R. & BARR, R.A. & VAN DYKE, P. " Studies of Ship and Barge Towing in Severe Environments." *Second International Symposium on Ocean Engineering and Ship Handling*, Swedish Maritime Research Center, 1983.

[6] TRIANTAFYLLOU, M. "The Dynamics of Taut Inclined Cables." *Journal*

of Mechanics and Applied Mathematics, Vol. 37, Pt.3, 1984.

[7] SHIN, H. *Non Linear Cable Dynamics*. PhD Thesis. M.I.T. Dept. of Ocean Engineering, Cambridge, Mass., 1987.

[8] BURGESS, J. *Natural Modes and Impulsive Motions of a Horizontal Shallow Sag Cable*. PhD Thesis, M.I.T. Dept. of Ocean Engineering, Cambridge, Mass., 1985.

[9] BLIEK, A. *Dynamic Analysis of Single Span Cables*. PhD Thesis, M.I.T. Dept. of Ocean Engineering, Cambridge, Mass., 1984.

[10] LONGUETT-HIGGINGS, M. S. "On the Statistical Distribution of the Heights of Sea Waves." *Journal of Marine Research*, Vol. XI:245-266, No.3, 1952.

[11] OCHI, M.K. "On prediction of Extreme Values." *Journal of Ship Research*. Vol. 17:29-37, 1973.

[12] LONGUETT-HIGGINGS, M. S. & CARTWRIGHT D. E. "The Statiscal Distribution of the Maxima of a Random Function." *Proceedings of the Royal Society of London*, Series A, Vol. 237:212-232, 1956.

[13] LONGUETT-HIGGINGS, M. S. "The Effect of Non-linearities on Statistical Distributions in the Theory of Sea Waves." *Journal of Fluid Mechanics*, Vol. 17:460-480, 1963.

[14] LONGUETT-HIGGINGS, M. S. "Modified Gaussian Distributions for Slightly Nonlinear Variables." *Radio Science Journal of Research*, Vol. 68D:1049-1062, No.9, 1964.

[15] VIDYASAGAR, M. *Nonlinear Systems Analysis*. Prentice-Hall Inc., Englewood Cliffs, NJ, 1978.

[16] KENDALL, M. G. & STUART A. *The Advanced Theory of Statistics*. 3rd. Edition, Vol. 1, Hafner Publishing Co., New York, NY, 1969.

[17] SALVESEN, N. & TUCK, E.O. & FALTINSEN O. "Ship motions and Sea loads," *Transactions of the Society of Naval Architects and Marine Engineers*, Vol.78, 1970

[18] LOUKAKIS, T. *Computer-Aided Prediction of Seakeeping Performance in Ship Design*, Technical Report, MIT-Department of Ocean Engineering, Cambridge, Mass., 1970

[19] ANAGNOSTOU, G. *Extreme Tension in a Ship's Towline*. M.S. Thesis, M.I.T. Dept. of Ocean Engineering, Cambridge, Mass., 1987.

[20] NIGAM, N. C. *Introduction to Random Vibrations*. MIT Press, Cambridge, Mass., 1983.

[21] FRIMM, F. C. *Part II - General Examination*, Report to Faculty Committee, Unpublished, August 1986.

[22] NAESS, A. "Extreme Values of a Stochastic Process Whose Peak Values Are Subject to the Markov Chain Condition." *Norwegian Maritime Research*, No.1, 1983

[23] DAVID, D.F. & KENDALL, M.G. & BARTON D.E. *Symmetric Functions and Allied Tables.* Cambridge University Press, Cambridge, 1966.

[24] VINJE, T. *On the Statistical Distribution of Maxima of Stochastic Non-linear Stochastic Variables.* Report No. SK/M 27, Division of Ship Structures - The University of Throndheim, Norway, 1974.

[25] VINJE, T. "On the Statistical Distribution of Second Order Forces and Motions," *International Shipbuilding Progress*, Vol. 30, No. 343:58-68, 1983.

[26] VINJE, T. *On the Calculation of the Maxima of Non-linear Wave Forces and Wave Induced Motions.* Report No. R-44.76, Division of Ship Hydrodynamics - The University of Throndheim, Norway, August 1976.

[27] NEUMANN, G. & PIERSON, W. J. *Principles of Physical Oceanography*, Prentice-Hall, Englewood Cliffs, N.J., 1966

[28] RICE, S. O. "Mathematical Analysis of Random Noise." In: *Noise and Stochastic Processes*, Ed. N. Wax, Dover Publications Inc., New York, NY, 1954.

[29] ABRAMOWITZ, M. & STEGUN, I.A. *Handbook of Mathematical Functions*, 9th Edition, Dover Publications Inc., New York, NY, 1970.

[30] WALLACE, D. L. "Asymptotic Approximations to Distributions," *Annals of Mathematical Statistics*, Vol.29:635-654, 1958.

[31] TRIANTAFYLLOU, M. *Cable Dynamics Simulation Program*, Private Communications, MIT-Department of Ocean Engineering, Cambridge, MA, 1986.

[32] BURGESS, J. *Derivation of the Twelve Degrees-of-Freedom Equation of Motion*, Unpublished Report, MIT, Cambridge, Mass, 1985.

[33] HARLKYARD, J.E. & JOHNSON R.P. *Model Basin Towline Response Tests - Final Report*, Technical Report, ARCTEC Offshore Corp., Escondido, CA, 1897.

Appendix A

Cable Models

In this appendix, the procedures applied to obtain the cable model used in the statistical analyses are described.

The theoretical model is the time domain differential equations that represent the cable's dynamic equations. These equations are integrated to provide the time domain simulations.

Model tests were carried out to verify the validity and accuracy of this dynamic model [33].

Finally, a numerical fit using a least minimum square error technique is applied to a wide range of time simulations in order to determine the relationship between the dynamic tension and the motions at the end of the cable.

A.1 The Time Simulation Model

The towing hawser, according to developments made by Triantafyllou [31], Burgess [8] and Shin [7], is a cable system to which some simplifying hypothesis apply:

- The hawser is assumed to be uniform with negligible bending stiffness,

- Only in-plane motions i.e., motions of the cable in the vertical plane are considered with excitation coming from one of its ends,

- The cable is assumed to be shallow sag, which means that the static tension is much larger that the hawser weight, and that the static tension and the curvature are constant along the cable.

Additionally, because the exciting frequencies are much lower than the first ellastic eigenfrequency of the cable (ellastic wave speed: $\sqrt{E/\rho_C}$), the longidutinal dynamics are not excited and can be neglected. The cable's dynamic equations can be written as [31]:

$$M \frac{\partial^2 q}{\partial t^2} = (\bar{T} + \tilde{T}) \left(\alpha + \frac{\partial^2 q}{\partial s^2} \right) - b \frac{\partial q}{\partial t} \left| \frac{\partial q}{\partial t} \right| - \bar{T} \, \alpha \qquad (A.1)$$

with

$$\tilde{T} = EA \left[\frac{p_0}{L} - \frac{\alpha}{L} \int_0^L q \, ds + \frac{1}{2L} \int_0^L \left(\frac{\partial q}{\partial s} \right)^2 ds \right] \qquad (A.2)$$

where:

M : cable mass per unit length

w : cable weigth per unit length

s : coordinate along the cable

q : $q(s)$ – normal motions along the cable

p : $p(s)$ – tangential motion along the cable

$\bar{T}$: static tension

$\tilde{T}$: dynamic tension

C_D : cable sectional drag coefficient

d : cable diameter

L : cable length

ρ_w : water density

b : $\frac{1}{2}\rho_w\,C_D\,d$ – sectional drag force

α : $\frac{wL}{T}$ – catenary stiffness

The simplifying assumptions in the previous page does not restrict the cable model in any sense. It includes the important non-linearities to be considered for modelling the towing hawser:

– the water drag:

$$b\,\frac{\partial q}{\partial t}\left|\frac{\partial q}{\partial t}\right| \tag{A.3}$$

– the non-linear geometric stiffness:

$$\frac{EA}{2L}\int_0^L\left(\frac{\partial q}{\partial s}\right)^2 ds \tag{A.4}$$

111

– the "clipping" model, for non-negative total tension:

$$\text{if} \quad \bar{T} + \tilde{T} \; < 0 \quad \text{then} \quad \bar{T} + \tilde{T} \quad \text{is set to} \quad 0. \tag{A.5}$$

The differential equation is integrated numerically using the Galerkin's Method with sinusoids. Examples of time simulations are shown elsewhere in this appendix.

A.2   Model Tests

Model tests were preformed in a ship model basin to verify the validity and accuracy of the cable dynamic model presented in the previous section [33].

The tests consisted of exciting one end of the cable (live end) sinusoidally with known amplitude and frequency, and measuring the tension at both ends.

The experimental arrangement is shown in the Figure A.1.

The cable used in these experiments had the characteristics, presented in Table A.1 which corresponds approximately to a $1/6^{\text{th}}$ model of an actual towing hawser, except for the stiffness (Young's Modulus), which was not scaled in the cable model material.

In order to reduce the stiffness of the hawser model a spring was connected in series with it at the dead end $(K = 564.7\text{lbs/ft})$, giving an equivalent average

Young's Modulus:

$$E_{eq} = E\left[1 + \frac{EA}{KL}\right]^{-1}$$

$$= 9.68 \times 10^5 \text{ lbs/in}^2$$

Three series of tests were carried out. In the first one, the static tension (T_0) was 130 lbs and no spring was used. For the second series, the static tension was maintained at 130 lbs and the spring was attached. Finally, in the third series the static tension was increased to 180 lbs and the spring remained attached. Table A.2 summarizes the exciting end-motion amplitudes (non-dimensionalized with the cable diameter) and frequencies (Hz) applied in each test.

Figures A.2, A.3 and A.4 present the maximum and minimum values of the dynamic tension in each one of the tests. For comparison, the simulated values from a numerical integration of equation A.1 are also presented in these Figures. The agreement is quite good, specially at low frequencies (0–0.6 Hz), which when scaled to the actual hawser (with $\sqrt{\alpha}$, α – the geometric scale) corresponds to the range of excitations in actual tow operations (0–1.6 rad/sec).

Figures A.5 and A.6 show time-histories of the simulated tension and the test results.

Diameter – D	in	0.375
Length – L	ft	220.0
Weight – w	lbs/ft	0.29
Young Modulus – E	lbs/in^2	6.97×10^6

Table A.1: Characteristics of Test Hawser

TEST I		TEST II		TEST III	
no spring $T_0 = 130$ lbs		with spring $T_0 = 130$ lbs		with spring $T_0 = 180$ lbs	
s/D	f	s/D	f	s/D	f
13.0	0.1	13.3	0.1	11.3	0.1
12.5	0.3	26.3	0.1	13.8	0.3
13.1	0.6	26.7	0.3	27.0	0.3
11.3	1.0	25.3	1.0	26.2	0.6
23.9	0.1	25.6	1.4	26.0	1.0
26.3	0.3	54.4	0.3	24.5	1.4
25.6	0.6	51.2	0.6	49.9	0.6
49.0	0.3	–	–	52.5	1.0

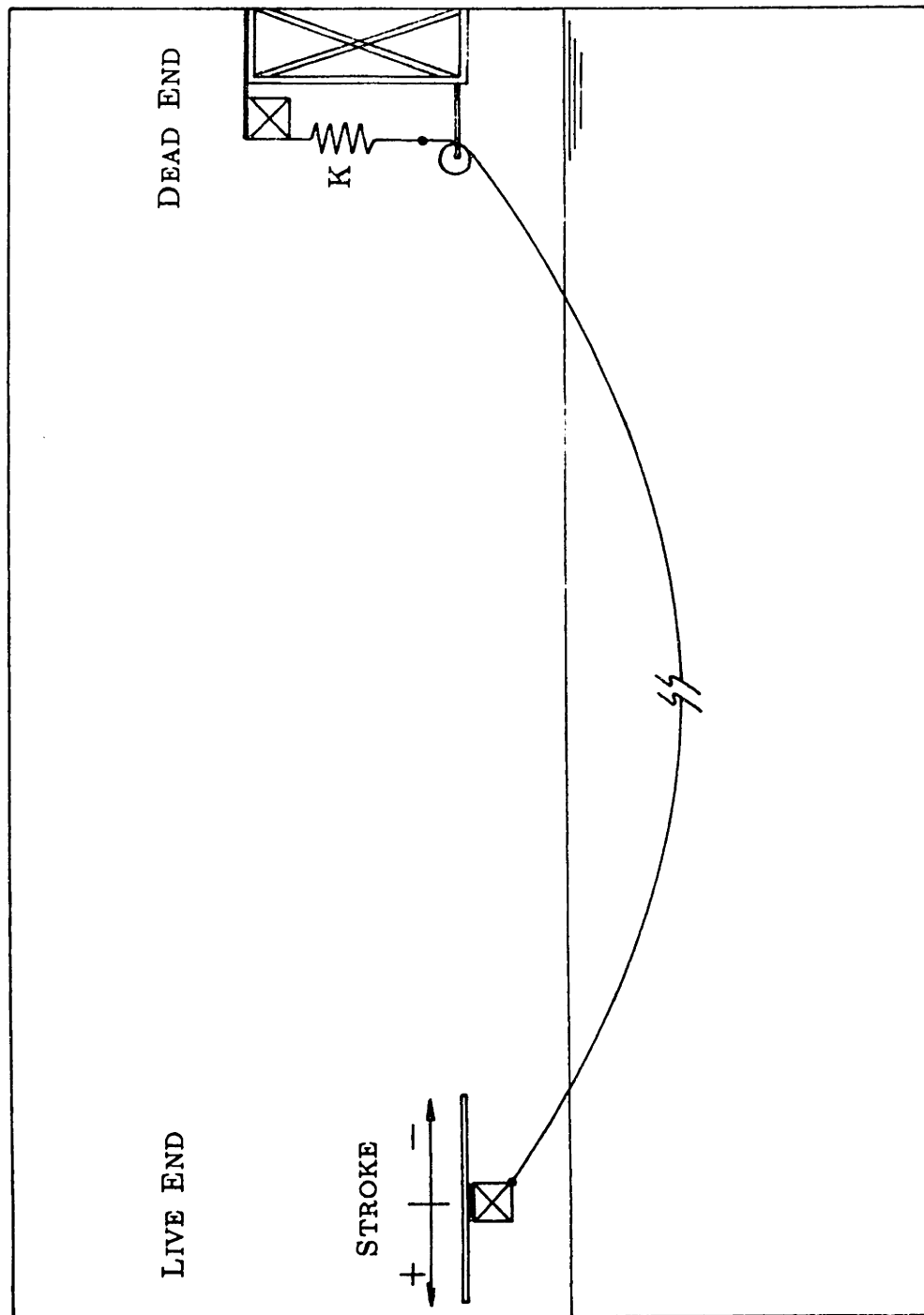Table A.2: End-Motion Amplitudes and Frequencies

Figure A.1: Experimental Arrangement for the Model Test

Figure A.2: Maximum and Minimum Dynamic Tension – TEST I
———— Time Domain Simulation with $s/D = 13$
– – – Time Domain Simulation with $s/D = 26$

Figure A.3: Maximum and Minimum Dynamic Tension – TEST II
——— Time Domain Simulation with $s/D = 13$
— — — Time Domain Simulation with $s/D = 26$
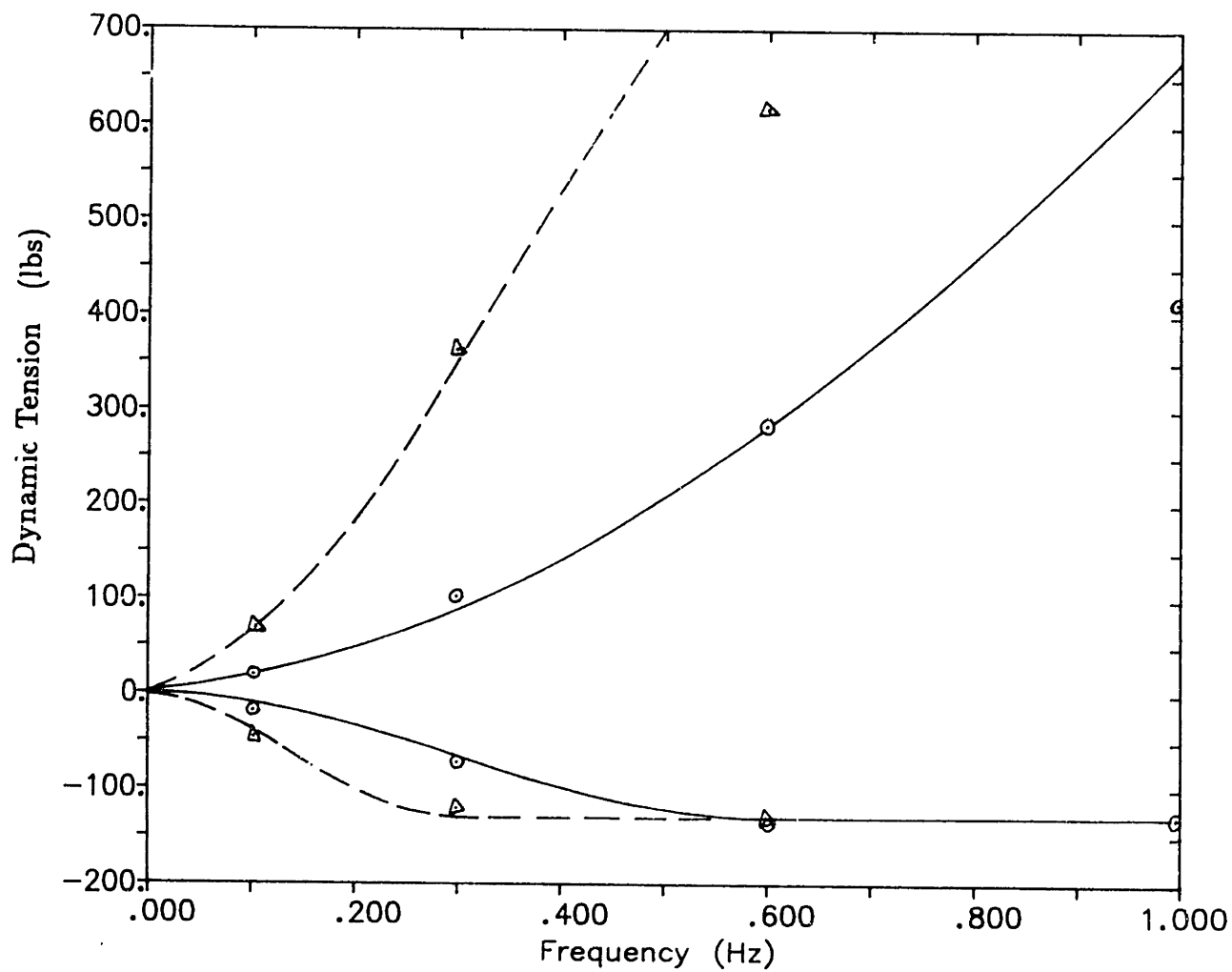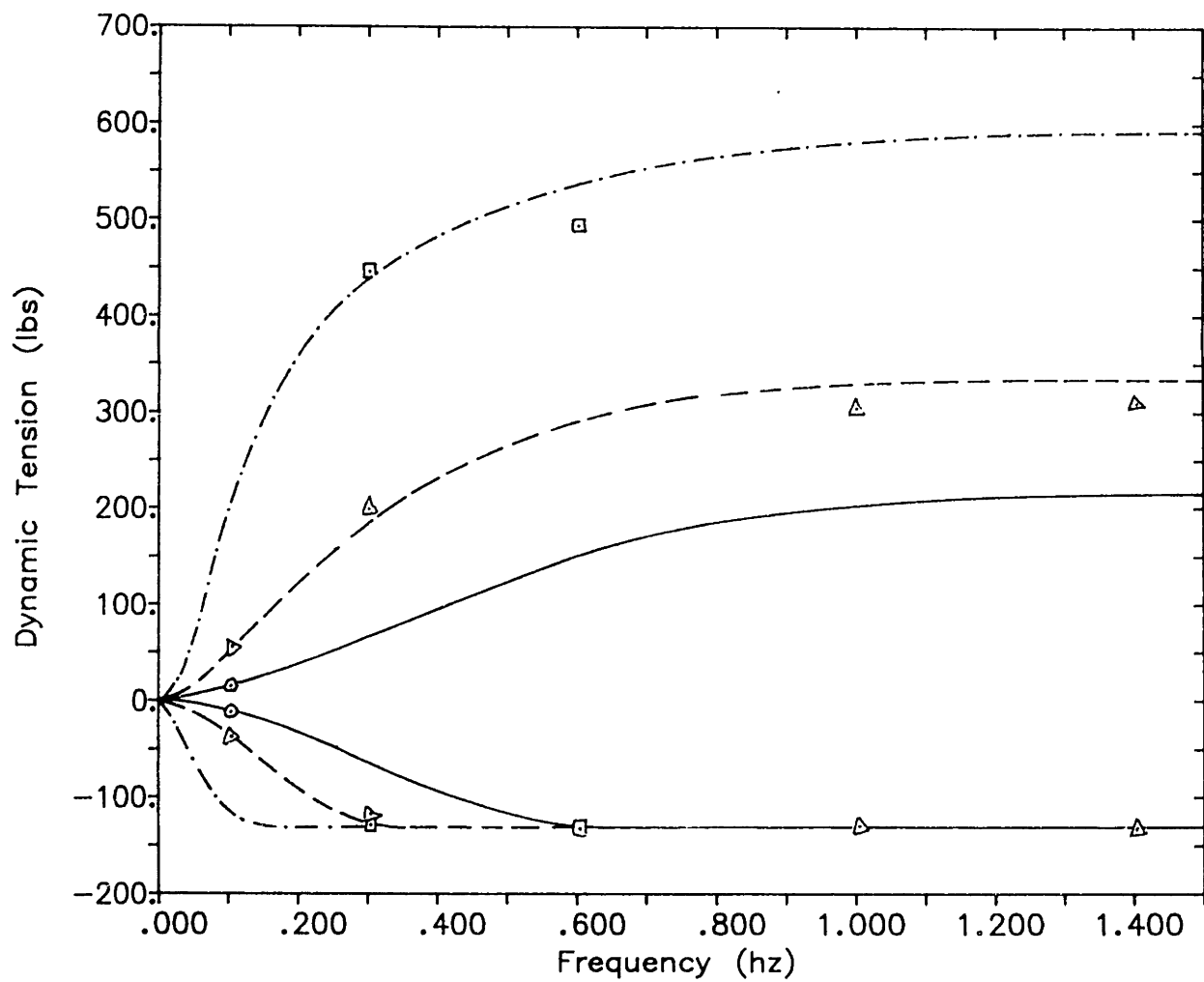— · — · — Time Domain Simulation with $s/D = 52$

117
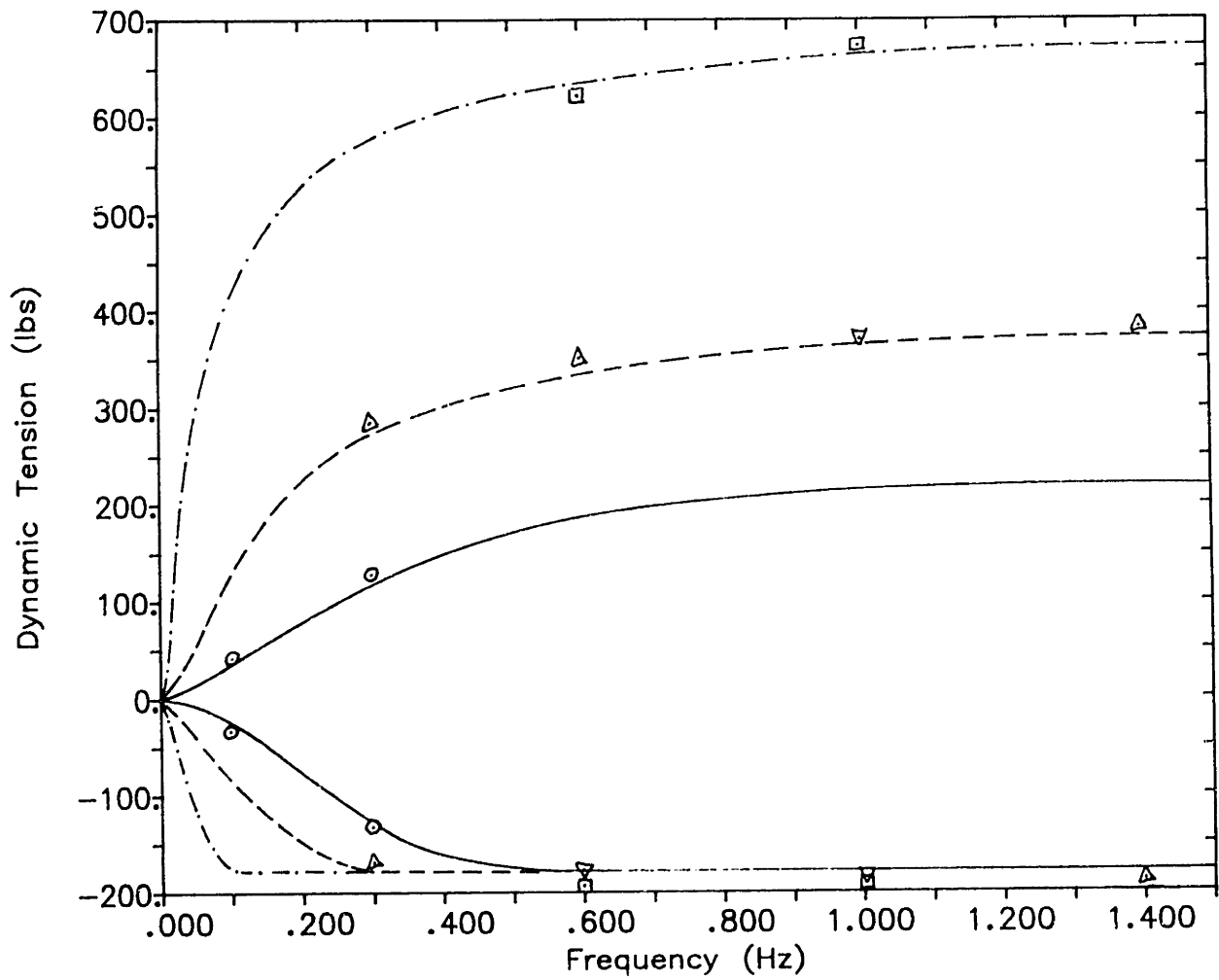
Figure A.4: Maximum and Minimum Dynamic Tension – TEST III

—————— Time Domain Simulation with $s/D = 13$

— — — Time Domain Simulation with $s/D = 26$

—.—.— Time Domain Simulation with $s/D = 52$

Figure A.5: Dynamic Tension versus Time
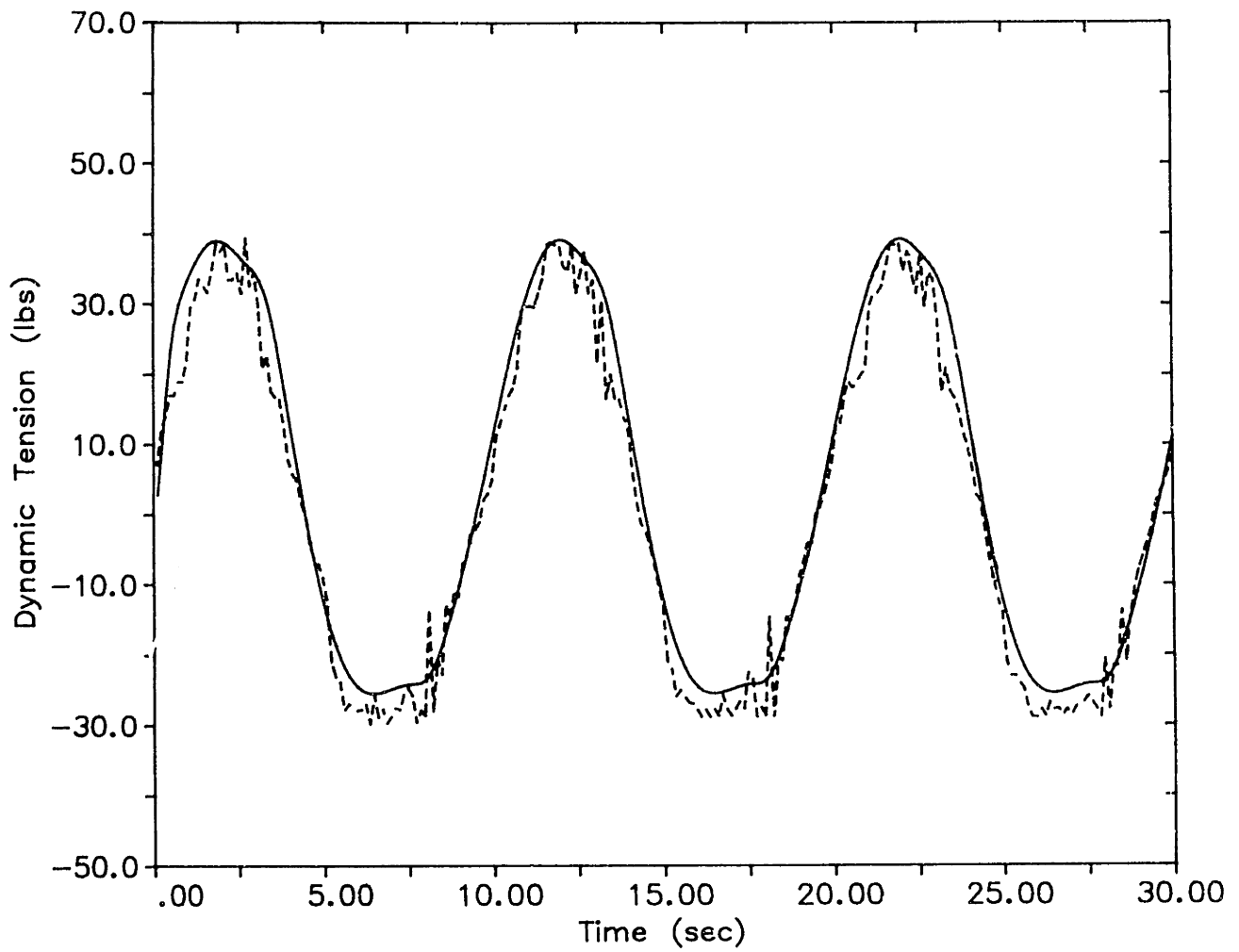$s/D = 11.3$ and $f = 0.1$ Hz
———— Time Domain Simulation
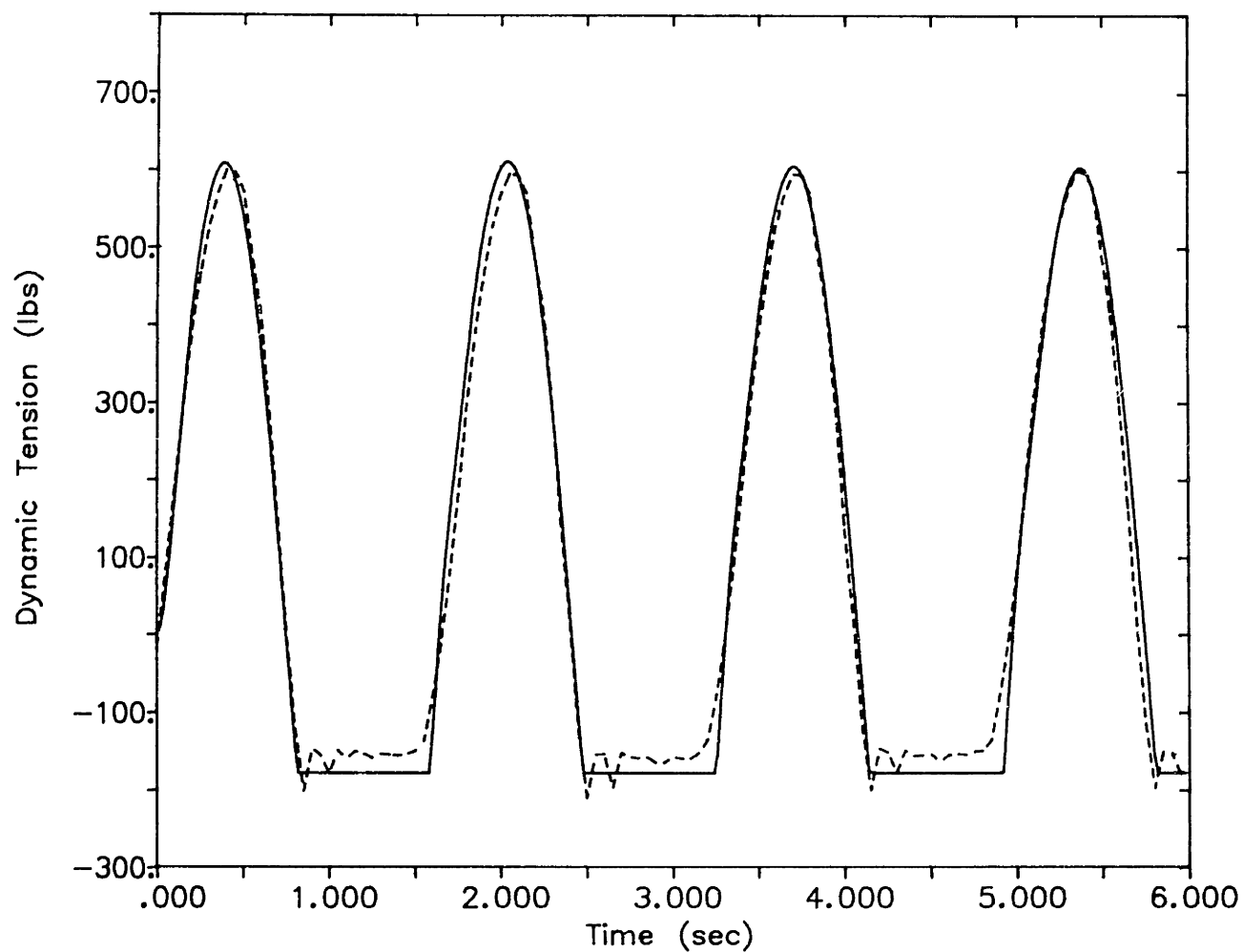- - - - - Model Test Measurement (TEST III).

Figure A.6: Dynamic Tension versus Time
$s/D = 49.9$ and $f = 0.6$ Hz
——— Time Domain Simulation
———— Model Test Measurement (TEST III).

A.3 The polynomial Tension Model

As introduced in Chapter 2 a polynomial model for the cable tension in terms of the end-point elongation, $x(t)$, and elongation time-derivative, $\dot{x}(t)$, was developed. This model was applied in the statistical analyses of extremes.

$$T(x, \dot{x}) = \sum_{m=0}^{3} \sum_{n=0}^{3} a_{mn} \, x^m(t) \, \dot{x}^n(t) \qquad \text{with:} \quad \begin{cases} m + n \leq 3 \\ (m, n) \neq (0, 0) \end{cases} \qquad (A.6)$$

The coefficients of this model are determined using a least minimum squares fit procedure applied to simulated data points, which are obtained from the time-domain solution of the cable dynamic equations presented in Section A.1.

For several different non-dimensional elongation amplitudes – (s/D), and frequencies – (w), data points are collected from the tension time-history and the linear system formed:

$$\alpha_i \left[\sum_{m=0}^{3} \sum_{n=0}^{3} a_{mn} \, x_i^m \, \dot{x}_i^n \right] = \alpha_i \, T(t_i) \qquad (A.7)$$

where: $x_i = s/D \, \sin \omega t_i$, are the elongations; and $\alpha_i = \dfrac{1}{\omega \, (s/D)} \dfrac{T_i}{T_0}$, are weights applied to the simulated data in order to assure that the resulting model is most accurate for larger tensions which are of consequence for ship motions and cable safety.

Some resulting coefficients were presented in Chapter 5, Table 5.2, and examples of simulated tension compared to the polynomial model are shown in Figures A.7 and A.8 for Hawser I.
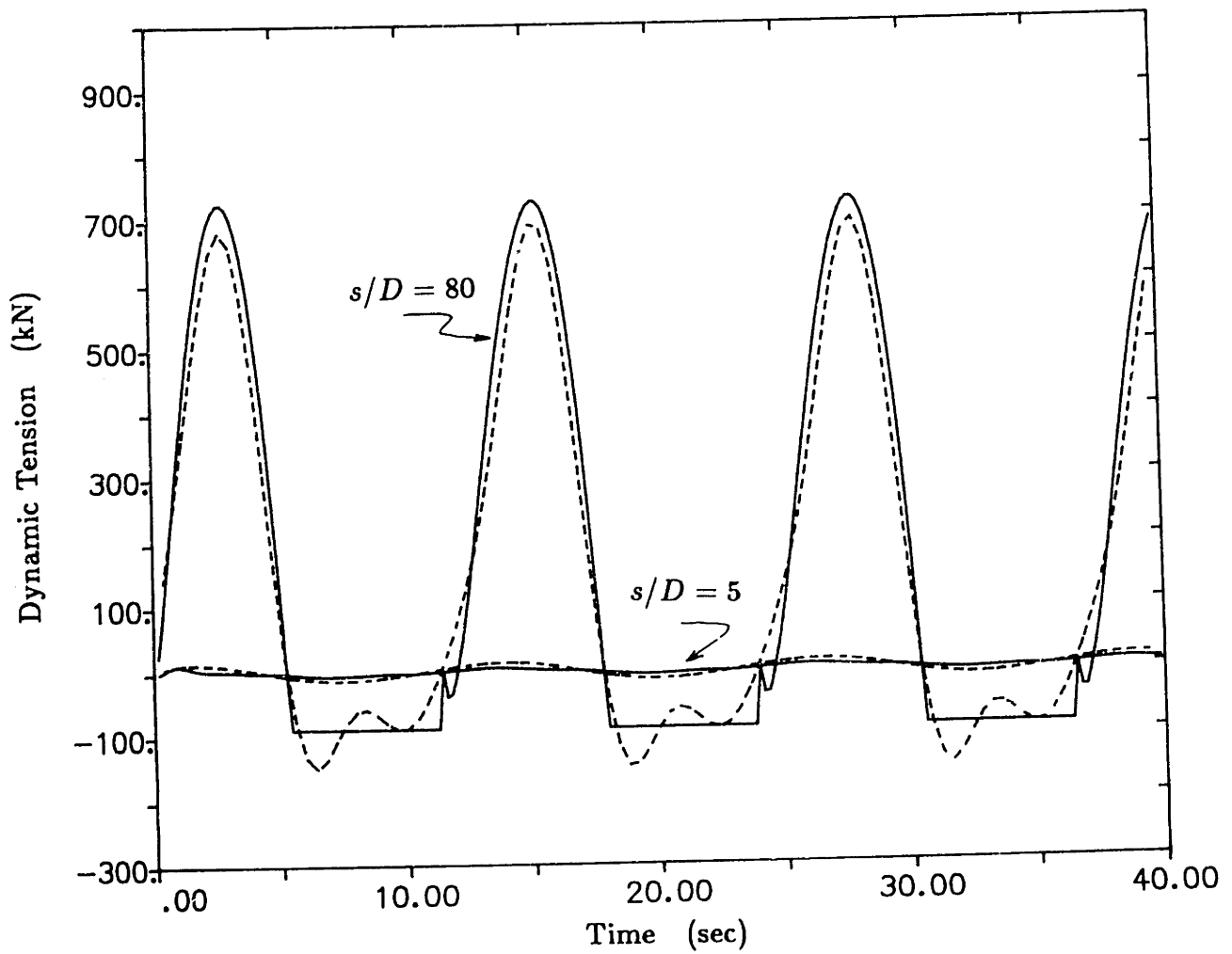
Figure A.7: Dynamic Tension versus Time
Hawser I - Static Tension: 20 kips (88,960 N)
$s/D = 5$ and 80 $f = 0.5$ Rad/sec
———— Time Domain Simulation
----- Polynomial Tension Model.
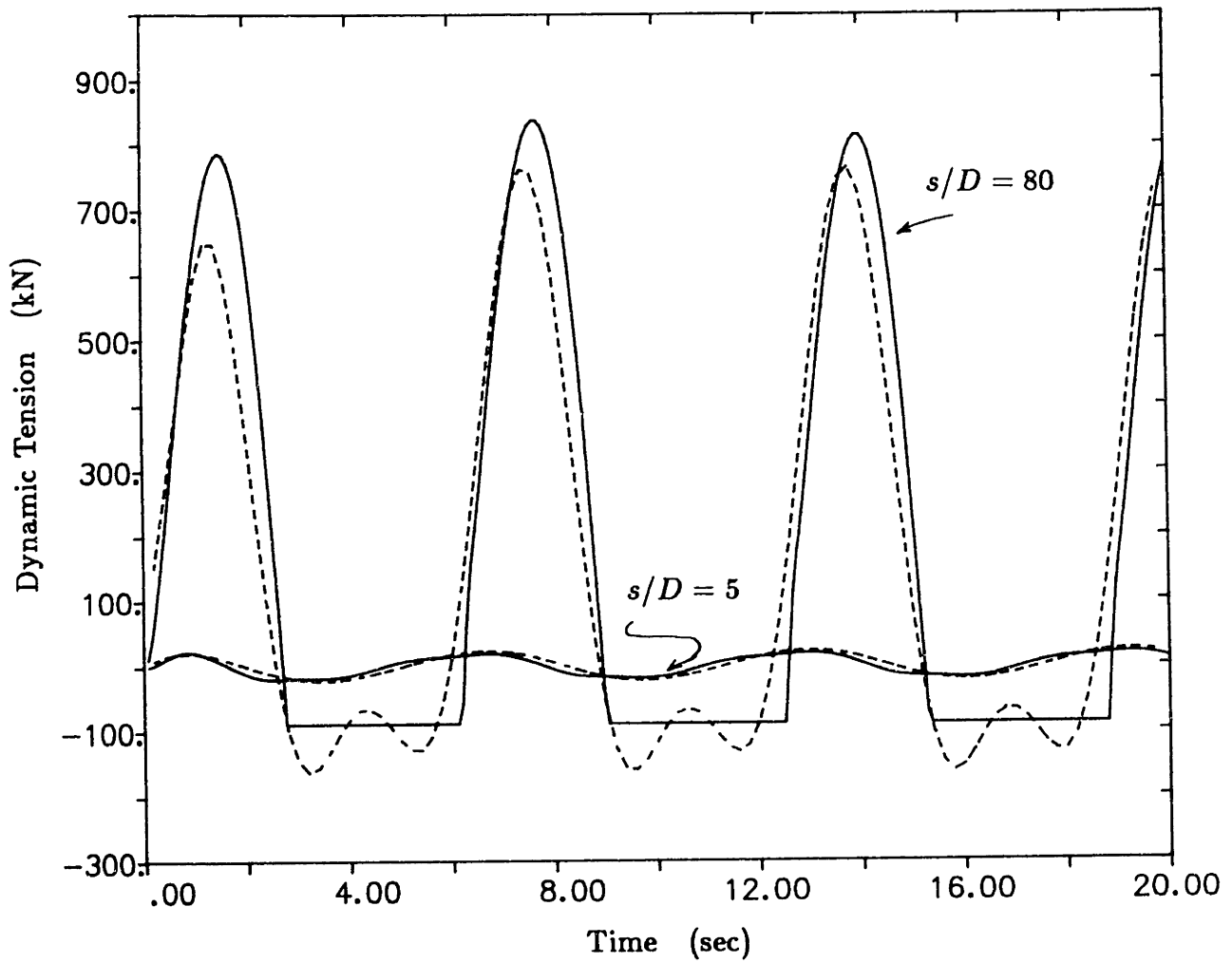
Figure A.8: Dynamic Tension versus Time
Hawser I - Static Tension: 20 kips (88,960 N)
$s/D = 5$ and 80 $f = 1.0$ Rad/sec
——— Time Domain Simulation
- - - - - Polynomial Tension Model.

Appendix B

Towing Dynamics Addendum

In this appendix, the geometry of the towing problem is introduced and the procedures for determining the cable elongation in terms of the ships motions are described. The hawser forces on each vessel are then determined, and the coupling matrices K_{ij} and D_{ij} presented.

In the second part, the developments for the surge motion computations are introduced especially: the surge Froude-Krylov force and the surge damping coefficients.

B.1 The Cable Elongation

Figure B.1 presents the geometry of the towing problem and the variables involved. Two inertial reference frames are defined: $O_1\,x_1\,y_1\,z_1$ at the tug and $O_2\,x_2\,y_2\,z_2$ at the towed vessel, with the origins O_1 and O_2 at the static equilibrium position of the vessels' center of mass. The angular motions: ϕ – roll, θ – pitch and ψ – yaw, are defined positive as indicated.

The cable extension, or elongation, due to the motions of the ships are determined by computing vectorially the cable end-point displacements at both ships when they move. First the tow is imagined fixed, and the end-point displacement vector evaluated displacing the tug vessel a small amount from its original position. Then, the tug is held fixed and the displacement of the tow point evaluated for a small motion of the tow ship.

From numerical simulations it was found that the hawser dynamic tension was most affected when the exciting end-motion was applied along the tangential direction at the extremities of the cable. Therefore, the displacement vectors are projected in this direction at both ends, and are summed up to determine tha cable elongation.

The undisturbed cable end-point positions: t_1 at the tug and t_2 at the tow,
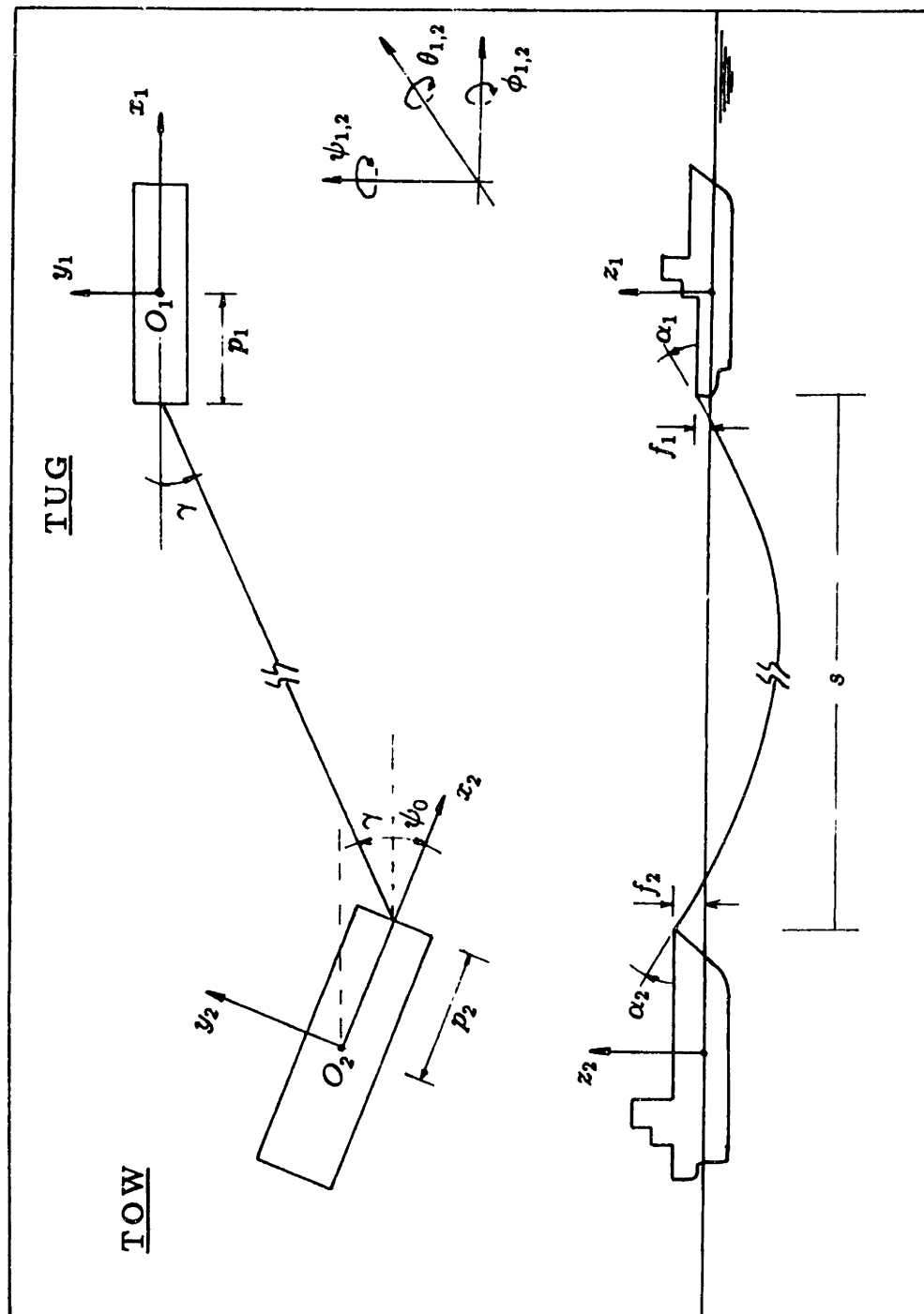
Figure B.1: Geometry of the Towing Problem

in the tug's reference frame $O_1 \, x_1 \, y_1 \, z_1$ are:

$$
t_1 \;=\; \begin{bmatrix} -p_1 \\[1em] 0 \\[1em] f_1 \end{bmatrix}
\qquad\qquad
t_2 \;=\; \begin{bmatrix} -p_1 - s\cos\gamma \\[1em] -s\cos\gamma \\[1em] f_2 \end{bmatrix}
\qquad\qquad \text{(B.1)}
$$

where f_1 and f_2 are the vertical cable end-point positions.

Keeping the tow fixed, and disturbing the tug a small amount (in comparison to the cable lenght) given by the motion vector [1] X_1 :

$$
X_1' \;=\; \begin{bmatrix} x_1 & y_1 & z_1 & \phi_1 & \theta_1 & \psi_1 \end{bmatrix}
\qquad\qquad \text{(B.2)}
$$

Making use of the rotation matrix for small motions [2] R_1 :

$$
R_1 \;=\; \begin{bmatrix} 1 & -\psi_1 & \theta_1 \\[1em] \psi_1 & 1 & \phi_1 \\[1em] -\theta_1 & -\phi_1 & 1 \end{bmatrix}
\qquad\qquad \text{(B.3)}
$$

---

[1] X_1' indicates the transpose of vector X_1.

The motion of the cable end-point at the tug can be expressed as:

$$
t_{1_D} = \begin{bmatrix} 1 & -\psi_1 & \theta_1 \\ \psi_1 & 1 & \phi_1 \\ -\theta_1 & -\phi_1 & 1 \end{bmatrix} \begin{bmatrix} -p_1 \\ 0 \\ f_1 \end{bmatrix} + \begin{bmatrix} x_1 \\ y_1 \\ z_1 \end{bmatrix} \tag{B.4}
$$

Thus, subtracting vectorially the original end-point position from the disturbed one, the cable end-point displacement due to small motions of tug, with the tow fixed is (in the fixed tug's frame $O_1 \, x_1 \, y_1 \, z_1$):

$$
\Delta l_1 = \begin{bmatrix} x_1 + f_1 \, \theta_1 \\ y_1 - p_1 \, \psi_1 + f_1 \, \psi_1 \\ z_1 + p_1 \, \theta_1 \end{bmatrix} \tag{B.5}
$$

Finally, the cable elongation due to small motions of the tug is determined projecting the displacement Δl_1 in the tangential direction to the cable. For that purpose the rotation matrix $R_{\alpha\gamma}$ is introduced. Defining: γ – the offset angle of the towed vessel and α_1 – the angle of the cable at the tug end - point, then:

$$
R_{\alpha\gamma} = \begin{bmatrix} \cos\alpha_1 & 0 & \sin\alpha_1 \\ 0 & 1 & 0 \\ -\sin\alpha_1 & 0 & \cos\alpha_1 \end{bmatrix} \begin{bmatrix} \cos\gamma & \sin\gamma & 0 \\ -\sin\gamma & \cos\gamma & 0 \\ 0 & 0 & 1 \end{bmatrix} \tag{B.6}
$$

The cable extension, in this new rotated frame is given by the product:

$$\Delta e_1 = R_{\alpha\gamma} \cdot \Delta l_1 \tag{B.7}$$

Since we are concerned with the displacement component in the tangential direction of the cable, the first line in the above matrix product gives the desired cable elongation, δ_1:

$$\delta_1 = \cos\alpha_1 \left[\cos\gamma \left(x_1 + f_1\,\theta_1 \right) + \sin\gamma \left(y_1 - p_1\,\psi_1 + f_1\,\phi_1 \right) \right] +$$
$$\sin\alpha_1 \left[\left(z_1 + p_1\,\theta_1 \right) \right] \tag{B.8}$$

The second contribution for the elongation is obtained displacing the tow vessel from its original position while the tow is fixed. As in the first part of these calculations, the small displacement is given by the tow's motion vector X_2. The disturbed cable end-point position is determined as before, expressed in the tow's fixed reference frame $(O_2\,x_2\,y_2\,z_2)$:

$$\Delta l_2 = \begin{bmatrix} x_2 + f_2\cos\theta_2 \\[2mm] y_2 + p_2\psi_2 + f_2\phi_2 \\[2mm] z_2 - p_2\theta_2 \end{bmatrix} \tag{B.9}$$

Again, the above vector is rotated by the angles $(\gamma + \psi_0)$ and α_2 which yields for

the component in the tangential direction to the cable:

$$\delta_2 \;=\; -\cos\alpha_2 \Big[(x_2 + f_2\,\theta_2)\cos(\gamma + \psi_0) - (y_2 + p_2\psi_2 + f_2\phi_2)\sin(\gamma + \psi_0) \Big] \;+$$

$$\sin\alpha_2 \Big[(z_2 - p_2\theta_2) \Big] \qquad\qquad (B.10)$$

The total elongation, the scalar x, can thus be determined by $x = \delta_1 + \delta_2$. According to the nomenclature introduced in Chapter 2,

$$\delta_1 = S_1' \cdot X_1 \qquad \text{and} \qquad \delta_2 = S_2' \cdot X_2 \qquad (B.11)$$

the influence vectors $S_{1,2}$, for determining the cable elongation from the ship motions, can be identified in equations $(B.8)$ and $(B.10)$:

$$S_1 \;=\; \begin{bmatrix} \cos\alpha_1 \, \cos\gamma \\[4pt] \cos\alpha_1 \, \sin\gamma \\[4pt] \sin\alpha_1 \\[4pt] f_1 \, \cos\alpha_1 \, \sin\gamma \\[4pt] -f_1 \, \cos\alpha_1 \, \cos\gamma - p_1 \, \sin\alpha_1 \\[4pt] -p_1 \, \cos\alpha_1 \, \sin\gamma \end{bmatrix} \qquad (B.12)$$

$$S_2 = \begin{bmatrix} -\cos\alpha_2 \cos(\gamma + \psi_0) \\ -\cos\alpha_2 \sin(\gamma + \psi_0) \\ \sin\alpha_2 \cos(\gamma + \psi_0) \\ f_2 \cos\alpha_2 \sin(\gamma + \psi_0) \\ -f_2 \cos\alpha_2 \cos(\gamma + \psi_0) - p_2 \sin\alpha_2 \\ p_2 \cos\alpha_2 \sin(\gamma + \psi_0) \end{bmatrix} \qquad (B.13)$$

B.2 Evaluation of The Coupling Matrices

As introduced in Chapter 2, the dynamic part of the hawser reaction forces acting on the ships, F_{DH}, can be written:

$$F_{DH} = \begin{bmatrix} K_{11} & K_{12} \\ K_{21} & K_{22} \end{bmatrix} \begin{bmatrix} X_1 \\ X_2 \end{bmatrix} + \begin{bmatrix} D_{11} & D_{12} \\ D_{21} & D_{22} \end{bmatrix} \begin{bmatrix} \dot{X}_1 \\ \dot{X}_2 \end{bmatrix} \qquad \text{(B.14)}$$

The objective is the evaluation of the coupling matrices K_{ij} and D_{ij} that translates the hawser forces on vessel - 1 at one end of the towline, due to the motions of the vessel - 2 at the other end. This development follows closely the ideas presented in Burgess [32].

B.2.1 The Hawser Forces

The total hawser tension acting on each one of the ships, $T_{H_{1,2}}$, can be written in terms of the cable's change in span, Δs, and its time derivative [2], $\Delta \dot{s}$:

$$
\begin{aligned}
T_{H_1}^o &= T_{0_1} + k_1 \, \Delta s + b_1 \, \Delta \dot{s} \\
T_{H_2}^o &= T_{0_2} + k_2 \, \Delta s + b_2 \, \Delta \dot{s}
\end{aligned}
\qquad \text{(B.15)}
$$

---

[2]The index 1 refer to the tug and 2 to the tow

which expressed in the inertial reference frames, fixed to ships' static equilibrium position, have the components:

$$
T^o_{H_1} = \begin{bmatrix} -H_{z_1} \\ -H_{y_1} \\ -V_1 \end{bmatrix} + \begin{bmatrix} -k_{z_1} \\ -k_{y_1} \\ -k_{z_1} \end{bmatrix} \Delta s + \begin{bmatrix} -b_{z_1} \\ -b_{y_1} \\ -b_{z_1} \end{bmatrix} \Delta \dot{s}
$$

(B.16)

$$
T^o_{H_2} = \begin{bmatrix} H_{z_2} \\ H_{y_2} \\ -V_2 \end{bmatrix} + \begin{bmatrix} k_{z_2} \\ k_{y_2} \\ -k_{z_2} \end{bmatrix} \Delta s + \begin{bmatrix} b_{z_2} \\ b_{y_2} \\ -b_{z_2} \end{bmatrix} \Delta \dot{s}
$$

T_0 is the static tension on the cable k_{eq} and b_{eq} are the spring and damping coefficients introduced in Chapter 2. The elements of the matrices in equation $(B.16)$ above, are (according to Figure B.1 nomenclature):

$$
H_{z_{1,2}} = T_0 \cos \alpha_{1,2} \cos \gamma
$$

$$
H_{y_{1,2}} = T_0 \cos \alpha_{1,2} \sin \gamma
$$

$$
V_{1,2} = T_0 \sin \alpha_{1,2}
$$

$$
k_{z_{1,2}} = k_{eq} \cos \alpha_{1,2} \cos \gamma
$$

$$
k_{y_{1,2}} = k_{eq} \cos \alpha_{1,2} \sin \gamma
$$

$$
k_{z_{1,2}} = k_{eq} \sin \alpha_{1,2}
$$

$$
b_{z_{1,2}} = b_{eq} \cos \alpha_{1,2} \cos \gamma
$$

$$
b_{y_{1,2}} = b_{eq} \cos \alpha_{1,2} \sin \gamma
$$

$$
b_{z_{1,2}} = b_{eq} \sin \alpha_{1,2}
$$

134

The hawser forces, as given in equation $(B.16)$, act on the ships while they move. For the equations of motion, these forces need to be described on the coordinate frames fixed to the moving ships. The transformation is accomplished using the rotation matrices $R_{1,2}$, equation $(B.3)$, and performing the matrix products [2]:

$$T_{H_{1,2}} = R_{1,2} \cdot T_{H_{1,2}}^o \tag{B.17}$$

which results in:

$$T_{H_1} = \begin{bmatrix} -H_{x_1} \\ -H_{y_1} \\ -V_1 \end{bmatrix} + \begin{bmatrix} & \vdots & 0 & -V_1 & H_{y_1} \\ [\,0\,]_{3\times3} & \vdots & -V_1 & 0 & -H_{x_1} \\ & \vdots & H_{y_1} & H_{x_1} & 0 \end{bmatrix} X_1 + \begin{bmatrix} -k_{x_1} \\ -k_{y_1} \\ -k_{z_1} \end{bmatrix} \Delta s + \begin{bmatrix} -b_{x_1} \\ -b_{y_1} \\ -b_{z_1} \end{bmatrix} \Delta \dot{s}$$

$$T_{H_2} = \begin{bmatrix} H_{x_2} \\ H_{y_2} \\ -V_2 \end{bmatrix} + \begin{bmatrix} & \vdots & 0 & -V_2 & -H_{y_2} \\ [\,0\,]_{3\times3} & \vdots & -V_2 & 0 & H_{x_2} \\ & \vdots & -H_{y_2} & -H_{x_2} & 0 \end{bmatrix} X_2 + \begin{bmatrix} k_{x_2} \\ k_{y_2} \\ -k_{z_2} \end{bmatrix} \Delta s + \begin{bmatrix} b_{x_2} \\ b_{y_2} \\ -b_{z_2} \end{bmatrix} \Delta \dot{s}$$

$$\tag{B.18}$$

According to the nomenclature introduced in Figure B.1, the cable end-point position vectors, at the tug ship and towed vessel are:

$$t_1 = \begin{bmatrix} -p_1 \\ 0 \\ f_1 \end{bmatrix} \quad \text{and} \quad t_2 = \begin{bmatrix} p_2 \\ 0 \\ f_2 \end{bmatrix} \tag{B.19}$$

The moments can be obtained by multiplying vectorially the cable end-point position vectors, given by equation $(B.19)$ above, and the tension vectors, equation

135

(B.18), for each one of the ships:

$$M_{H_{1,2}} = t_{1,2} \times T_{H_{1,2}} \qquad (B.20)$$

such that the hawser action on the ships can be written in terms of their force and moment components:

$$F_{H_{1,2}} = \begin{bmatrix} T_{H_{1,2}} \\ \\ t_{1,2} \times T_{H_{1,2}} \end{bmatrix} \qquad (B.21)$$

Performing the vector products for the moments (to first order) and using equation (B.18), the resulting expression for the components of the hawser reaction vectors at the tug and tow, according to (B.21) above, are:

$$F_{H_1} = F_{0_1} + \begin{bmatrix} [\,0\,]_{6\times3} & \vdots & 0 & -V_1 & H_{y_1} \\ & \vdots & -V_1 & 0 & -H_{z_1} \\ & \vdots & H_{y_1} & H_{z_1} & 0 \\ & \vdots & f_1 V_1 & 0 & f_1 H_{z_1} \\ & \vdots & p_1 H_{y_1} & -f_1 V_1 + p_1 H_{z_1} & f_1 H_{y_1} \\ & \vdots & p_1 V_1 & 0 & p_1 H_{z_1} \end{bmatrix} X_1 + \mathbf{k}_1 \cdot \Delta s + \mathbf{b}_1 \cdot \Delta \dot{s}$$

$$F_{H_2} = F_{0_2} + \begin{bmatrix} [\,0\,]_{6\times3} & \vdots & 0 & -V_2 & -H_{y_2} \\ & \vdots & -V_2 & 0 & H_{z_2} \\ & \vdots & -H_{y_2} & -H_{z_2} & 0 \\ & \vdots & f_2 V_2 & 0 & -f_2 H_{z_2} \\ & \vdots & p_2 H_{y_2} & -f_2 V_2 + p_2 H_{z_2} & -f_2 H_{y_2} \\ & \vdots & -p_2 V_2 & 0 & p_2 H_{z_2} \end{bmatrix} X_2 + \mathbf{k}_2 \cdot \Delta s + \mathbf{b}_2 \cdot \Delta \dot{s}$$

$$(B.22)$$

$F_{0_{1,2}}$ are the vectors with the components of the hawser static force and moment on the tug and tow in their own reference frames:

$$
F_{0_1} = \begin{bmatrix} -H_{x_1} \\ -H_{y_1} \\ -V_1 \\ f_1 H_{y_1} \\ -f_1 H_{x_1} - p_1 V_1 \\ p_1 H_{y_1} \end{bmatrix}
\quad \text{and} \quad
F_{0_2} = \begin{bmatrix} H_{x_2} \\ H_{y_2} \\ -V_2 \\ -f_2 H_{y_2} \\ f_2 H_{x_2} + p_2 V_2 \\ p_2 H_{y_2} \end{bmatrix}
\tag{B.23}
$$

In equation $(B.22)$ the vectors $k_{1,2}$ and $b_{1,2}$ represent the components of the spring and damping forces (for unit changes in span and its rate of change), in the tug and tow reference frames, respectively:

$$
k_1 = \begin{bmatrix} -k_{x_1} \\ -k_{y_1} \\ -k_{x_1} \\ f_1 k_{y_1} \\ -f_1 k_{x_1} - p_1 k_{x_1} \\ p_1 k_{y_1} \end{bmatrix}
\quad \text{and} \quad
k_2 = \begin{bmatrix} k_{x_2} \\ k_{y_2} \\ -k_{x_2} \\ -f_2 k_{y_2} \\ f_2 k_{x_2} - p_2 b_{x_2} \\ -p_2 k_{y_2} \end{bmatrix}
\tag{B.24}
$$

$$
b_1 = \begin{bmatrix} -b_{x_1} \\ -b_{y_1} \\ -b_{x_1} \\ f_1 b_{y_1} \\ -f_1 b_{x_1} - p_1 b_{x_1} \\ p_1 b_{y_1} \end{bmatrix}
\quad \text{and} \quad
b_2 = \begin{bmatrix} b_{x_2} \\ b_{y_2} \\ -b_{x_2} \\ -f_2 b_{y_2} \\ f_2 b_{x_2} - p_2 b_{x_2} \\ p_2 b_{y_2} \end{bmatrix}
\tag{B.25}
$$

B.2.2 The Change in Span

The change in span can be written in terms of influence row vectors, which are linear transformations from the motions vectors to the scalar change in span:

$$\Delta s = \begin{bmatrix} E_1' & \vdots & E_2' \end{bmatrix} \begin{bmatrix} X_1 \\ X_2 \end{bmatrix} \qquad (B.26)$$

The vectors $E_{1,2}$ are evaluated in a similar manner as were the elongation influence vectors in section B.1. The distance between the cable end-points is calculated for small displacements of tug or tow vessels, from the static equilibrium position, while one of them is held fixed. According to the nomenclature introduced in Figure B.1, to first order, these vectors are [32]:

$$E_1 = \frac{1}{d_0} \begin{bmatrix} s\cos\gamma \\ s\sin\gamma \\ \Delta f \\ s f_1 \sin\gamma \\ p_1 \Delta f + s f_1 \cos\gamma \\ s p_1 \sin\gamma \end{bmatrix} \qquad E_2 = \frac{1}{d_0} \begin{bmatrix} -s\cos(\gamma+\psi_0) \\ -s\sin(\gamma+\psi_0) \\ -\Delta f \\ -s f_2 \sin(\gamma+\psi_0) \\ p_2 \Delta f - s f_2 \cos(\gamma+\psi_0) \\ -s p_2 \sin(\gamma+\psi_0) \end{bmatrix} \qquad (B.27)$$

where $d_0 = \sqrt{s^2 + (f_2 - f_1)^2}$ is the distance between the two vessels at the static equilibrium position, and $\Delta f = f_1 - f_2$.

B.2.3 The matrices K_{ij} and D_{ij}

The expression for the hawser reaction forces and moments, equation $(B.22)$, can be rewritten considering the relationship between motions and change in span, equation $(B.26)$. Then, eliminating the static reaction forces and moments, $F_{0_{1,2}}$, gives the dynamic hawser forces and moments, $F_{DH_{1,2}}$, which, when compared to equation $(B.14)$, allows the identification of the coupling matrices:

$$K_{11} = \mathbf{k}_1 \cdot E_1' + \begin{bmatrix} & \vdots & 0 & -V_1 & H_{y_1} \\ & \vdots & -V_1 & 0 & -H_{x_1} \\ [\,0\,]_{6\times 3} & \vdots & H_{y_1} & H_{x_1} & 0 \\ & \vdots & f_1 V_1 & 0 & f_1 H_{x_1} \\ & \vdots & p_1 H_{y_1} & -f_1 V_1 + p_1 H_{x_1} & f_1 H_{y_1} \\ & \vdots & p_1 V_1 & 0 & p_1 H_{x_1} \end{bmatrix}$$

$$K_{22} = \mathbf{k}_2 \cdot E_2' + \begin{bmatrix} & \vdots & 0 & -V_2 & -H_{y_2} \\ & \vdots & -V_2 & 0 & H_{x_2} \\ [\,0\,]_{6\times 3} & \vdots & -H_{y_2} & -H_{x_2} & 0 \\ & \vdots & f_2 V_2 & 0 & -f_2 H_{x_2} \\ & \vdots & p_2 H_{y_2} & -f_2 V_2 + p_2 H_{x_2} & -f_2 H_{y_2} \\ & \vdots & -p_2 V_2 & 0 & p_2 H_{x_2} \end{bmatrix} \qquad (B.28)$$

$$K_{12} = \mathbf{k}_1 \cdot E_2'$$

$$K_{21} = \mathbf{k}_2 \cdot E_1'$$

$$D_{ij} = \mathbf{b}_i \cdot E_j'$$

B.3   The Surge Exciting Force

The wave exciting force for the surge motion is computed by means of the Froude-Krylov approximation, i.e. through the integration of the wave pressures on the hull surface, assuming that the ship does not affect the wave potential:

$$F_{FK} = \int\int_S p\,\vec{n}\,dS$$

Closing the hull surface with the horizontal water plane, the Gauss Theorem can be applied, and the force determined by the integration of the pressure gradient in the ship's immersed volume:

$$F_{FK} = \int\int\int_V \nabla p\,dV$$

In the case of the surge force, since there is no horizontal force component on the water plane surface, the Gauss Theorem can be applied to the sectional force:

$$
\begin{aligned}
F(x) &= \int_C p\,n_1\,dl \\
&= \int\int_S \frac{\partial p}{\partial x}\,dS
\end{aligned}
\qquad\text{(B.29)}
$$

where, $C = C(x)$ and $S = S(x)$ are the section contour and area, respectively. Considering these contours as given by the section half beams in terms of the vertical

z - coordinate, i.e.: $C(x) = b_x(z)$ then:

$$dS = 2\, b_x(z)\, dz \qquad\qquad (B.30)$$

and the sectional surge force is given by:

$$F(x) = 2 \int_z \frac{\partial p}{\partial x}\, b_x(z)\, dz \qquad\qquad (B.31)$$

The waves pressure field is:

$$p = \rho\, g A\, e^{k_0 z}\, Re\Big\{ \exp[\, -i\, k_0\, (x\cos\beta + y\sin\beta) + iw_e t\,]\Big\} \qquad (B.32)$$

where:

A : wave amplitude,

k_0 : wave number,

β : wave angle w.r.t. ship's longitudinal axis,

w_e : wave encounter frequency,

x : longitudinal coordinate along the ship,

y : lateral coordinate, $y = b_x(z)$ (half beams).

Evaluating $\frac{\partial p}{\partial x}$ and using it with equation $(B.31)$, the sectional surge force is obtained.

For long waves it is difficult to do the numerical integration in equation $(B.31)$ accurately. This can be remedied by the following procedure. For large wave lengths compared to the beam, $\sin k_0 \, b(z) \approx k_0 \, b(z)$, then (leaving $e^{iw_e t}$ aside):

$$F(x) = -2 \, \rho \, g A \, k_0 \, \cos \beta \, \sin(k_0 \, x \, \cos \beta) \int_z b_x(z) \, e^{k_0 z} \, dz \qquad (B.33)$$

A further simplification can be applied for the case of the low frequency surge. Assuming: $\exp[k_0 z] \approx [1 + k_0 z]$, the z - integral can be performed analytically, resulting in:

$$F(x) \, k_0 \overset{\approx}{\to} 0 \; -2 \, \rho \, g A \, k_0 \, \cos \beta \, \sin(k_0 \, x \, \cos \beta) \, S(x) \, [\, 1 + k_0 z_C(x) \,] \qquad (B.34)$$

where $z_C(x)$ is the vertical center of the sectional area $S(x)$. The total surge force is determined by integrating $F(x)$ along the ship's length:

$$F_{FK} \, k_0 \overset{\approx}{\to} 0 \; -2 \, \rho \, g A \, k_0 \, \cos \beta \int_{-\frac{L}{2}}^{\frac{L}{2}} \sin(k_0 \, x \, \cos \beta) \, S(x) \, [1 + k_0 \, z_C(x)] \, dx \qquad (B.35)$$

B.4 The Surge Damping Coefficients

For the towed vessel, the surge damping coefficient is evaluated as the slope of the resistance curve at the towing speed. R_T is the total resistance,

$$R_T = \frac{1}{2} \rho \, g S_W \, C_T \, V^2 \qquad (B.36)$$

where:

C_T : total resistance coefficient,

S_W : hull's wetted surface,

V : towing speed

The damping coefficient is then given by:

$$
\begin{aligned}
b_R &= \frac{dR_T}{dV} \\
&= \rho \, g S_W \, C_T \, V
\end{aligned}
\qquad (B.37)
$$

For the tug, besides b_R, given by $(B.37)$ above, one must also consider the propeller effects on the damping through the evaluation of the change in thrust, T, due to changes in velocity, V. For a constant torque (Diesel Engine) propulsion plant, the analysis that follows determines this coefficient:

$$b_T = \frac{dT}{dV} \qquad (B.38)$$

Considering the open water characteristic curve for the tug propeller, and the thrust, torque and advance coefficients:

$$K_t = \frac{T}{\rho\,N^2 D^4} \qquad K_q = \frac{Q}{\rho\,N^2 D^5} \qquad J = \frac{V(1-w)}{N\,D} \qquad \text{(B.39)}$$

where:

Q : torque at the propeller shaft,

N : propeller speed (RPS),

D : propeller diameter,

w : wake fraction coefficient.

The propeller thrust can be expressed in terms of the torque as:

$$T = \frac{K_t}{K_q}\frac{Q}{D} \qquad \text{(B.40)}$$

For a constant torque plant, differentiating this expression with respect to the speed V, yields:

$$\frac{dT}{dV} = \rho\,N^2 D^4 \left[\frac{dK_t}{dV} - \frac{K_t}{K_q}\frac{dK_q}{dV} \right] \qquad \text{(B.41)}$$

The right hand side derivatives are:

$$\frac{dK_q}{dV} = \alpha_q \frac{dJ}{dV} \qquad \text{and} \qquad \frac{dK_t}{dV} = \alpha_t \frac{dJ}{dV} \qquad \text{(B.42)}$$

where: $\alpha_q = \frac{dK_q}{dJ}$ and $\alpha_t = \frac{dK_t}{dJ}$ are respectively, the slopes of the curves $K_q \times J$

and $K_t \times J$ in the open-water propeller diagram.

Therefore, using the relationships $(B.42)$ above, in equation $(B.41)$:

$$\frac{dT}{dV} = \rho \, N^2 D^4 \left[\alpha_t - \alpha_q \frac{K_t}{K_q} \right] \frac{dJ}{dV} \qquad (B.43)$$

To determine $\frac{dJ}{dV}$, write $N = \left[\frac{\rho D^5 K_q}{Q} \right]^{-\frac{1}{2}}$, and consider the following:

$$\begin{aligned} \frac{dJ}{dV} &= \frac{d}{dV} \left[\frac{V(1-w)}{D} \left(\frac{\rho \, D^5 K_q}{Q} \right)^{\frac{1}{2}} \right] \\ &= \left(\frac{\rho \, D^3 K_q}{Q} \right)^{\frac{1}{2}} (1-w) + \frac{1}{2} V (1-w) \left(\frac{\rho \, D^3}{Q \, K_q} \right)^{\frac{1}{2}} \frac{dK_q}{dV} \end{aligned} \qquad (B.44)$$

also:

$$\left(\frac{\rho \, D^5 K_q}{Q} \right)^{\frac{1}{2}} = \frac{1}{ND} \qquad \text{and} \qquad \left(\frac{\rho \, D^3}{Q \, K_q} \right)^{\frac{1}{2}} = \frac{\rho \, ND^4}{Q} \qquad (B.45)$$

which, substituted in $(B.44)$ gives:

$$\frac{dJ}{dV} = \frac{J}{V} + \frac{J}{2 \, K_q} \frac{dK_q}{dV} \qquad (B.46)$$

Using equation $(B.42)$ in above,

$$\frac{dJ}{dV} = \frac{J}{V} \frac{1}{1 - \frac{J \, \alpha_q}{2 \, K_q}} \qquad (B.47)$$

Thus, substituting $\frac{dJ}{dV}$, as given in equation $(B.47)$ above, into equation $(B.43)$,

gives after some algebraic simplification:

$$\frac{dT}{dV} = 2\,\rho\,D^2\,\frac{V}{J}\left[\frac{\alpha_t\,K_q - \alpha_q\,K_t}{2\,K_q - J\,\alpha_q}\right] \tag{B.48}$$

which constitutes the propeller surge damping coefficient for the tug, that can be

determined once the propeller operation point is known.